universität wien

DIPLOMARBEIT

Titel der Diplomarbeit

Possible mechanism of the eating-inhibitory effect of DGAT-1-inhibition

angestrebter akademischer Grad

Magistra der Naturwissenschaften (Mag.rer.nat.)

Verfasserin:	Gudrun Schober
Matrikel-Nummer:	0155276
Studienrichtung:	Ernährungswissenschaften
Betreuer:	Prof. Dr. Wolfgang Langhans

Schwerzenbach, am 16. Dezember 2008

ACKNOWLEDGMENTS

In the first place I would like to thank my Professor Dr. Wolfgang Langhans, who gave me the great opportunity to work within his research group and for his support, trust and guidance throughout the thesis. His door was always open to solve any problems.

I wish to convey my sincere appreciation to Myrtha Arnold, who gave me the chance to learn from her and for her permanent and unforgettable support and assistance during my thesis. She has been present all the time whenever help was needed. Thanks!!

I am also very thankful to Prof. Nori Geary, for his support and his endurance in mastering the English language.

I am sincerely thankful to all my colleagues here in Schwerzenbach, Isabelle Baumgartner, Lily Kuo, Elizabeth Rüttimann, Viktoria Gloy, Brigitte Kopf, Jacquelien Hillebrand, Gustavo Pacheco Lopez, Loredana Asarian, Michael Koss and Markus Senn, for always being helpful.

Further I would like to thank:
Mandy Sütö and Ana Hemmersbach for there support with animal care and cleaning. The technical service team of Roland Morscher, Pascal Bernhard and Christian Schlatter for always providing any technical help and support. Marcel Morf for his help in solving all my computer problems and Ruth Hauser, for taking charge of all the administrative and financial affairs.

From the bottom of my heart I want to thank my boyfriend Damian for the never-ending support and love, and special thanks goes to my best friends, Nadja and Natascha, for struggling together through our study.

Finally, I am deeply grateful to my family for being there for me and for giving me the great opportunity for such an education.

I TABLE OF CONTENTS

II. TABLE OF FIGURES:

III. LIST OF ABBREVIATIONS:

AA	amino acids
AAT	acyl-CoA acyltransferase
ACAT	acyl-CoA:cholesterol acyltransferase
ad lib	ad libitum
Ad-hDGAT1	recombinant adenovirus containing human DGAT1
AGPAT	1-acylglycerol-3-phosphate acyltransferase
AgRP	agouti-related protein
apo AI	apoprotein AI
apo A-IV	apoprotein AIV
apo B48	apolipoprotein B48
ARC	arcuate nucleus
ASO	antisense oligonucleotide
$A^y/_a$	Agouti yellow mice
BAT	brown adipose tissue
BBB	blood-brain barrier
BS	bile salt
BW	body weight
C/EBPα	cytidine-cytidine-adenosine-adenosine-thymidine-enhancer-binding protein α
cAMP	cyclisches adenosine monophosphat
CART	cocaine and amphetamine-related transcript
CCK	Cholecystokinin
CL	cholesterol
CM	chylomicron
CNS	central nervous system
CPT-1	carnitine O-palmitoyltransferase 1
CSF	cerebrospinal fluid

DAG	sn-1,2-diacylglycerol
DGAT	Acyl-CoA:1,2-diacylglycerol O-acyltransferase
DHAP	dihydroxyacetone phosphate
DIO	diet-induced obesity
DMH	dorsamedial nucleus
DPP-4	dipeptidyl peptidase-4
EB	energy balance
EE	energy expenditure
EI	energy intake
ER	endoplasmic reticulum
FA	fatty acids
FAO	fatty acid oxidation
FAS	fatty acid synthase
FATP4	fatty acid transport protein 4
FFAs	free fatty acids
FI	food intake
GH	growth hormone
GHS-R	growth hormone secretagogue receptor
GI	gastrointestinal
GLP-1, 2	Glucagon-like peptide-1, 2
GLP-1R	Glucagon-like peptide-1 receptor
GLUT-2	glucose-transporter-2
GPAT	glycerol-phosphate acyltransferase
ICV	intracerebroventricular
IFABP	intestinal fatty acid binding protein
IP	intraperitoneally
IR	insulin receptor
LHA	lateral hypothalamic area
LPA	lysophosphatidic acid
LXR	liver X receptors

MAG	monoacylglycerols
MC	melanocortin
MC3/4-R	melanocortin type 3 and 4 receptors
MGAT	acyl CoA: monoacylglycerol acyltransferase
MM	molecular mass
MP	methyl palmoxirate
Mr	*Mortierella ramanniana* (fungi)
mRNA	messenger RNA
MTP	microsomal triglyceride transfer protein
NPY	neuropeptide Y
NTS	nucleus of the solitary tract
ob	obese
ODN	oligodeoxynucleotide
OXM	Oxyntomodulin
PAP	phosphatidic acid phosphohydrolase
PC	phosphatidylcholine
PCTV	prechylomicron transport vesicle
PFA	perifornical area
PI-3K	phospatidylinositol-3 kinase
PKA	protein kinase A
PKC	protein kinase C
PL	phospholipids
POMC	pro-opiomelanocortin
PP	pancreatic polypeptide
PPARα, γ	peroxisome proliferator-activated receptor α, γ
$pPLA_2$	phospholipase A_2
PVN	paraventricular nucleus
PYY	peptide tyrosine-tyrosine
rER	rough endoplasmic reticulum

sn	stereospecific numbering
SREBP-1c	sterol-regulatory-element-binding protein-1c
T2DM	Type 2 diabetes mellitus
TG	triglycerides
TNF-α	tumor necrosis factor α
UCP1	uncoupling protein 1
VMH	ventromedial nucleus
WAT	white adipose tissue
WHO	World Health Organization
WT	wild type
α-MSH	α-melanocyte stimulating hormone

1 GENERAL INTRODUCTION

The prevalence of overweight and obesity has been increasing markedly over the past two decades, and obesity is now regarded as a global epidemic affecting both, adults and children [BAYS, 2004; GALE et al., 2004; OGDEN et al., 2006; RONNETT et al., 2005; WANG et al., 2006]. The World Health Organization (WHO) has declared overweight as one of the top ten risk conditions in the world and one of the top 5 in developed countries [WHO, 2006]. Increased mortality and significant morbidity are directly associated with obesity, mainly due to cardiovascular diseases (hypertension, coronary heart disease), metabolic disorders (Type 2 diabetes mellitus (T2DM), hyperlipidemia and insulin resistance), as well as respiratory diseases, gastrointestinal disorders (fatty liver and cirrhosis), and some cancers (cervical, breast, gallbladder and colon) [CALLE et al., 2004; CROWLEY, 2008; FLEGAL et al., 2005; NAMMI et al., 2004; WILBORN et al., 2005]. The basic cause of overweight and obesity is an imbalance between energy intake (EI) and energy expenditure (EE), which leads to abnormal or excessive fat accumulation in adipose tissue in form of triglycerides (TG) [CAMPFIELD et al., 1998; HILL et al., 2003; MORTON et al., 2006; NAMMI et al., 2004]. However, the relationship between TG synthesis and the development of obesity has not been critically examined yet. Specifically, it is still unclear whether inhibition of TG synthesis might be a feasible strategy for the treatment of obesity and T2DM [CHEN et al., 2000; SHI et al., 2004]. Over the past decade some studies about the biology of TG synthesis and the roles of the main enzymes that are involved in lipid metabolism were performed and attention was drawn to Acyl CoA:diacylglycerol acyltransferase 1 (DGAT1), one of two known key enzymes that catalyze the final and only committed step in mammalian TG synthesis [CASES et al., 1998]. Selective inhibition of DGAT1-mediated TG synthesis may be an approach to treating hypertriglyceridemia or obesity in humans [CASES et al., 1998]. Thus, it

has been shown that genetic DGAT1 deficiency in mice makes mice resistant to diet-induced obesity and leads to increased leptin sensitivity, to increased energy expenditure and to improved glucose sensitivity [CHEN et al., 2002a]. However, the effects of a pharmacological inhibition of DGAT1 have not been systematically investigated yet. Some patent documentations have described weight loss with pharmacological DGAT1 inhibition in rodents that is associated with decreased food intake [ZHAO et al., 2008], but the mechanisms and the generality of this eating-inhibitory effect remain unclear.

In this thesis I performed three experiments to address these open questions. The specific research aims were 1) to determine whether intragastric infusions of a DGAT1-inhibitor (DGAT1i01) can inhibit eating in chow-fed or high fat diet (HFD)-fed rats, respectively; 2) to investigate the effects of intragastric infusion of a DGAT1i01 on serum and plasma metabolites in HFD fed rats and 3) to determine whether enhanced fatty acid oxidation in small intestinal enterocytes is a possible mechanism for the eating-inhibitory effect after intragastric infusion of DGAT1i01. The molecular DGAT1i01 used in all three experiments was provided by AstraZeneca.

2 LITERATURE SURVEY

2.1 The control of food intake

Food intake (FI) provides energy, all the macronutrients, vitamins, minerals, and a variable amount of water. Energy intake and energy expenditure, in the form of cellular metabolism and exercise, are precisely coupled over long time intervals in healthy adults resulting in stable body fat stores [WOODS et al., 2000]. The composition and amount of food that we eat varies from meal to meal and from day to day [SCHWARTZ et al., 2000; WOODS, 2004a]. Changes in food intake are more often due to changes in meal size rather than frequency [WOODS et al., 2000]. Satiation, i.e., the process that leads to meal termination, results from the coordinated interaction of neural and humoral signals that emanate from the gut in response to mechanical and chemical stimuli of ingested food (gastrointestinal signals, e.g. CCK, see below), and signals generated in proportion to body fat mass (adiposity signals, e.g. leptin and insulin, see below) [CUMMINGS et al., 2007; GALE et al., 2004; KENNEDY, 1953; SCHWARTZ et al., 2000; WOODS et al., 1998]. These signals cause changes in the neuronal activity in several brain areas, such as the nucleus of the solitary tract (NTS) in the hindbrain and different nuclei in the hypothalamus that control energy homeostasis (see Chap. 2.1.3) [SCHWARTZ et al., 2000; WOODS et al., 1998; WOODS et al., 2000].

Energy homeostasis is achieved when anabolic and catabolic effects are in balance over long periods of time (see Figure 2.1) [WOODS et al., 1998]. Short-term gastrointestinal signals that are acutely affected by ingested nutrients and that influence individual meals, and long-term adiposity hormones, such as leptin and insulin, contribute to the regulation of energy homeostasis [BEGLINGER et al., 2006; MORTON et al., 2006; SCHWARTZ et al., 2000].

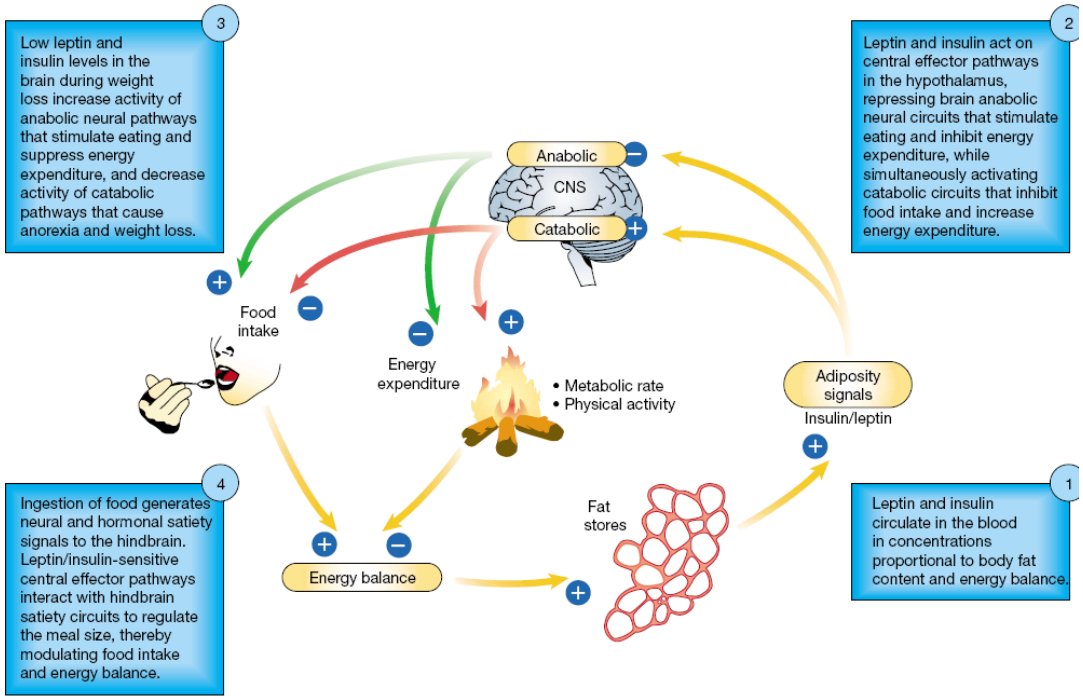

Figure 2.1: The general circuitry underlying the control of food intake and regulation of body adiposity.
[Source: [SCHWARTZ et al., 2000]]

Most of the gastrointestinal signals act through specific receptors on peripheral nerves (e.g. vagus nerve) connecting the GI tract with neurons in the NTS, an area of the caudal brain stem that integrates sensory information from the GI tract and abdominal viscera, as well as taste information from the oral cavity [SCHWARTZ et al., 2000]. Alternatively, gastrointestinal hormones may reach the hindbrain or other brain sites via the circulation [MORTON et al., 2006; WOODS, 2004a]. From the hindbrain, the principal central site for the control of meal size [CUMMINGS et al., 2007], afferent neural information then passes through the brainstem to the hypothalamus (see Figure 2.2), where several nuclei such as the arcuate nucleus (Arc), the paraventricular nucleus (PVN), the ventromedial nucleus (VMH), the dorsomedial nucleus (DMH), and the lateral hypothalamic area (LHA) are implicated in the control of eating (see below Chap. 2.1.3) [HOLST et al., 2004; SMITH et al., 2008; WOODS et al., 1998].

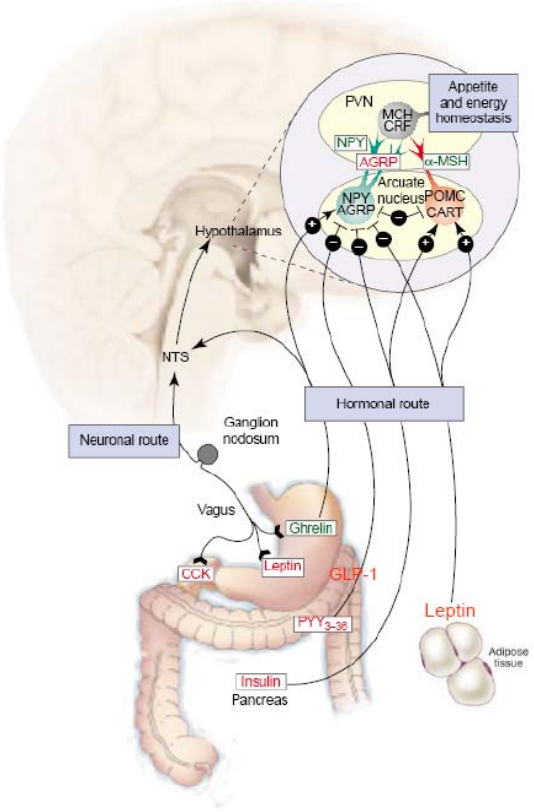

Figure 2.2: Hormonal and neural routes involved in regulation of appetite.
[Source: adapted from [HOLST et al., 2004]]

2.1.1 Gastrointestinal signals in the control of eating

The gastrointestinal (GI) tract is the body's largest endocrine organ and produces about 30 different peptidic hormones, which act on several tissues. GI peptides are released from enteroendocrine cells in response to ingested food, e.g. specific carbohydrates, fats or proteins, or the mixtures of these macronutrients, or through mechanical stimulation such as gastric distension (see Figure 2.3) [COLL et al., 2007; CUMMINGS et al., 2007; MORTON et al., 2006]. Different GI peptides are then secreted from multiple sites in the GI tract, including the stomach, pancreas,

proximal small intestine, distal small intestine and colon (see Figure 2.4) [CUMMINGS et al., 2007; WOODS, 2004a]. Cholecystokinin (CCK), glucagon-like peptide-1 and 2 (GLP-1, GLP-2), peptide tyrosine-tyrosine (PYY) and oxyntomodulin (OXM) [reviewed by [COLL et al., 2007; MENDIETA-ZERÓN et al., 2008; SMITH et al., 2008] are peptides which inhibit eating, whereas ghrelin is the only GI peptide that stimulates eating [CUMMINGS, 2006; HOLST et al., 2004; WREN et al., 2001].

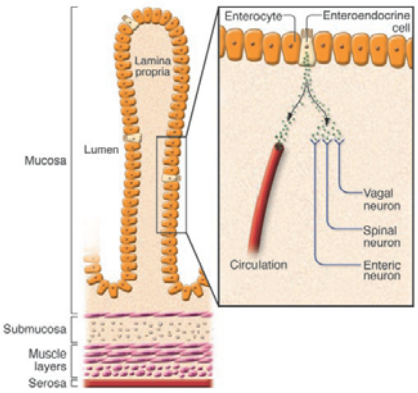

Figure 2.3: Topography of enteroendocrine cells and absorptive enterocytes on a villus within the intestinal wall.
[Source: CUMMINGS and OVERDUIN, 2007]

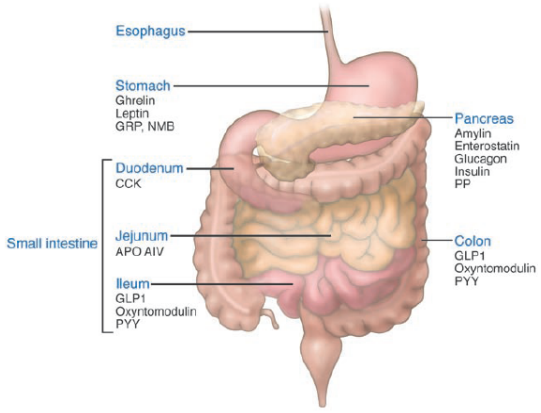

Figure 2.4: Principal sites of synthesis of GI peptides implicated in the control of FI.
[Source: CUMMINGS and OVERDUIN, 2007]

2.1.1.1 Cholecystokinin (CCK)

CCK is the first described and most studied GI peptide that acts as a postprandial satiation signal. It is secreted in response to digested foods, mainly lipids (especially long-chain free fatty acids) (reviewed by [BEGLINGER et al., 2004]) and proteins. CCK exists in several molecular forms, primarily CCK-8, CCK-33, CCK-39 and CCK-58 in rats. CCK is produced by I-cells in the duodenal and jejunal mucosa, as well as in the central nervous system (CCK-4) [COLL et al., 2007; CUMMINGS et al., 2007]. CCK peptides interact with two G-protein coupled receptors termed CCK_1 (formerly known as CCK-A, for 'alimentary') and CCK_2

(formerly known as CCK-B, for 'brain'). Both receptors are widely expressed in the central nervous system (CNS) and in the periphery (GI system). The key receptors for the reduction of FI, the CCK_1-receptors, are expressed on sensory fibers of the vagus nerve innervating the tissue around the pyloric sphincter and the proximal duodenum. The CCK signal carried in the vagus nerve enters the hindbrain and reaches the NTS (reviewed by [CUMMINGS et al., 2007; MENDIETA-ZERÓN et al., 2008]). The physiological relevance of CCK's satiating effect has been confirmed in humans, in whom the carboxy-terminal octapeptide CCK-8 reduces FI and meal duration [BEGLINGER et al., 2004]. CCK is considered as a short-acting satiation signal because its anorectic effect is short-lived and undetectable if the peptide is administered more than 15 min prior to the start of a meal. By increasing doses of CCK a greater decrease in FI is obtained [GIBBS et al., 1973]. CCK also slows down gastric emptying, thereby prolonging postprandial gastric distension (reviewed by [BEGLINGER et al., 2004]).

2.1.1.2 Glucagon-like peptide-1 (GLP-1)

GLP-1 is a peptide product of the gene encoding preproglucagon which is widely expressed in the gut, pancreas and NTS [BEGLINGER et al., 2006; COLL et al., 2007]. It is synthesized in two major molecular forms, as GLP-1(7-36)amide (the most common circulating form) and as GLP-1(7-37)amide (reviewed by [DRUCKER, 2006; GUTZWILLER et al., 2004; MENDIETA-ZERÓN et al., 2008]). GLP-1 is released primarily by L-cells in the distal small intestine and colon, where it co localizes with OXM, which is also produced from the preproglucagon gene in the intestine and brain, and PYY (see below) [BEGLINGER et al., 2006; COLL et al., 2007; CUMMINGS et al., 2007; SMALL et al., 2004]. Ingested nutrients, especially free fatty acids (FFA) and carbohydrates, stimulate GLP-1 secretion rapidly within minutes by indirect, duodenally activated neurohumoral mechanisms, as well as by direct contact within the L-cells of the distal intestine, which is

temporally delayed [BRUBAKER, 2006]. The release of GLP-1 initiates a decrease in FI and an inhibition of gastric emptying, and it enhances the glucose-dependent insulin release from the pancreatic B cells (insulinotropic effect). GLP-1 also enhances insulin biosynthesis, thereby replenishing insulin stores, and lowers glucose via inhibition of glucagon secretion from pancreatic islet α cells (reviewed by [BRUBAKER, 2006; CUMMINGS et al., 2007; DRUCKER, 2006]). These pleiotropic and clinically relevant actions of GLP-1 have spurred the development of GLP-1 receptor agonists (e.g. exendin-4), or agents that reduce GLP-1 degradation (e.g. dipeptidyl peptidase-4 (DPP-4) inhibitors) that are promising therapeutics for the treatment of T2DM [DRUCKER, 2006]. Many studies in rodent models of diabetes as well as in patients with T2DM have demonstrated that GLP-1 receptor (GLP-1R) agonists and DPP-4 inhibitors lead to significant reductions in glycemia and HbA1c levels (reviewed by [BRUBAKER, 2006]). The effect of GLP-1 on eating may be mediated via a heptahelical G-protein-coupled GLP-1R) expressed in hypothalamus, brainstem and periphery (pancreatic islets, lung, stomach and duodenum). GLP-1R activation leads to increases in intracellular Ca^{2+} and is coupled to activation of cyclic adenosine 3´,5´-monophosphate/protein kinase A (cAMP/PKA)-dependent signaling as well as activation of PKC, phospatidylinositol-3 kinase (PI-3K) and MAPK signaling pathways (reviewed by [BAGGIO et al., 2007; BEGLINGER et al., 2006; BRUBAKER, 2006]).

2.1.1.3 Peptide tyrosine-tyrosine (PYY)

Peptide PYY exists in two main forms, PYY_{1-36} and the active anorectic form PYY_{3-36}, and is a member of the pancreatic polypeptide family that also includes pancreatic polypeptide (PP; a pancreatic satiation peptide) and neuropeptide Y (NPY; a orexigenic hypothalamic neuropeptide) [CUMMINGS et al., 2007; SMITH et al., 2008]. PYY is mainly produced by the same cells in the distal-intestinal cells (ileum, colon and rectum) that secrete GLP-1, and its secretion is correlated with

caloric intake, with larger release after ingestion of larger meals. Fat is the strongest macronutrient stimulus for PYY release, followed by carbohydrates (reviewed by [CUMMINGS et al., 2007; MENDIETA-ZERÓN et al., 2008; SMALL et al., 2004]). Receptors that mediate the effects of PYY belong to the NPY receptor family and include the Y1, Y2, Y4, Y5, and Y6 receptors [BEGLINGER et al., 2006]. PYY_{1-36} binds Y1R, Y2R, Y4R and Y5R while PYY_{3-36} binds with high affinity to the arcuate Y2R, and with lower affinity to the Y1R and Y5R [SMITH et al., 2008]. Systemic PYY crosses the blood-brain barrier (BBB) and probably exerts its activation via the Y2R in the hypothalamic Arc. In the hypothalamus, the Y2R is a presynaptic autoinhibitory receptor on orexigenic neurons that express both NPY and agouti-related protein (AgRP). Inhibition of these AgRP/NPY neurons through Y2R leads to a disinhibition of adjacent anorectic pro-opiomelanocortin (POMC) neurons, which are inhibited by AgRP/NPY neurons. PYY therefore inhibits eating [BATTERHAM et al., 2002]. Peripheral administration of PYY_{3-36} has been shown to delay gastric emptying [MORAN et al., 2005] and secretion, and it decreases FI and weight gain in rodents, primates and humans. The appetite inhibitory effect was also seen with a Y2R-specific agonist and was absent in the Y2R-deficient mouse [BATTERHAM et al., 2002; MORAN et al., 2005]. However, central administration of either PYY_{1-36} or PYY_{3-36} potently increases FI [HAGAN, 2002].

2.1.1.4 Apolipoprotein A-IV (apo A-IV)

Apo A-IV is a circulating glycoprotein (molecular weight of 46-kDa) secreted primarily by the small intestine in humans and rodents, in which small amounts of apo A-IV are also secreted from the liver. In the intestine, apo A-IV is released in association with chylomicrons during fat absorption. It is used to package digested lipids for their transit through the lymphatics to the blood (reviewed by [CUMMINGS et al., 2007; GOTOH et al., 2006; TSO et al., 2004]). Apo A-IV is also synthesized in the hypothalamus, with the Arc having a higher content of apo A-IV

relative to other areas of the CNS [LIU et al., 2001; SHEN et al., 2008; TSO et al., 2004]. It has been demonstrated that the level of apo A-IV messenger RNA (mRNA) in the hypothalamus is influenced by an animal's nutritional status. Fasting causes a marked reduction in apo A-IV gene expression in both, the hypothalamus and jejunum. However, lipid re-feeding rapidly restores hypothalamic apo A-IV mRNA levels to the levels observed in ad libitum (ad lib) fed animals [LIU et al., 2001; SHEN et al., 2008; TSO et al., 2004]. Systemic or intracerebroventricular (ICV) administration of apo A-IV significantly inhibits food intake and body weight of rats in a dose-dependent manner [FUJIMOTO et al., 1993], whereas apo A-IV-specific antibodies (goat anti-rat apo A-IV serum), infused into the third cerebral ventricle, elicit eating in rats [FUJIMOTO et al., 1993]. It has been demonstrated that central apo A-IV reduces FI by potentiating the anorectic effect of central melanocortin (MC) agonists by acting downstream of the Arc, and that there is a synergism between apo A-IV and MC type 3 and 4 receptor, (MC3/4-R) signaling that causes anorexia [GOTOH et al., 2006]. Because both, intestinal and hypothalamic apo A-IV are regulated by fat absorption but not by carbohydrates, apo A-IV is hypothesized to represent a link between short- and long-term regulation of lipid-related energy balance (EB) [reviewed by [TSO et al., 2001]]. Apo A-IV may also interact with other metabolic signals involved in the regulation of energy homeostasis such as leptin and insulin (see below), which contribute to the regulation of body adiposity [LIU et al., 2001].

2.1.1.5 Ghrelin

Ghrelin, an acylated 28 amino acid peptide, was first described in 1999 as the endogenous ligand of the growth hormone (GH) secretagogue receptor (GHS-R; 'ghrelin receptor'), which is expressed in the Arc and other hypothalamic and brain stem nuclei, as well as in peripheral tissues (reviewed by [COLL et al., 2007; CUMMINGS, 2006; MENDIETA-ZERÓN et al., 2008; SMALL et al., 2004]). Ghrelin

is produced and secreted primarily by the gut, in the gastric oxyntic cells (A/X cells) in the fundus of the stomach, as well as by proximal small intestinal cells (reviewed by [CUMMINGS, 2006; MENDIETA-ZERÓN et al., 2008]). Ghrelin is the only peripheral orexigenic hormone known to date (for review, see [CUMMINGS, 2006; GEARY, 2004]). Peripheral administration of ghrelin potentially increases FI in diverse species, including humans [TSCHOP et al., 2000; WREN et al., 2001]. Ghrelin also stimulates gastric acid secretion and motility and the release of GH (reviewed by [CUMMINGS, 2006; HELLSTROM et al., 2004; MENDIETA-ZERÓN et al., 2008]). Ghrelin is normally secreted prior to meals [CUMMINGS, 2006; HOLST et al., 2004; MENDIETA-ZERÓN et al., 2008], and its levels decrease during eating or when nutrients are infused into the stomach [SHIIYA et al., 2002] These findings suggest that plasma ghrelin reflects an acute feeding state and may also serve as an indicator of short-term EB [SHIIYA et al., 2002]. Chronic peripheral ghrelin administration leads to significant increases in cumulative FI and body weight (BW) gain, with the latter being mainly the result of increased fat deposition with some contribution by decreased energy expenditure [TSCHOP et al., 2000]. Beyond its proposed role in the short-term control of eating, ghrelin also appears to play a role in the long-term BW regulation. Interestingly, basal ghrelin levels are also decreased in obese humans and increased in weight loss [TSCHOP et al., 2001]. Furthermore it is reported that fasting plasma ghrelin concentration negatively correlates with percentage of body fat, and fasting insulin and leptin concentration [CUMMINGS, 2006; TSCHOP et al., 2001]. In addition to being produced in the stomach, ghrelin may also be produced in the brain, playing an important role in signaling hypothalamic Arc neurons, which co-express the potent orexigenic neuropeptides, NPY and AgRP (blocking the MC3 and MC4 receptors) [CUMMINGS, 2006; HOLST et al., 2004; TSCHOP et al., 2000]. Almost all Arc NPY/AgRP neurons express ghrelin receptors and respond to ghrelin by increasing their firing rate [CUMMINGS, 2006; MONDAL et al., 2005; NOGUEIRAS et al., 2008]. The anorectic pools of Arc neurons (POMC/CART (cocaine and

amphetamine-related transcript) do not posses ghrelin receptors [HOLST et al., 2004] (for effects of the NPY/AgRP activation see Chap. 2.1.3).

2.1.2 Adiposity signals in the control of eating and BW

Circulating signals generated in proportion to body fat stores (adiposity signals) influence FI and EE in a coordinated manner to keep body fat and, hence, body weight stable. This concept of 'lipostasis' was proposed by Gordon Kennedy [KENNEDY, 1953] about 50 years ago. The two best known long-acting adiposity signals are the pancreatic hormone insulin and the adipose tissue hormone leptin, both acting in the brain, with the hypothalamus being a critical CNS site for their catabolic effects. A change in the their plasma levels indicates a state of altered energy homeostasis and adiposity, and the brain responds by adjusting FI and EE to restore adipose tissue mass to a regulated level [BASKIN et al., 1999].

2.1.2.1 Leptin

Leptin, the obese (ob) gene product [ZHANG et al., 1994], is a cytokine-like, glycosylated protein, predominantly synthesized and secreted by adipose tissue. Lower levels of expression are also detected in the hypothalamus, pituitary, placenta, skeletal muscle, and gastric and mammary epithelia (reviewed by [GALE et al., 2004; SCHWARTZ et al., 2000]). Leptin is secreted in direct proportion to the amount of fat stored in the adipocytes. Thus, circulating leptin increases as an individual becomes more obese. However, obesity is often accompanied by 'leptin resistance', which presumably underlies the failure to regulate energy stores [TARTAGLIA et al., 1995]. Humans with a genetic lack of leptin are hyperphagic and severely obese and respond strongly to leptin administration [COLL et al., 2007].

The importance of leptin as an adiposity signal to the brain has been discovered in animal models, such as the *ob/ob* mice, which have a mutation in the ob gene rendering them unable to synthesize leptin [ZHANG et al., 1994]. Other animals have genetic mutations that comprise functioning of the leptin receptor (*db/db* mice (diabetes mutation) and fatty Zucker, *fa/fa* rats) [CHUA, JR. et al., 1996]. The phenotype of *db/db* mice and *fa/fa* rats, which includes severe, early onset obesity and extreme insulin resistance, is identical to that of *ob/ob* mice. Central administration of small amounts of leptin reverses these syndromes in *ob/ob* mice (for reviews see [WOODS et al., 2000]) without causing signs of illness [WOODS et al., 2001]. Leptin enters the CNS by a saturable, receptor-mediated transport across brain capillary endothelial cells. The leptin concentration of human cerebrospinal fluid therefore correlates directly with plasma concentrations [WOODS et al., 1998]. Numerous studies support the hypothesis that the activation of hypothalamic receptors [SCHWARTZ et al., 2000] is a major pathway for leptin's catabolic effects on EB.

Leptin inhibits Arc neurons containing (orexigenic) peptides, NPY and the MCR antagonist AgRP, whereas POMC/CART neurons are stimulated [COLL et al., 2007; WOODS et al., 2001]. This induces the synthesis of α-melanocyte stimulating hormone (α-MSH), which is cleaved from the POMC precursor molecule. It exerts its effect by binding to MC3R and MC4R in the PVN, which engages the MC circuitry that decreases FI and increases EE [SCHWARTZ et al., 2000]. Thus, leptin impacts the EB equation by decreasing FI and increasing EE, which in turn causes a decrease in BW.

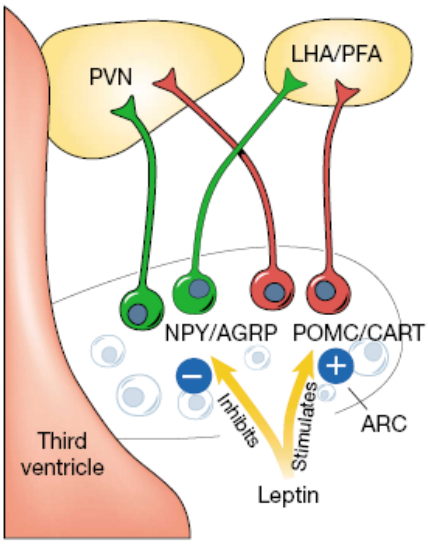

Figure 2.5: Control of food intake by the hypothalamic leptin-melanocortin pathway.
[Source: [SCHWARTZ et al., 2000]]

2.1.2.2 Insulin

Insulin is secreted from pancreatic β-cells in response to sensory stimuli (cephalic phase insulin release), GI peptides, and increases of glucose or certain amino acids. The basal plasma and cerebrospinal fluid (CSF) insulin levels are directly correlated with body adiposity [WOODS et al., 2001]. Obese individuals have higher basal and CSF insulin levels than lean individuals [WOODS et al., 2001]. As an adiposity signal, insulin crosses the BBB via a saturable, receptor-mediated transport mechanism that involves insulin receptors; they are highly expressed in the hypothalamic Arc cells that synthesize NPY and POMC [BASKIN et al., 1999; BENOIT et al., 2002; SCHWARTZ et al., 2000; WOODS et al., 1998]. Insulin acts through the same hypothalamic neuropeptide systems as leptin to control FI and to regulate BW [BENOIT et al., 2002]. Central administration (ICV) of exogenous insulin results in a dose-dependent decrease in FI [BENOIT et al., 2002] and BW [OBICI et al., 2002; WOODS et al., 2001], and conversely, the chronic central administration of insulin antibodies leads to increased FI and BW (reviewed by [BENOIT et al., 2002]). Consistent with this, a selective decrease in insulin receptor (IR) expression in a discrete region of the hypothalamus, generated by ICV infusion of antisense oligodeoxy-nucleotide (ODN) designed to blunt the expression of the IR protein in rat hypothalamic areas, results in a rapid and significant hyperphagia and rapid onset of hepatic insulin resistance [OBICI et al., 2002; WOODS et al., 1998].

According to the concept of the regulation of energy homeostasis by leptin and insulin, a negative EB (low insulin and leptin) results in a disinhibition of the anabolic pathway and an inhibition of the catabolic pathway, a condition that favors increased FI and energy storage. Conversely, during states of positive EB (high insulin and leptin) the opposite is observed, i.e., inhibited anabolic and disinhibited catabolic pathways. In this state, FI and the size of the adipose mass are reduced (see Figure 2.6; [WOODS et al., 1998]). Hence, insulin and leptin share many

common activities regarding the regulation of energy homeostasis, suggesting that both act mainly in the hypothalamic Arc to control caloric intake and expenditure [BASKIN et al., 1999; BENOIT et al., 2002].

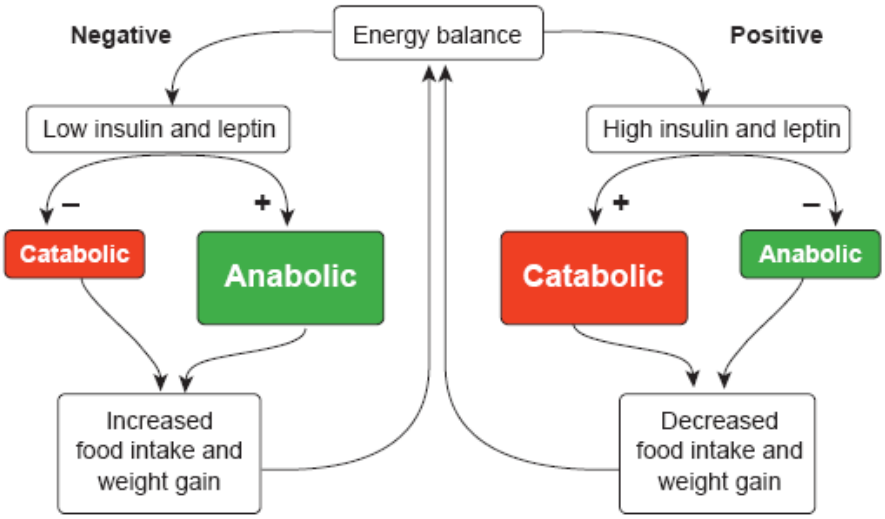

Figure 2.6: The general circuitry underlying the regulation of body weight. [Source: [WOODS et al., 1998]]

2.1.3 Integration of peripheral and central signals within the hypothalamic arcuate nucleus

Integration of peripheral and central anabolic and catabolic inputs within the hypothalamic Arc is believed to be central to the maintenance of EB [VAN DEN TOP et al., 2006; WOODS, 2004a]. Consistent with this, administration of leptin and insulin enhances the central sensitivity to input from short-acting peripheral satiation signals such as CCK, resulting in smaller meals that have the cumulative effect of reducing BW [BASKIN et al., 1999; MORTON et al., 2006; SCHWARTZ et al., 2000; WOODS, 2004a]. These findings suggest that hypothalamic pathways that are sensitive to leptin and insulin have anatomical connections with caudal brainstem neurons, e.g., with the NTS, which respond to meal-related signals and control meal size [BASKIN et al., 1999]. The site of integration of meal-related

signals with other signals that influence meal size begins within individual vagal afferent fibers and continues into the NTS in the hindbrain, where meal size is finally determined [WOODS, 2004a; WOODS, 2004b]. At the same time, the Arc continuously receives signals related to adiposity as well as information concerning ongoing meals from the hindbrain, and it also contains neurons that monitor ongoing metabolism directly (see Figure 2.7) [WOODS, 2004a]. Hence, the Arc contains multiple neuronal systems with different populations of cells, which are important in the regulation of energy homeostasis [WILLIAMS et al., 2001; WOODS et al., 1998].

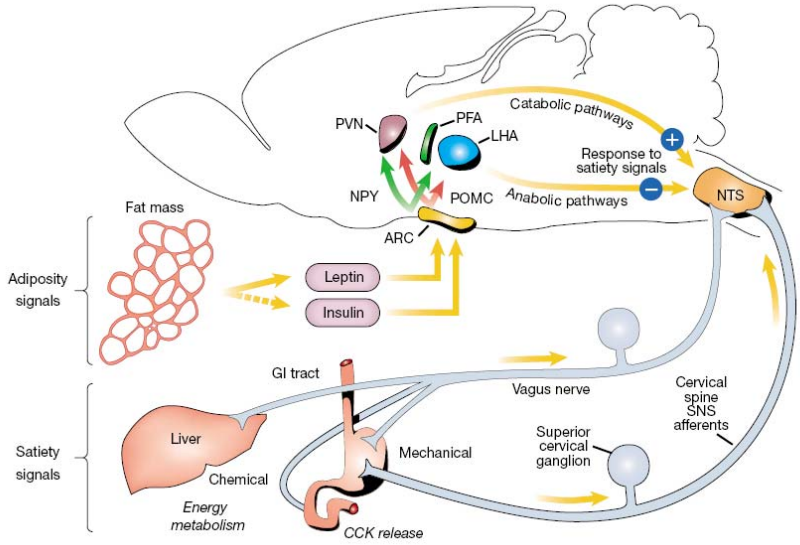

Figure 2.7: Neuroanatomical model of pathways by which the adiposity signals leptin and insulin interact with central autonomic circuits controlling meal size.
[Source: [SCHWARTZ et al., 2000]]

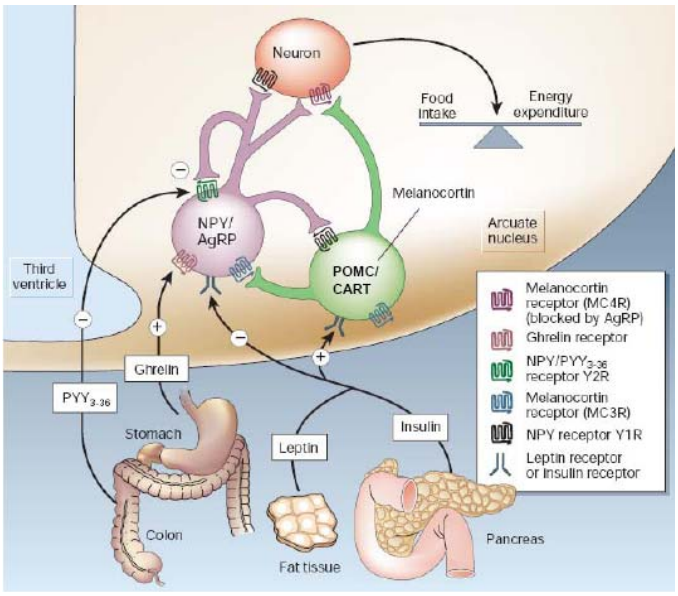

Figure 2.8: NPY/AgRP and POMC neurons act as an interconnected circuit.
[Source: modified from [SCHWARTZ et al., 2002]]

One of these cell populations contains two neuropeptides, i.e. NPY and AgRP, which are powerful stimulators of eating behavior in animals, whereas the other contains POMC, which is split into α-MSH; this then inhibits eating by acting on MC4R (see Figure 2.8; reviewed by [GALE et al., 2004; HELLSTROM et al., 2004; SCHWARTZ et al., 2000]).

Both subsets of neurons project to adjacent hypothalamic areas including the PVN, where neurons that reduce FI are concentrated (anorexigenic), and the LHA as well as the perifornical area (PFA), which contain neurons that stimulate FI (orexigenic) [MORTON et al., 2006; SCHWARTZ et al., 2000]. The PVN and LHA have direct descending connections to caudal brainstem centers that process food-related signals (see Figure 2.7; [BASKIN et al., 1999; SCHWARTZ et al., 2000]).

2.1.4 Metabolic signals in the control of eating

Metabolic signals generated by the supply and utilization of metabolic fuels influence food choice and how much food is consumed in the short-term. Metabolic signals also determine FI in the long-term and are important in maintaining EB over a nutritionally significant time interval [FRIEDMAN et al., 2005]. Hence, nutrients such as glucose, FA, and amino acids (AA) act as signaling molecules informing the CNS about the energy status of the organism [SANDOVAL et al., 2008].

2.1.4.1 Signals derived from glucose

In 1955 Mayer [MAYER, 1955] proposed that the CNS uses glucose as a signal to control FI ('glucostatic theory'). According to this theory, hypo- or hyperglycemia should induce changes in eating behavior (hunger or satiety). Consistent with the glucostatic theory, a brief pre-meal decline in blood glucose levels appears to contribute to meal initiation [CAMPFIELD et al., 2003]. Some evidence for a role of glucose in the control of FI has been provided by the use of specific glucose utilization inhibitors, in particular 2-deoxy-D-glucose. This glucose analog inhibits glucose metabolism and potently increases FI (reviewed by [SANDOVAL et al., 2008]). Stronger evidence for a regulatory role of glucose in eating is derived from studies in transgenic mice lacking the glucose-transporter-2 (GLUT-2). These GLUT-2-KO mice eat more than corresponding wild type mice and they show an increase in orexigenic and a decrease in anorexigenic neuropeptide expression in the hypothalamus [BADY et al., 2006]. In fact, there are several glucose-sensing neurons present in different regions of the brain, from the hindbrain to the hypothalamus (VMH, LHA), that increase or decrease their activity in response to glucose [LEVIN, 2006]. Together with peripheral glucose sensors, such as the taste buds and the vagal afferents in the hepatic portal vein [HEVENER et al., 2000], they form a network that monitors glucose availability. Interestingly, glucose influences the expression and turnover of anorexigenic POMC and orexigenic AgRP/NPY neurons in the Arc (see above) which presumably mediate the effects of glucose-sensing on eating. Indeed, POMC neurons are considered as glucose-excited cells, whereas NPY neurons belong to the glucose-inhibited cells [LEVIN, 2006; SANDOVAL et al., 2008]. In most of these neurons glucokinase, an enzyme that catalyses glucose phosphorylation, which is the rate limiting step in ATP production, appears to be the primary regulator of glucose-sensing [LEVIN, 2006]. Furthermore, these neurons also respond to peripheral hormones (insulin, leptin; see above) which inform the brain about metabolic status and body adiposity.

2.1.4.2 Signals derived from fatty acids

Circulating lipids such as TG, glycerol and LCFAs can also be sensed in the CNS and appear to be involved in the control of eating and hepatic glucose production. In the hypothalamus an energy 'surfeit' signal has been proposed to be generated by increased cellular LCFA-CoA pools, which activate neural pathways that in turn curtail FI and liver glucose production [LAM et al., 2005; MIGRENNE et al., 2007]. The physiological relevance and the exact molecular mechanism of this effect are still unclear; however, β-oxidation seems to play an important role, and FA metabolites such as malonyl- and acyl-CoA may relay their effects [LAM et al., 2005].

2.1.5 Control of food intake by fatty acid oxidation

In 1986 Scharrer and Langhans [SCHARRER et al., 1986] first demonstrated that an inhibition of peripheral fatty acid oxidation (FAO) by mercaptoacetate (MA) stimulates eating in rats fed a medium fat diet (18% fat), but not in rats fed a low fat diet (3.3% fat). MA inhibits FAO by interfering with the acyl-CoA dehydrogenases (EC 1.3.99.3) that catalyze the first step of β-oxidation in the mitochondrial matrix [BAUCHE et al., 1981]. These and other results suggest that FAO is involved in the control of FI when dietary fat levels are high [SCHARRER et al., 1986]. Furthermore, this eating-stimulatory effect of FAO inhibition seems to be signaled to the brain by vagal afferents. A role of vagal afferents was suggested early on (reviewed by [LEONHARDT et al., 2004]). More recently [BRANDT et al., 2007], the failure of MA to stimulate eating in rats after subdiaphragmatic vagal deafferentation, a procedure that surgically eliminates all vagal afferents while leaving about 50% of the efferents intact, convincingly demonstrated the necessity of vagal afferents for the eating-stimulatory effect of MA. Further support for a causal relationship between inhibition of fatty acid oxidation and stimulation of eating is derived from findings of an increase in food intake in response to

administration of other inhibitors of fatty acid oxidation. Thus, Friedman et al. [FRIEDMAN et al., 1986], showed an increase in FI in rats fed a HFD using the FAO inhibitor methyl palmoxirate (MP; methyl 2-tetradecylglycidate). MP reduces FAO by inhibiting carnitine O-palmitoyltransferase 1 (CPT-1; EC 2.3.1.21), the rate-limiting enzyme for the transport of long-chain FAs into the mitochondria [DECLERCQ et al., 1985]. Etomoxir, like MP, inhibits CPT-1 and FAO, and also stimulates FI in rats and in humans [HORN et al., 2004; KAHLER et al., 1999]. Moreover, etomoxir decreased plasma β-hydroxybutyrate in humans, indicating a decrease in hepatic FAO [KAHLER et al., 1999]. Both, MP and etomoxir also reduced hepatic energy status (ATP/ADP ratio) and phosphorylation potential [HORN et al., 2004]. In contrast to the strong eating-stimulatory effect of FAO inhibition, the evidence for an eating-inhibitory effect of FAO stimulation is inconsistent and weak. This discrepancy still needs to be explained.

Thupari et al. [THUPARI et al., 2002] showed that intraperitoneally (IP) injected C75 (α-methylene-γ-butyrolactone), a known inhibitor of fatty acid synthase (FAS; EC 2.3.1.85) [KUHAJDA et al., 2000], increases FAO in adipose tissue and liver in spite of high levels of malonyl-CoA, and also reduces FI [THUPARI et al., 2002]. The increased FAO and ATP levels, which might be due to increased CPT-1 activity, led to enhanced cellular energy turnover and decreased hepatic fat content (see Figure 2.9) [THUPARI et al., 2002]. This eating-inhibitory effect of IP C75 is not vagally mediated, because total subdiaphragmatic vagotomy or selective subdiaphragmatic vagal deafferentation failed to diminish it [MANSOURI et al., 2008a].

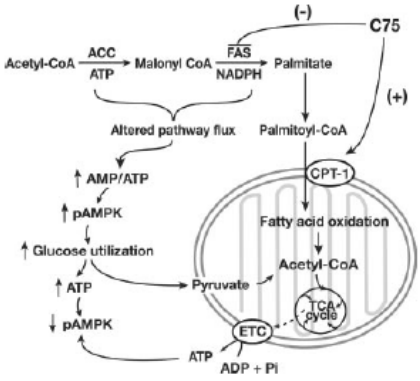

Figure 2.9: Model for C75 action on energy metabolism.
(Tricarboxylic acid cycle (TCA), electron transport chain (ETC), phosphorylated AMP-activated protein kinase (p-AMPK))
[Source: [LANDREE et al., 2004]]

2.2 Dietary fat in the digestive tract

The most important function of the digestive tract is the transformation of energy from ingested food into absorbable and usable sources of energy. This process is closely linked to the digestion and physicochemical transformation of macromolecular nutrients (carbohydrates, triglycerides (TG), proteins) to monomers (glucose, AA) or reconstituted aggregates (chylomicrones) and, moreover, to the transport of these substrates through the intestinal mucosal cells into the blood and the lymphatic system. Dietary fat consists mostly (approximately 90%) of TGs, and the remaining 10% consist of cholesterol esters, phospholipids, and plant sterols (reviewed by [BUHMAN et al., 2002; FRIEDMAN et al., 1980]).

2.2.1 Digestion and Absorption of dietary fat

Lipid digestion and absorption is a complex process that requires several enzymatic components to convert insoluble lipids (nonpolar) into water soluble and thus absorbable products [FRIEDMAN et al., 1980]. The absorption of TG by the intestine is very efficient because more than 95% of dietary TGs are absorbed [MANSBACH et al., 2007; ROS, 2000].

2.2.1.1 Digestion

Dietary fat digestion is initiated in the stomach, where lipids (mostly TG; see Chap. 2.2.2) are partially broken down to sn (stereospecific numbering)-1,2-diacylglycerol (DAG) and free FAs (FFAs) by lingual and gastric lipase, which accounts for 10-30% of dietary fat hydrolysis [FRIEDMAN et al., 1980; SHEN et al., 2001; SHI et al., 2004]. Subsequently, lipids are formed into large fat globules with hydrophobic TG cores surrounded by polar molecules resulting in an initial emulsion (chyme).

This emulsion is stabilized by cholesterol (CL; see Figure 2.10), phospholipids (PL; predominantly phosphatidylcholine (PC); see Figure 2.10), ionized proteins and limited amounts of FFAs from the hydrolysis of TG by gastric lipase. The emulsification of dietary fat is an important precondition for efficient hydrolysis by the pancreatic lipase (see below) (for review see [ROS, 2000; SHEN et al., 2001; SHI et al., 2004]). The digestive process is then completed in the lumen of the small intestine (luminal digestion), where the emulsion of fat globules is mixed with bile salts, molecules that have an amphipathic structure [FRIEDMAN et al., 1980] (BS; see Figure 2.10), and pancreatic juice, including the pancreatic lipase (EC 3.1.1.3), the principal lipolytic enzyme, and colipase, a cofactor of lipase activity [FRIEDMAN et al., 1980]. Pancreatic lipase acts only on the oil-water interface and breaks down TG at the position sn-1 and sn-3, leading to the formation of 2-MAG and FFAs. Colipase first attaches to the aqueous interface of TG to maximize exposure to the catalytic site of the pancreatic lipase, and subsequently lipase binds to colipase. Adequate concentrations of bile salts must be available for effective lipase activity and micellar solubilization [SHEN et al., 2001; SHIAU, 1981]. PLs are hydrolyzed by the pancreatic phospholipase A_2 ($pPLA_2$) (EC 3.1.1.4) at the sn-2 position, which generates lysophospholipids (e.g. lysophosphatidylcholine) and FFAs [SHEN et al., 2001; SHI et al., 2004]. Cholesteryl ester must be hydrolyzed first by the pancreatic esterase (EC3.1.1.13) before they can be absorbed as free CL [SHEN et al., 2001].

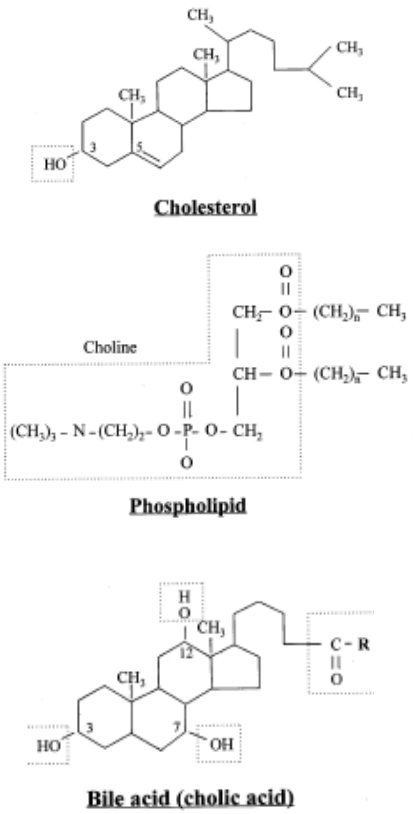

Figure 2.10: Chemical structure of cholesterol, phospholipid and bile acid. Their hydrophilic domains are shown inside broken lines.
[Source: [ROS, 2000]]

2.2.1.2 Absorption by enterocytes

After digestion, MAG, DAG, FFAs, lysophosphatidic acid (LPA), CL, fat-soluble vitamins and BS are assembled to mixed micelles, in which the polar groups project into the water phase, whereas the nonpolar hydrocarbons form the center, resulting in a high water solubility. These micelles are then absorbed by enterocytes via diffusion across the intestinal brush border membrane (see Figure 2.11a) (reviewed by [ROS, 2000; SHI et al., 2004; SHIAU, 1981]). Monomers of FFAs and MAG are also able to cross the microvillous membrane by diffusion and active transport, facilitated by transporters, such as intestinal fatty acid binding protein (IFABP), CD36 and FA-transport-protein-4 (FATP4) [MANSBACH et al., 2007; SHI et al., 2004; SHIAU, 1981]. Intracellularly, MAG and FFAs are then carried to the endoplasmic reticulum (ER), where they are sequentially re-esterified to TG. This process consists predominantly of the acylation from MAG to sn-1,2-DAG by MAG acyltransferase (MGAT), and the acylation from DAG to TG by diacylglycerol acyltranserase (DGAT) (see below, Chap. 2.2.2.2). LPA and CL are also acylated to phosphatic acid (PA) and CL ester, respectively, by 1-acylglycerol-3-phosphate acyltransferase (AGPAT) or acyl-CoA:cholesterol acyltransferase (ACAT), respectively. PA is then converted to TG (see Figure 2.11b) [SHEN et al., 2001; SHI et al., 2004].

2.2.1.3 Formation of intestinal chylomicrons

CMs are heterogeneous particles, which mainly transport dietary fat in the postprandial state. The CM formation begins in the ER lumen and terminates with the exit of mature CM from the Golgi complex. Newly synthesized TGs along with PLs, CL, and protein from LPs are incorporated into chylomicrons (CM) by a sequential multistep process [MANSBACH et al., 2007; SHI et al., 2004; SHIAU, 1981]. Apolipoprotein B48 (apo B48), synthesized by the rough ER (rER) and the microsomal TG transfer protein (MTP), are required for the CM assembly. ApoB48

forms stable complexes (dense particles) with PL, CL, and small amounts of TG, and is chaperoned by the MTP, it is merged in the smooth ER (sER) with a large light particle consisting of neutral lipids (TG and CL esters), and apo A-IV. The resulting lipid particles that consist of a core of TG and CL ester, coated by a monolayer of PLs, apo B48 and apo A-IV, buds then from the sER as a nascent protein transport vesicle. This prechylomicron transport vesicle (PCTV) is able to fuse with the Golgi complex, and further, delivers its content into the lumen. Within the Golgi lumen, apoprotein AI (apo AI) sticks to the prechylomicrons to create a mature CM. The mature CMs are then released from the Golgi complex into the intercellular space where they enter the circulation via the lymph system (see Figure 2.11). The blood transports the CM to other organs (e.g. liver, muscle and adipose tissue) where TG are released again from the CM to be used as a source of energy [HUSSAIN, 2000; MANSBACH et al., 2007].

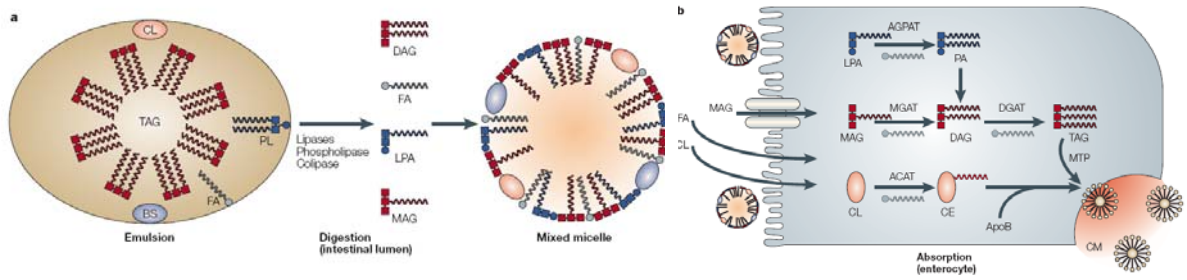

Figure 2.11: The process of dietary lipid digestion (a) and absorption (b).
[Source: [SHI et al., 2004]]

2.2.2 TG

Triglycerides (TGs) (also known as triacylglycerols; TAGs) are a heterogeneous group of hydrophobic, neutral lipids with a glycerol backbone. The glycerol is esterified with three fatty acids (FAs), which can differ in chain length (16, 18 and 20 carbons are the most common) and degree of unsaturation [FRIEDMAN et al., 1980; YEN et al., 2008].

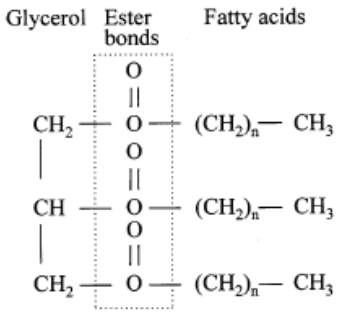

Figure 2.12: Chemical structure of a triglycerid.
[Source: [ROS, 2000]]

The primary sources of these FAs are the diet (see Chap. 2.2.1 for intestinal fat digestion and absorption) and *de novo* synthesis, secondary sources are the FA released from body stores and those generated by chain elongation and desaturation [LEHNER et al., 1996].

2.2.2.1 Biosynthesis of TG

All humans, animals, plants, bacteria and yeast are capable of synthesizing TG. In mammals, TGs are primarily synthesized and secreted in the liver and small intestine, while adipocytes predominantly store TGs and release FAs into plasma, where they form albumin-bound complexes [COLEMAN et al., 2004; FARESE, JR. et al., 2000]. Because of their hydrophobicity, TGs play a major role in dietary fat absorption and fat transportation. They are concentrated in cytosolic lipid droplets in cells or are found in the plasma incorporated into very-low-density lipoprotein (VLDL). TGs are also an essential component of milk [CASES et al., 2001; YEN et al., 2008; ZAMMIT, 1996]. The liver plays an important role in the regulation of TG synthesis and partitioning, between retention of TG in form of cytosolic lipid droplets and secretion. This, on the other hand, is of primary importance in determining the rate of VLDL production [OWEN et al., 1997].

In eukaryontes, TGs are quantitatively the most important energy storage form in muscle and adipose tissue, and they have a crucial function as source of essential and non-essential FAs and as a source of precursors for phospholipid biosynthesis (e.g. phosphatidylcholine) [COLEMAN et al., 2004]. But an excess accumulation of TG in adipocytes or a high level of TG in the bloodstream can be linked to many human diseases, such as obesity, T2DM, atherosclerosis, nonalcoholic steatohepatitis and pancreatitis. There is also an elevated risk of heart diseases and stroke [CASES et al., 2001; UNGER, 2002; YEN et al., 2008].

2.2.2.2 Pathways of TG synthesis

There are two major pathways of TG synthesis in mammalian tissues [CLARK et al., 1961]: 1) the glycerol phosphate or phosphatidic acid pathway, associated with the liver and adipose tissue, and 2) the monoacylglycerol (MAG) pathway, associated with the intestine [LEHNER et al., 1996]. In the glycerol phosphate pathway phosphatidate is formed by adding two fatty acyl CoAs to glycerol-3-phospate. Subsequently, a phosphate is removed from the phosphatidate, catalyzed by phosphatidate dephosphorylase, resulting in a diacylglycerol (DAG), which can then be joined to a fatty acyl CoA to form TG (see below, Figure 2.14). The monoacylglycerol pathway is considered as the main pathway for the TG biosynthesis, whereas the phosphatidic acid pathway, representing the *de novo* route to TG formation, accounts for only about 20-30% of formed TG [LEHNER et al., 1996]. Both pathways use fatty acyl-coenzymes A (FA CoAs) as acyl donors and glycerol (glycerol-3-phosphate and/or dihydroxyacetone phosphate (DHAP)) or 2-monoacylglycerol (2-MAG), respectively, as acyl acceptor, to produce DAG intermediates (see Figure 2.14). DAG and fatty acyl-CoA are then used to form TG, catalyzed by acyl-CoA:1,2-diacylglycerol O-acyltransferase (see below) (reviewed by [CHEN et al., 2000; FARESE, JR. et al., 2000; GRIGOR et al., 1982; LEHNER et al., 1996; YEN et al., 2008]). The rate of TG synthesis is dependent on the availability of the substrates, i.e., glycerol-3-phosphate precursors and long-chain FA, and the activities of the enzymes involved [MAYOREK et al., 1985].

2.2.2.3 Regulation of TG synthesis

The complex regulation of TG formation and hydrolysis involves transcriptional and post-transcriptional controls that respond to food-derived metabolites and specific hormones as well as exercise-mediated energy expenditure [COLEMAN et al., 2000].

Crucial lipogenic transcription factors, such as sterol regulatory-element-binding protein-1c (SREBP-1c), peroxisome proliferator-activated receptor γ (PPARγ), liver X receptors (LXR) and the nutritional and hormonal regulators insulin, carbohydrate, and FA (e.g. poly-unsaturated FA (PUFAs)), play an important role in the regulation. The regulation can differ greatly in various tissues, e.g., TG synthesis in liver and adipose tissues is unlike that in milk producing breast epithelial cells [COLEMAN et al., 2004].

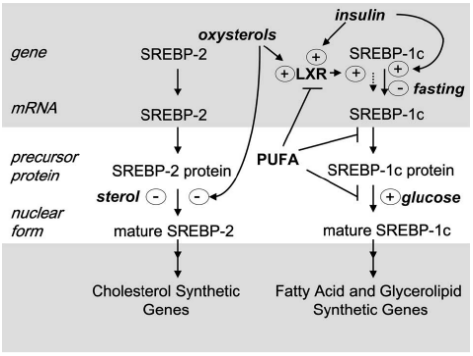

Figure 2.13: Regulation of lipogenic and TG genes by SREBP, LXR, PUFAs, glucose, and insulin. [Source: [COLEMAN et al., 2004]]

2.3 Enzymes of triglyceride synthesis

The sequential re-esterification of 2-MAG to TG in enterocytes has been suggested to be catalyzed by a 'TG synthetase complex'. This complex contains acyl-CoA:monoglyceride acyltransferase (MGAT), acyl-CoA:diacylglycerol acyl transferase (DGAT) and a FA activating enzyme for the initial enzymatic step, acyl-CoA synthetase (including acyl-CoA ligase and acyl-CoA acyltransferase) [LEHNER et al., 1995; RAO et al., 1966].

2.3.1 Diacylglycerol O-acyltransferase 1

Acyl-CoA:1, 2-diacylglycerol O-acyltransferase 1 (DGAT1; EC 2.3.1.20), an integral membrane protein, is the key enzyme in TG synthesis. It contains 6-12 transmembrane domains, which form a homotetramer [CASES et al., 1998; CHENG et al., 2001; LEHNER et al., 1996]. DGAT1 catalyzes the final and rate-limiting step [MAYOREK et al., 1989] in the glycerol phosphate and mono-acylglycerol pathway, in which sn-1,2-diacylglycerol (DAG) is covalently bound to

long chain FA CoA (see Figure 2.14 and Figure 2.15) [CHEN et al., 2000; COLEMAN et al., 2004; FARESE, JR. et al., 2000; YEN et al., 2008].

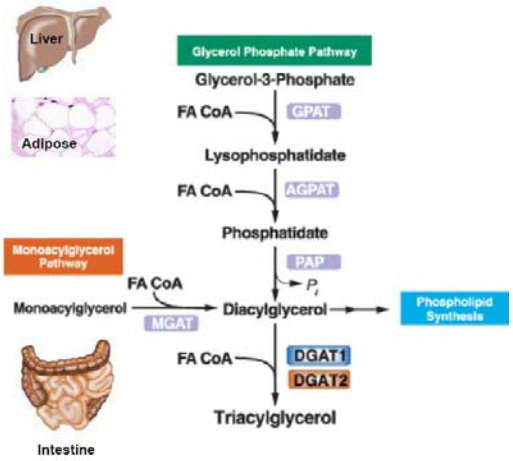

Figure 2.14: Triglyceride synthesis in the diacylglycerol acyltransferase reaction.
GPAT, glycerol-phosphate acyltransferase; AGPAT, acyl-glycerol-phosphate acyltransferase; PAP, phosphatidic acid phosphohydrolase; MGAT, acyl CoA: monoacylglycerol acyltransferase.
[Source: adapted from [YEN et al., 2008]]

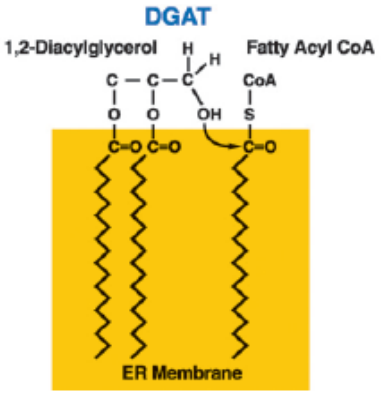

Figure 2.15: Formation of an ester linkage between fatty acyl CoA and 1,2-diacylglycerol to form TG.
This reaction is catalyzed by DGAT at the surface of the endoplasmic reticulum (ER).
[Source: [YEN et al., 2008]]

DGAT1 activity (first reported by [WEISS et al., 1960] has been localized predominantly to the cytosolic (‘overt’ activity) and luminal (‘latent’ activity) surface of the endoplasmic reticulum (ER) membrane in rat liver cells [ABO-HASHEMA et al., 1999; FARESE, JR. et al., 2000; OWEN et al., 1997; WATERMAN et al., 2002]. One model suggests that the overt DGAT activity catalyzes the synthesis of TG which are then incorporated into cytosolic lipid droplets (storage form), whereas the latent DGAT activity catalyzes the synthesis of TG-rich LP (e.g. nascent VLDL) for secretion. This model proposes that DAG freely crosses the ER membrane and that FA CoA moieties are transported by a carnitine acyltransferase through the ER membrane into the lumen (see Figure 2.16 and Figure 2.17) [FARESE, JR. et al., 2000; WATERMAN et al., 2002; YEN et al., 2008].

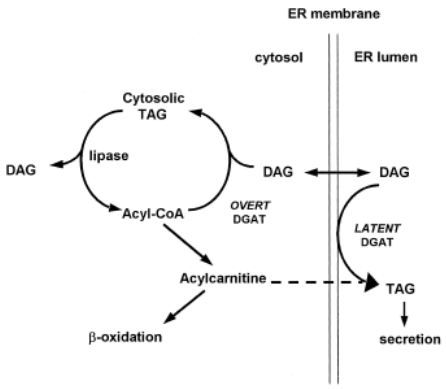

Figure 2.16: Metabolic scheme illustrating the suggested functions of the overt (cytosolic) and latent (luminal) DGAT enzymes in the ER by rat liver.
[Source: [WATERMAN et al., 2002]]

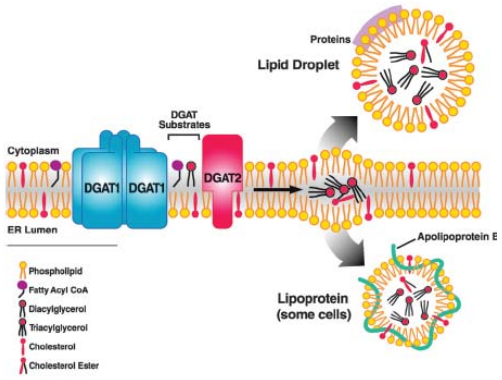

Figure 2.17: The role of DGAT enzymes in the synthesis and secretion of TG in the ER (a hypothetical model).
[Source: [YEN et al., 2008]]

Because of its essential role in TG synthesis, DGAT1 is involved in intestinal fat absorption, regulation of plasma TG concentration and lipoprotein (LP) assembly, as well as fat storage in adipose tissue, energy metabolism in muscle and lactation (reviewed by [CASES et al., 1998]). Although DGAT1 was originally identified as a TG synthesis enzyme, recent findings indicate that DGAT1 also catalyzes the formation of DAG, monoester and diester waxes, and retinyl esters (from retinol) *in vitro* [KALSCHEUER et al., 2003; LUNG et al., 2006; YEN et al., 2005].

2.3.1.1 Identification and cloning of a DGAT gene

In 1998, a mammalian cDNA encoding a DGAT (now known as DGAT1), which shares homology with sequences in the acyl CoA:cholesterol acyltransferase (ACAT; EC 2.3.1.26) C terminus, was identified and cloned by Cases *et al*.. In humans, the DGAT1 gene is located on chromosome 8 and encodes about 500 AA (calculated molecular mass (MM) ~55kDa) [CASES et al., 1998]. DGAT mRNA is widely expressed in mouse and human tissues, with the highest activity in tissues typically associated with TG synthesis. Particularly high levels occur in small intestine, liver, and skeletal muscle, but high DGAT mRNA expressions have also

been found in adipose tissue and mammary glands [CASES et al., 1998; FARESE, JR. et al., 2000]. In fungi and plants, DGAT is associated with the membrane and oil body fractions, mainly in oil seeds, where it contributes to the formation of storage lipids [LUNG et al., 2006].

2.3.1.2 Regulation of DGAT enzymes

In cultured hepatocytes (HepG2 hepatoma cells), DGAT1 mRNA levels are regulated by the MEK/ERK signaling pathway, showing a 2-fold increase due to inhibition of this signaling pathway (reviewed by [YEN et al., 2008]). DGAT1 gene expression in adipocytes is subject to transcriptional and posttranscriptional regulation, which was shown to be the principle mechanism. This is indicated by a marked increase in DGAT1 activity (~100-fold), DGAT1 protein (~90-fold) and mRNA level (~8-fold) in mature mouse 3T3-L1 adipocytes (a model for mammalian adipocytes) compared with preadipocytes [CASES et al., 1998; YU et al., 2002]. These findings indicate an upregulation of DGAT enzymes during adipogenesis and suggest the involvement of CCAAT (cytidine-cytidine-adenosine-adenosine-thymidine)-enhancer-binding protein α (C/EBPα) or PPARγ. C/EBPα and PPARγ are transcription factors that are involved in gene expression in adipogenesis (reviewed by [YEN et al., 2008]). Glucose also controls DGAT mRNA expression in 3T3-L1 adipocytes, showing an increased expression in response to glucose (25mM) [HIRATA et al., 2006; MEEGALLA et al., 2002]. Moreover, glucose administration also induces tumor necrosis factor α (TNF-α; a cytokine implicated in obesity-related insulin resistance) mRNA expression in these cells [HIRATA et al., 2006]. This suggests an important role of DGAT in the control of cytokine expression in visceral adipocytes. Therefore, an inhibition of DGAT1 leads to an inhibition of TNF-α gene expression [HIRATA et al., 2006]. Otherwise, when an improperly high level of mRNA is produced, (e.g. in Ad-hDGAT1-transduced cells), the rise in protein expression is curbed at the posttranscriptional level, in order to

maintain intracellular TG homeostasis. Consistent with these findings, it is also clear that the steady-state level of DGAT1 protein primarily determines DGAT1 activity, and that this protein level is crucially regulated by posttranscriptional mechanisms [YU et al., 2002]. Any changes, e.g., over expression of DGAT genes, actually seem to be linked to lipotoxicity, as demonstrated by an increased TG accumulation [CHEN et al., 2002d; MILLAR et al., 2006] and intramyocellular lipid increase [ROORDA et al., 2005], respectively, in insulin-sensitive tissues other than adipocytes (liver, skeletal muscle, and intestine) [CASASCHI et al., 2005; CHEN et al., 2002d; UNGER, 2002; YU et al., 2002]. These findings may point to a potential role of DGAT1 enzyme in the development of obesity, insulin resistance and T2DM [CASASCHI et al., 2005; YU et al., 2002]. Evidence for this association between insulin resistance and TG accumulation comes from insulin-resistant animal models [CASASCHI et al., 2005].

2.3.1.3 DGAT1 deficiency in mice

DGAT1-deficient ($DGAT^{-/-}$) mice have been generated to investigate the biological functions of the DGAT1 gene in energy and glucose metabolism, and in particular in TG synthesis [CHEN, 2006; SMITH et al., 2000]. $DGAT^{-/-}$ mice are viable and fertile, but their white adipose tissue (WAT), liver and muscle TG content are lower than in wild-type (WT) ($DGAT^{+/+}$) mice [BUHMAN et al., 2002; SMITH et al., 2000]. Also, $DGAT^{-/-}$ mice tend to have lower DAG levels in these tissues (liver, skeletal muscle) [CHEN, 2006]. Their adipocytes are protected from high-fat diet-induced hypertrophy compared to WT mice, whose fat cell size doubles in this situation [CHEN et al., 2002b]. DGAT1 deficiency also alters the FA composition of TG in adipose tissue and muscle, resulting in a relative increase in saturated FAs (C16:0 and C18:0) and a relative decrease in monounsaturated FAs (C16:1 and C18:1) [CHEN et al., 2002b]. Although this mechanism remains incompletely understood, it may reflect a kind of preference for unsaturated FAs in the DGAT1-mediated TG

synthesis. DGAT$^{-/-}$ females have a complete absence of lactation because DGAT deficiency also alters TG metabolism in the mammary glands, characterized by a lack in lipid droplets in epithelial cells [SMITH et al., 2000]. DGAT$^{-/-}$ mice show an increased sensitivity to insulin (for insulin, see Chap. 2.1.2.2) and leptin (for leptin, see Chap. 2.1.2.1). This enhanced insulin sensitivity can be ascribed to the increased glucose transport in skeletal muscle and adipose tissue [CHEN et al., 2002b; CHEN et al., 2004]. In addition, key molecules in the insulin signaling pathway, e.g., PKB (or Akt), PKC-λ and phosphatidylinositol-3 kinase, are increased. Otherwise, there is a decrease in serine phosphorylation of IR-substrate-1, a molecule involved in insulin resistance. These findings were observed in chow-fed DGAT1$^{+/+}$ mice transplanted with DGAT1$^{-/-}$ WAT [CHEN et al., 2004]. Moreover, the increase in insulin sensitivity is associated with a reduced TG content in liver and skeletal muscle as well as a decreased adipocyte size [CHEN et al., 2002b]. It has also been demonstrated that the effects of DGAT1 deficiency on glucose and energy metabolism only occur in the presence of leptin, as shown in leptin-resistant Agouti yellow ($A^y/_a$) mice and leptin-deficient (ob/ob) mice, respectively, two genetic models of insulin resistance and obesity [CHEN et al., 2002a]. But surprisingly, there is no change of the effect of ICV leptin infusion on food intake in energy balance in DGAT$^{-/-}$ mice, suggesting an enhanced leptin action directly in peripheral tissues and not in the hypothalamus [CHEN et al., 2002a]. DGAT$^{-/-}$ mice are also resistant to high-fat diet-induced obesity (DIO) (see Figure 2.18), accompanied by an increase in total EE, i.e., a ~20% higher metabolic rate compared with WT mice [BUHMAN et al., 2002; SMITH et al., 2000]. These mice also tend to have improved glucose disposal after a glucose load [SMITH et al., 2000]. Increased physical activity contributes to the elevated EE in DGAT deficiency, but alternative mechanisms mediating the increased EE are subjects of current studies

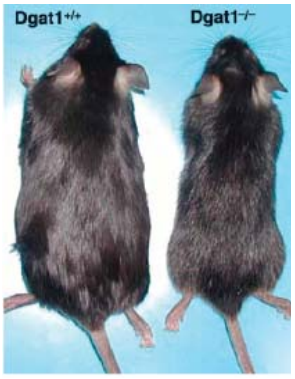

Figure 2.18: Phenotype of DGAT1 deficiency in mice. [Source:[YEN et al., 2008]]

(e.g. increased thermogenesis or β-oxidation of FA) [CHEN et al., 2000; SMITH et al., 2000]. In DGAT1$^{-/-}$ mice, brown adipose tissue (BAT) uncoupling protein 1 (UCP1) expression as well as WAT UCP3, PPARα, and acyl-CoA oxidase expression (genes involved in FAO) are increased, whereas the expression of PPARγ and FA synthase (genes involved in adipogenesis) are decreased. The leptin mRNA expression is also decreased by ~50 %. The reduced leptin levels are consistent with the observation that DGAT$^{-/-}$ mice have increased leptin sensitivity, which primarily affects EE without a comparable effect on FI [CHEN et al., 2002b]. To show the importance of WAT in endocrine functions, Chen et al. transplanted WAT from DGAT$^{-/-}$ mice into DGAT$^{+/+}$ recipient mice. As a result, obesity resistance, enhanced glucose disposal and increased activation of insulin signaling pathway were conferred to DGAT$^{+/+}$ recipient mice [CHEN et al., 2003; CHEN et al., 2004]. Furthermore, DGAT1 deficiency in adipocytes seems to increase the expression of adiponectin, an adipose tissue hormone that enhances FAO and insulin sensitivity and, hence, increases resistance to obesity [CHEN et al., 2003]. These findings demonstrate that the altered endocrine function of the DGAT-deficient WAT has a beneficial effect on systemic energy turnover and glucose metabolism.

Although DGAT$^{-/-}$ mice are unable to express a functional DGAT enzyme, they are still capable of synthesizing TG, resulting in similar fasting serum TG levels when compared to WT mice [CHEN et al., 2000; SMITH et al., 2000]. Furthermore, DGAT1 is not essential for dietary TG absorption or for CM synthesis. There is only a reduction in postabsorptive chylomicronemia in the cytoplasm of enterocytes, suggesting a reduced rate of TG absorption after a lipid load [BUHMAN et al., 2002]. All these findings indicate that alternative mechanisms must exist, and there are in fact at least two other enzymes, a second DGAT (DGAT2) and diacylglycerol transacylase, that contribute to TG synthesis in liver and intestine, and which may compensate for the absence of DGAT1 [BUHMAN et al., 2002].

2.3.2 DGAT2 – an isoform of DGAT1

The DGAT2 enzyme is an integral membrane protein in the ER bilayer (like DGAT1) which contains two transmembrane domains. Both, the N and C termini are exposed to the cytosol, i.e., most of the protein (~87%) faces the cytosol. This suggests that DGAT2 has its active site on the cytoplasmic side of the ER membrane and thus contributes only to the overt DGAT activity (cytosolic lipid droplet synthesis; see above Figure 2.16 and Figure 2.17) Furthermore, DGAT2 may be important in the initial TG synthesis [STONE et al., 2006].

The human DGAT2 gene is located on the chromosome 11 and encodes a protein of 350-400 AA (calculated MM ~40 to 44 kDa) [YEN et al., 2008]. In human tissues, two mRNA species (~1.8 and ~2.4 kilobases) are identified, and the highest DGAT2 expression levels are observed in liver and WAT. Lower levels are found in the mammary gland, testis and in the peripheral blood leukocytes. Surprisingly, DGAT2 expression is absent in the small intestine of humans, however, gene expression in mouse small intestine exists [CASES et al., 2001]. Because of its high expression in liver, DGAT2 is more likely to play an important role in the LP VLDL assembly of the de novo synthesized of FA from surplus of carbohydrates [MEEGALLA et al., 2002].

DGAT2-deficient mice were generated by Stone et al. to investigate the role of DGAT2 in TG synthesis and energy homeostasis [STONE et al., 2004]. In comparison to DAGT1$^{-/-}$, DGAT2-/- mice are smaller, and they die shortly after birth, because inactivation of DGAT2 leads to lethal abnormalities in energy homeostasis and skin functions (defective skin-barrier function, e.g. transepidermal water loss, and necrotic tail (arrow); see Figure 2.19).

Figure 2.19: Phenotype of DGAT2 deficiency in mice. [Source: [STONE et al., 2004]]

2.3.3 Inhibition of DGAT

Inhibition of DGAT2 expression in liver and adipose tissue of adult DIO and *ob/ob* mice has been achieved by using an optimized antisense oligonucleotide (ASO). This DGAT2 ASO treatment caused a noticeable reduction in hepatic TG content [CHOI et al., 2007; YU et al., 2005] and secretion rate; it also improved hepatic steatosis, possibly due to activation of hepatic FAO and inhibition of hepatic lipogenesis. There are also several naturally occurring compounds from fungal and plant extracts, e.g. xanthohumol (a natural product from *Humulus lupulus*) [TABATA et al., 1997], amidepsine A (produced by *Humicola sp.*) [TOMODA et al., 1995], roselipins (produced by *Gliocladium roseum*) (see Figure 2.20) [TOMODA et al., 1999], that can inhibit DGAT activity. Many other plant-derived inhibitors, e.g., taxifolin, polyacetylens, and tanshinone have been discovered by different groups (reviewed by [TOMODA et al., 2007]). Inhibition of DGAT by long-chain 2-bromooctanoate in cultured rat hepatocytes (first reported by [MAYOREK et al., 1985]) leads to an inhibition in TG synthesis in a dose-dependent manner, accompanied by accumulation of DAG but not by restriction of general neutral lipid synthesis. Betulinic acid (3β-hydroxy-lup -20(29)-en-28-oic acid (see Figure 2.21), a naturally pentacyclic triterpene) from *Alnus hirsuta* [CHUNG et al., 2006] and eicosapentaenoic acid (C20:5) are also reported to be potent inhibitors of DGAT in rat liver microsomes [BERGE et al., 1999; RUSTAN et al., 1988]. Studies on DGAT1$^{-/-}$ mice suggest that

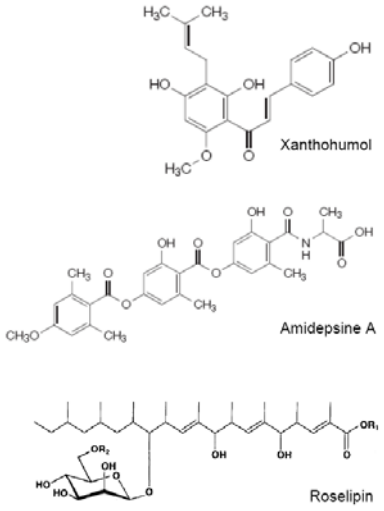

Figure 2.20: Chemical structure of Xanthohumol, Amidepsine A and Roselipin.
[Source: [SHI et al., 2004; TOMODA et al., 1999]]

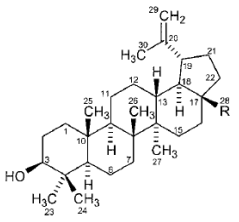

Figure 2.21: Chemical structure of Betulinic acid.
[Source: [KUMAR et al., 2008]]

pharmacological inhibition of DGAT1 may be a possible strategy for the treatment of obesity and T2DM, but further investigations need to address the selectivity toward the DGAT isoenzymes [CHEN et al., 2000; TOMODA et al., 2007].

This thesis focuses on a pharmacological inhibition of DGAT1, in particular on its possible effect on food intake and metabolism.

3 MATERIALS AND METHODS

3.1 Animals and housing

Ten male Sprague-Dawley (SD) rats (240-270 g BW) at the time of arrival) from Charles River (Sulzfeld, Germany) were caged individually in custom-made Macrolon plastic cages (44 x 20 x 36 cm) with stainless steel grid floors in a temperature controlled test room (22 ± 2°C) with a 12:12-h light-dark cycle (lights off at 10:00). All cages were fitted with appropriately sized plastic “sleeping tubes” where animals could rest. The animals were adapted to housing conditions for at least one week before gastric and jugular vein catheter surgery. Beginning two days before surgery, the animals were adapted to a 16 h deprivation 8h feeding schedule (food access from 10:00 to 18:00, i.e. during the first 8 h of the dark phase). At 18:00 food was taken out of the cage and the food intake (FI) of each animal was recorded daily. The BW and wellbeing of the animals were checked daily at the same time. Routine checks included observing that the animals were normally alert and active, had food and water and clean bedding. All procedures were approved by the Canton of Zurich Veterinary Office.

3.2 Surgery

After six days adaption to the housing conditions all animals were equipped with jugular vein catheters and with gastric catheters (see Chapter 3.2.4). The BW on the day of surgery (19.03.2008) was 270-300 g. After surgery animals were allowed to recover for 21 days before the first experiment (see Chapter 3.6.1).

3.2.1 Chronic Jugular vein (JV) catheter

3.2.1.1 Introduction

The method and volume of blood to be collected from laboratory animals depends on the animal species, frequency of collection, and experimental needs. Blood can be sampled for example by puncture of the ophthalmic venous plexus, puncture of the heart, cutting the tail or even by decapitation. With all these methods the animal has to be either anesthetized or handled and restrained. All these techniques may therefore induce stress, i.e., endocrine changes such as an elevation of circulating catecholamine and corticosteroid levels, which may change the target variable. To avoid these effects it is preferable to take blood samples from less disturbed animals through a previously implanted catheter. We therefore decided to equip all our rats with a jugular vein catheter according to a cannulation procedure described by Steffens [STEFFENS, 1969], with some modifications [FERRARI et al., 2005; REMIE et al., 1990].

3.2.1.2 Preparation of materials for cannulation

The jugular vein catheter consisted of silastic tubing (ID: 0.508mm, OD: 0.939 mm, length 10.5 cm; ID: 1.47 mm, OD: 2.159 mm, length 1.3 cm; Gore W.L., Newark, DE, USA), a 20 gauge (G) Vacutainer cannula as adapter (Becton-Dickinson, Basel, Switzerland) and a polypropylene surgical mesh (Bard, New Jersey, NY, USA) to improve adhesion to skin and fascia.

For the adapter the yellow tip of the cannula was broken off with a pincer and the end of the cannula was polished to obtain a smooth and round surface. The next step was to bend the cannula with a round pincer in an L-shaped form with an angle of more than 100°. The plastic Vacutainer hub was broken off in the same way as the tip and the end was polished, too. Afterwards the adapter was fit into one end of the 10.5 cm tubing (ID: 0.508 mm, OD: 0.939 mm). To be able to slide

the silicon tube over the adapter, the end of the tube was soaked in ether for some seconds to make it more stretchable. After the tube-adapter-construct was dried and shrunk again, a 1.3 cm piece of thicker tubing (ID: 1.47 mm, OD: 2.159 mm) which had been placed in ether before was fit over this end of the cannula as a reinforcement. After complete drying the adapter-tubing-construct was checked for possible leakage. A 1 ml syringe (Omnifix®, B.Braun, Melsungen, Germany) with a rounded 20 G-cannula was filled with ethanol and connected to the catheter with a short piece of PE-tubing (Tube PE-60; 0.76x1.22 mm; Smiths Medical, London, England). The system was considered tight when no ethanol leaked through the adapter tubing connection part. In a next step the catheter was fixed to a piece of non absorbable surgical mesh (2.2x6 cm) to facilitate adhesion to the skin and fascia. The mesh was folded into a square (2.2x3 cm) of two layers. The adapter piece of the catheter was led through a hole in the top fold of the mesh so that the catheter was positioned between the two layers of mesh. The adapter was then fixed to the mesh with cross stitches of a 3/0 silk thread (B.Braun, Melsungen, Germany) and all edges were rounded. Finally, the tightness of the catheter was checked again (see above).

With a rounded 20 G-needle two holes were made 0.5 mm distant to the end of the silastic tubing to ensure that the catheter would not attach to the wall of the atrium when aspirating blood. For the fixation of the catheter in the vein a small band of silicon was applied around the tubing, 3.8 mm away from the distal end. The liquid silicon (Silicone Adhesive, Cook Veterinary Products, Queensland, Australia) was applied using a 1 ml syringe and a polished 18 G-cannula in order to achieve a uniform circle. For this procedure the catheter was fixed on a small rack with the end of the tubing hanging down loosely. Finally the catheter was dried for one hour at 50°C. Before catheter implantation all catheters were gas sterilized with ethylene-oxid.

3.2.2 Chronic intragastric (IG) catheter

3.2.2.1 Preparation of materials for cannulation

The gastric catheter was assembled from silastic tubing (ID: 0.762 mm, OD: 1.651 mm, Gore W.L., Newark, DE, USA length 17 cm), with one end reinforced with another piece of silastic tubing (ID: 1.47 mm, OD: 1.95 mm, Gore W.L., Newark, DE, USA, length 1.3 cm), a 20 G Vacutainer cannula as adapter (Becton-Dickinson, Basel, Switzerland), and polypropylene surgical mesh (Bard, New Jersey, NY, USA). The adapter was made in a similar way as for the jugular vein catheter described above, except that the cannula was bend into a U-form (see figure) instead of an L-form and that three (instead of one) silicon bands were applied in different positions in order to help keep the catheter in place. The three silicon bands around the tubing were applied at 7 mm (small circle), 8 mm (medium size circle) and 4 cm (medium size circle) from the distal end. Also, we did not puncture holes into the end of the catheter because no fluids were aspirated.

3.2.3 Combined JV and IG catheter

A gastric catheter and a jugular vein catheter were assembled as described above. Both adapter-tubing constructs were fixed between two layers of non absorbable surgical mesh (2.2x3 cm). The adapter pieces protruded from the mesh in one line with a 7-10 mm distance between them. The adapter of the IG catheter was placed cranial of the IV catheter adapter and its tubing was directed caudally, whereas the tubing of the JV catheter was directed cranially.

3.2.4 JV and IG cannulation

3.2.4.1 Preoperative evaluation and preparation

Prior to surgery, each animal was examined for the presence of any clinical signs that could affect its ability to survive the anesthetic and surgical protocol. On the eve of the surgery food was removed from the first five rats (2-3 standard chow or high fat pellets were left in the cage overnight). The rats had ad lib access to tap water until one hour before surgery. Three hours prior to anesthesia all animals received a subcutaneous (SC) injection of 200 µl of the broad-spectrum antibiotics Borgal 24% (Intervet, Veterinaria AG, Zurich, Switzerland), diluted 1:6 with saline (NaCl 0.9%, B.Braun Medical AG, Sempach, Switzerland) for infection prophylaxis and food was removed from the remaining animals. Fifteen to 30 min prior to anesthesia the animals were pretreated with 100 µl/100g atropine SC [0.05mg/kg/day] (Sintetica S.A, Mendrisio, Switzerland), diluted with saline 1:10. Inhalation anesthesia was induced in an induction chamber (animals were adapted to the chamber) with 4-5 % isoflurane (Minrad Inc. USA, Provet AG) in oxygen 1000 ml/min (Pan Gas Dübendorf, Switzerland). When surgical tolerance was reached, anesthesia was maintained with 1-3 % isoflurane, oxygen and dinitrogenoxide, 300 ml/min each. Throughout surgery the depth of anesthesia was checked frequently by testing of reflexes (e.g., corneal reflex) and lack of response to stimuli (such as pinching a toe). The depth and frequency of breathing was also monitored.

The sites of surgery (the back from the lumbar region over the whole neck; the abdomen from the pubic bones to the sternum; the right ventral side of the neck from the right clavicle to the mandible) were shaved and disinfected with Braunol (Braunol®2000, B.Braun Medical AG, Emmenbrücke, Switzerland). The cornea of the animals was protected from drying out with an eye ointment (Vitamin A 15000 IE/g, Bausch&Lomb, Steinhausen, Switzerland), and the animals were kept on heating pads (39°C) throughout the surgery to prevent hypothermia. All

instruments and catheters were sterilized (autoclave and diethylene dioxid, respectively) and all surfaces in the surgery room were disinfected using 70 % ethanol.

3.2.4.2 Surgical Procedure

A 2.5 cm long median dorsal cutaneous incision was made just caudal to the interscapular area, and the positions for the JV and IG cannula access ports were marked rostral to the incision between the scapulae (Figure 3.1). Starting from the incision, straight hemostats were pushed in cranial direction through the subcutaneous connective tissue to the marked ports to generate the space for the double layer of polypropylene surgical mesh. The skin was then pierced with a bent 18 G needle for the two cannula ports (Figure 3.2).

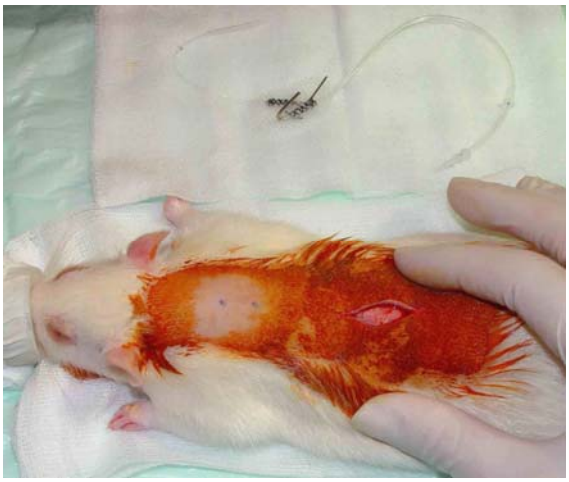

Figure 3.1: Cutaneous median dorsal incision caudal to the interscapular area.
Marking of the JV and IG cannula position between the scapulae where the cannula ports were exteriorized.

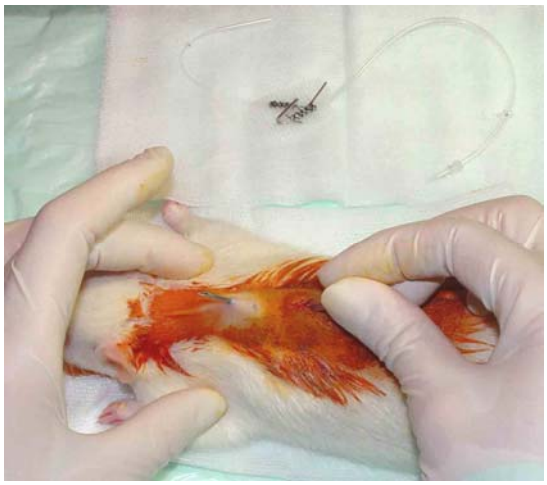

Figure 3.2: Perforation of the skin with a bent 18G needle to generate the catheter ports.

Next, a 2 cm ventral cervical skin incision was made right of the midline with its caudal end at the level of the clavicle (Figure 3.7). Small artery forceps were then pushed under the skin to generate a tunnel from the ventral cervical incision to the median dorsal cutaneous incision. The distal end of the JV cannula was then

grasped with forceps and led subcutaneously from the dorsal incision to the right clavicle by pulling the forceps back (Figure 3.3).

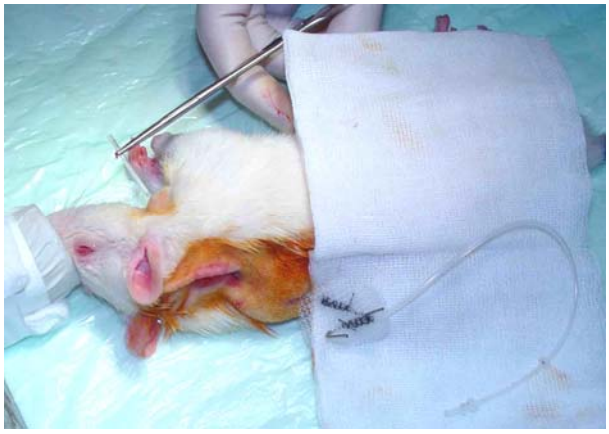

Figure 3.3: Subcutaneous tunneling of the JV cannula.

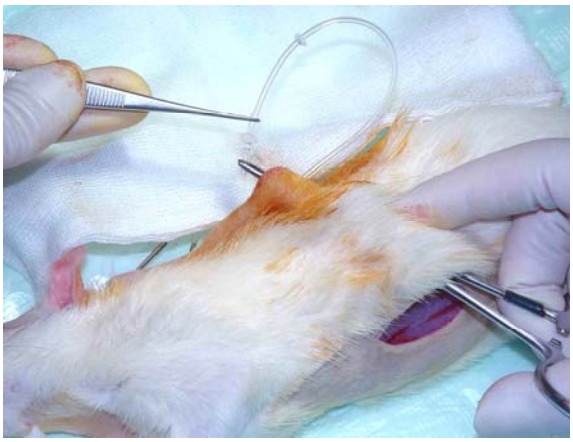

Figure 3.4: Subcutaneous tunneling of the IG cannula.

The folded mesh with the adapters was placed in the correct position under the skin so that the adapters of both the JV and IG cannulas protruded out of the puncture wounds. Each adapter was then connected via PE-tubing (0.76x1.22 mm) to a syringe containing saline (Figure 3.5). Afterwards, a 4 cm ventral midline skin incision was made using a scalpel from the level of the xiphoid cartilage with the caudal end at the level of the pubic bones. The IG cannula was then led through a lateral subcutaneous tunnel from the median dorsal incision to the abdominal skin incision on the left side of the rat (Figure 3.4). Subsequently, the dorsal incision was closed with a 3/0 absorbable Vicryl thread by surgeon's knots (4-5) (Figure 3.6).

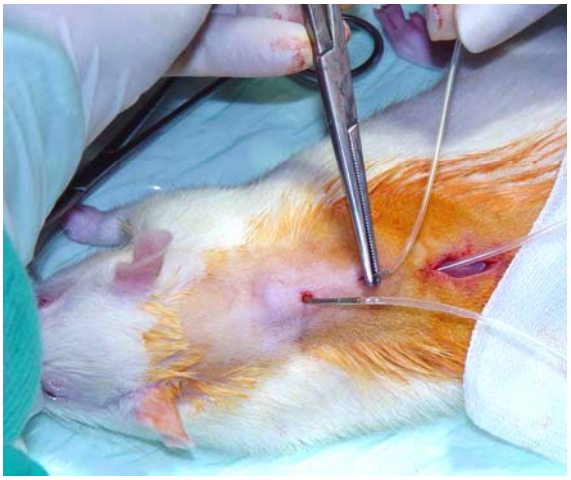

Figure 3.5: Connection of the IG and JV port with PE-tubing.

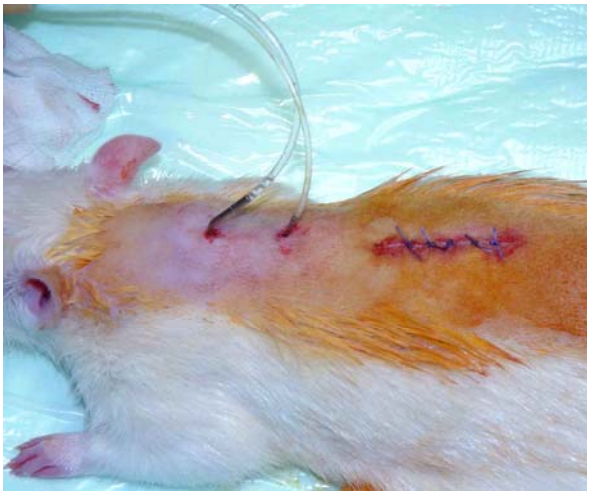

Figure 3.6: Suture of the dorsal incision.

The rat was then turned into a supine position with its head towards the surgeon and the 2 cm ventral cervical skin incision (see above) was draped with sterile gauze (5x5 cm; IVF, Neuhausen, Switzerland). Blunt forceps were used to push aside connective and adipose tissue to expose the division of the external jugular vein into the maxillary vein, and the linguofacial vein (Figure 3.8). At this point the largest vessel was chosen for cannulation and mobilized over a distance of about 5 mm. A loose ligature (3/0 silk thread) was placed caudally on the external jugular vein, and the maxillary vein as well as the linguofacial vein were ligated 3mm rostral from the bifurcation (3/0 silk thread) (B.Braun, Melsungen, Germany).

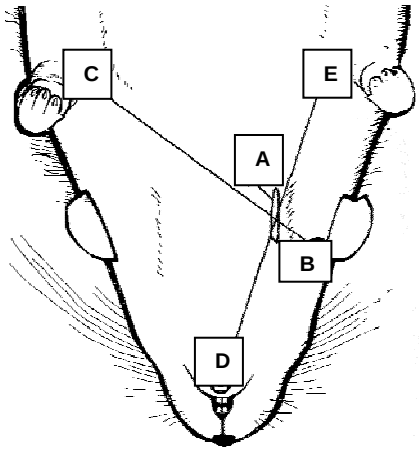

Figure 3.7: Place of incision.
Imaginary lines to determine the exact location of the jugular vein bifurcation.
(A) Incision, (B-C) line between the left arm pit and the right ear, (D-E) line between the right arm pit and the chin. [Source: adapted from [REMIE, 2000]].

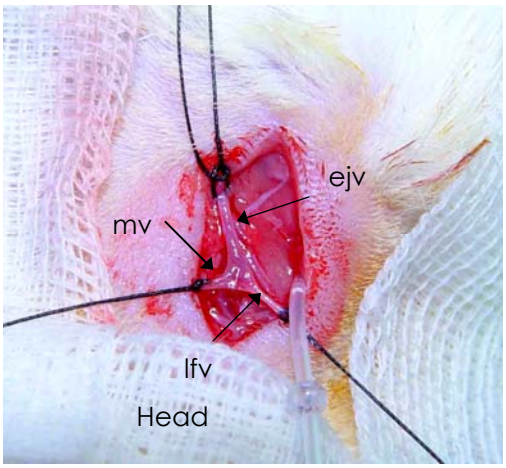

Figure 3.8: Dissection of the external jugular vein. View of the ventral surface of the rat's neck with the external jugular vein (ejv), the linguofacial vein (lfv), and the maxillary vein (mv).

With a 20 G needle the wall of the linguofacial vein was pierced 2 mm rostral to the bifurcation (Figure 3.9). The vessel was dilated by sharp-pointed jeweller's forceps to be able to insert the distal end of the sterile jugular vein catheter between the legs of the forceps (Figure 3.10). Prior to its insertion the catheter was flushed and filled with saline. The catheter was pushed gently into the vessel until the silicon band reached the point of perforation (Figure 3.11). Previous studies indicated that the end of the cannula was then located at the level of the right atrium. The catheter was secured in place by two ligatures. First the loose caudal ligature around the catheterized vessel was tied and the rostal ligature was used to anchor the cannula to the vessel. The two ligatures were cross tied with each other to ensure that the cannula could not move. Subsequently, the catheter was checked for patency by aspirating some blood and flushing with saline. The cervical skin incision was closed in two layers, using a continuous subcutaneous suture for the muscular layer and single knot skin suture with 5/0 and 3/0 absorbable Vicryl (Ethicon® 3/0, Johnson &Johnson, Spreitenbach, Switzerland).

The jugular vein catheter was finally filled with 100 µl heparinized polyvinylpyrrolidone (PVP; preparation see Chap.3.3.2) and the outer part of the cannula (3-4 cm PE-60 tubing (0.76x1.22 mm) was sealed with a stainless steel pin ("stopper"), which was made out of an obturated, blunt 20 G needle.

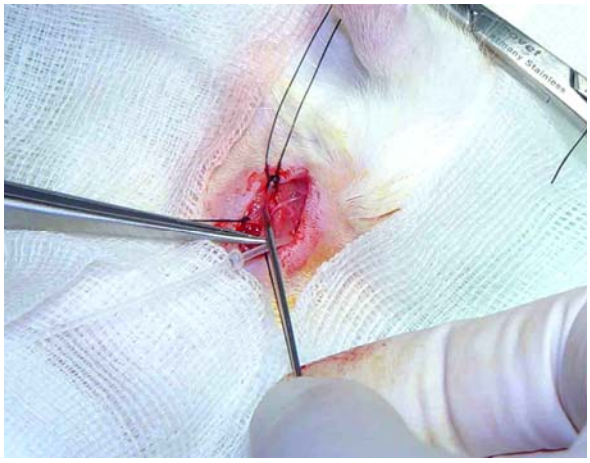

Figure 3.9: Piercing of the maxillary wall 2 mm rostral from the bifurcation with a 20 G needle.

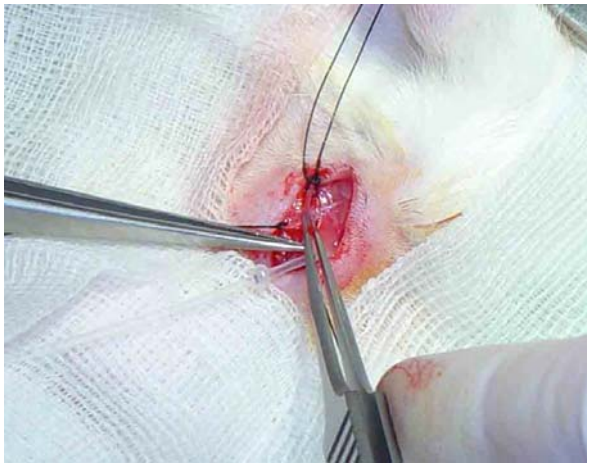

Figure 3.10: Dilation of the vessel with a sharp-pointed jeweller's forceps.

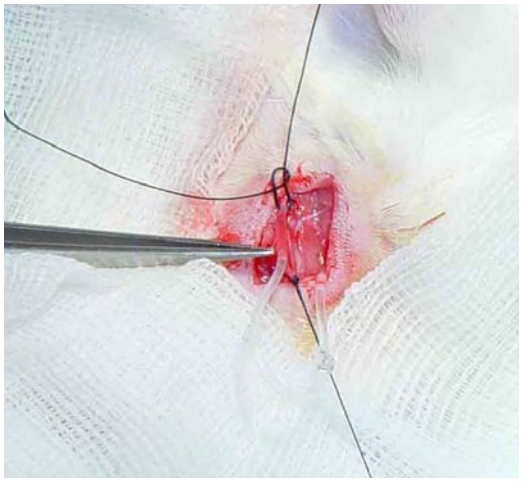

Figure 3.11: Insertion of the JV catheter into the vessel.

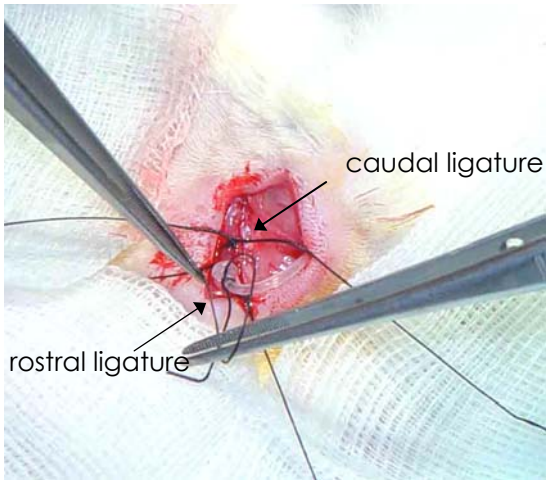

Figure 3.12: Fixation of the JV catheter to the vein.

After the JV catheter implantation the abdominal cavity was opened in the linea alba with a sharp-blunt pair of scissors. A hole was made through the abdominal muscle using a 18 G needle and the distal end of the IG cannula was led through it

until the third silicon circle (most proximal to the adapter part) was inside the abdominal cavity. The stomach was then partially exteriorized and held in place with cotton swabs (Novamed, St.Gallen, Switzerland) dampened with warm saline. A 3 mm diameter purse-string suture with a 4/0 non-absorbable silk (Johnson & Johnson, Spreitenbach, Switzerland), was loosely placed on the greater curvature (Figure 3.13). The center of the purse-string was punctured with an 18 G needle and the catheter was inserted until the first silicon band (small one, most distal) was inside the stomach and the second silicon band was outside the stomach wall (Figure 3.14).

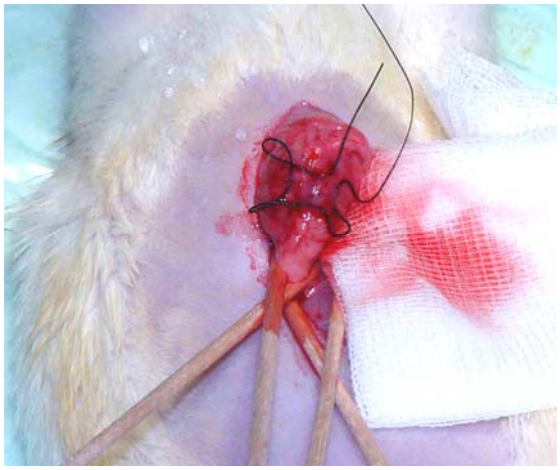

Figure 3.13: Placing a 3mm diameter purse-string suture on the greater curvature of the gastric corpus.

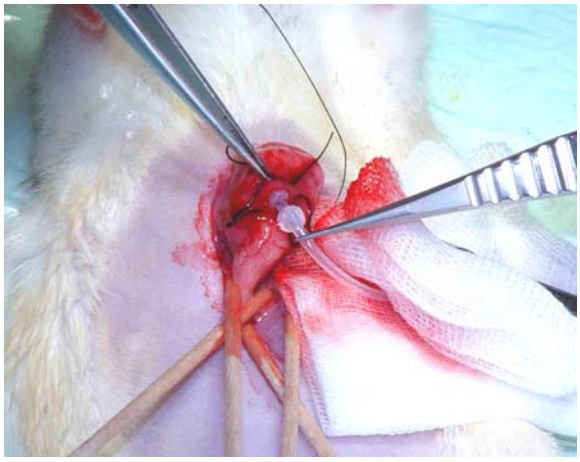

Figure 3.14: Insertion of the IG cannula into the stomach.

The purse-string was then tightened around the catheter and a 3/0 silk thread was placed rostal to the first silicon band and connected to the purse-string suture (Figure 3.15). In addition, the cannula was fixed to the abdominal wall using the third silicon band and non-absorbable 4/0 silk. The abdominal muscle layer was closed using an interrupted suture technique with 3/0 absorbable Vicryl, and the skin incision was then closed with an interrupted 5/0 absorbable Vicryl suture. Subsequently, the catheter was filled with sterile saline and the tubing was sealed with a stopper (Figure 3.16).

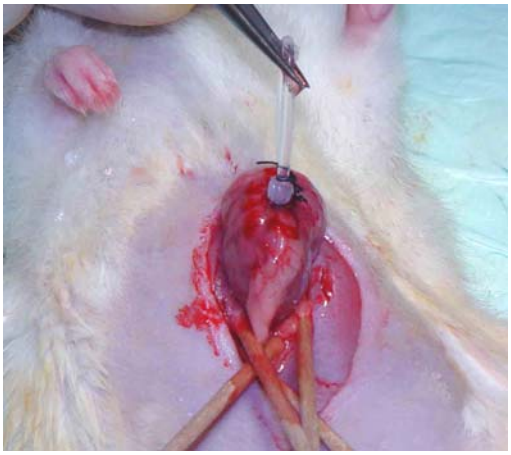

Figure 3.15: Fixation of the IG cannula on the stomach wall.

Figure 3.16: JV and IG catheter access ports.

3.2.4.3 Post-operative care

During immediate recovery from the anesthesia, all animals were closely monitored and single bedded in clean recovery cages under an infrared lamp to assure thermoneutrality and to prevent heat loss. One-two hours after surgery the animals received a SC injection of 100 µl/100 g of the analgesic carprofen (Rimadyl®, Pfizer AG, Zurich, Switzerland), diluted 1:10 with saline [5 mg/kg/day]. Normal husbandry practices were resumed after the animals had recovered from anesthesia and regained mobility. On the following day all rats received SC antibiotics (Borgal®, see above) and analgesics (Rimadyl®, see above), and two days after surgery only analgesics. During the first week after surgery the JV catheters were flushed regularly (see Chap.3.3.3). All sutures as well as the animals' wellbeing and BW (illustrated in Figure 3.17) were controlled daily, and all animals were allowed to recover for at least ten days before experiments began.

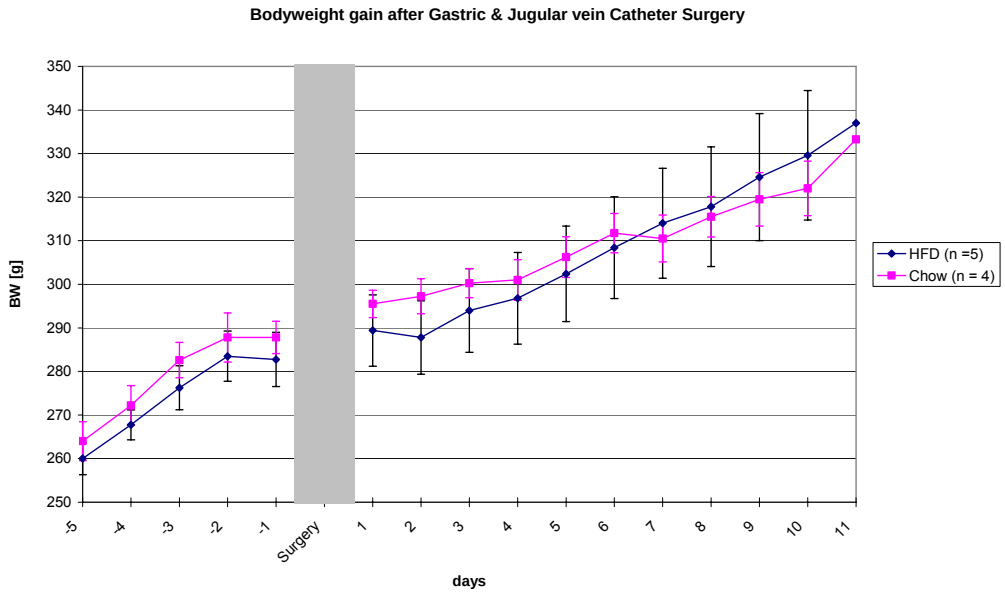

Figure 3.17: Body weight gain for rats after jugular vein and gastric cannulation fed ad libitum (i) HFD (ii) Standard Chow

3.3 JV and IG catheter maintenance

3.3.1 Preparation of materials for catheter maintenance

For catheter maintenance the following materials were needed: PE-tubing (PE-60, 0.76x1.22 mm, ~20 pieces, length: ~25 cm), syringe assemblies (1 and 10ml syringe attached to a 20G blunted cannula), custom-made “connectors” (made out of a 20 G Vacutainer cannula from which the yellow cap and the tip were broken off and the ends were polished), heparinized polyvinylpyrrolidone (PVP) as a catheter “lock” solution (see Chapter 3.3.2), sterile saline and 70% ethanol.

All PE-tubing was filled with 70% ethanol, and stoppers and connectors were left in ethanol for more than 20 minutes. The blunted 20 G cannula was autoclaved (1 bar, 50 minutes) before use.

3.3.2 Preparation of the catheter lock solution (heparinized PVP)

As mentioned above, heparinized polyvinylpyrrolidone (PVP-10; Sigma, St. Louis, USA) was used as a catheter lock solution for the JV catheter. Twenty-one g PVP (powder) was filled in a 50 ml Falcon tube and 12.0 ml 0.9 % NaCl was added. The tube was closed immediately and shaken vigorously for some minutes. Under light heating (<50°C) in a water bath and with frequent shaking the PVP was dissolved in saline until a homogeneous viscous solution was generated. This solution was aliquoted into three glass vials, loosely closed with a lid and autoclaved (1 bar, 50 min). The resulting highly viscous solution was then stored in the refrigaretor at 4°C. Before use the PVP solution was warmed (<37°C) and 1 ml Heparin (25000 IU/ml) (Heparin-Na (50000 IU/5ml), B.Braun) was added.

3.3.3 Flushing regime to maintain catheter patency

After successful intravenous catheter implantation, the amount of time that it remains patent sets limits to its use. Therefore, a maintenance program of regular flushing was necessary to allow for repeated blood sampling and infusions over longer periods of time. During the first week after surgery, JV and IG catheters were flushed daily, during the second week every second day and thereafter every third day. Before flushing the catheters, the PE-tubings, which were filled with 70 % ethanol before (see above) were rinsed with sterile saline. One ml syringes were then filled with sterile saline and attached to the 20 G blunted needles. Afterwards the syringe assemblies were connected to the PE tubing with a connector on one end, and each tube was rinsed thoroughly to remove all air inside. The PVP was prepared as described above and filled in 1ml syringes which were then also connected to PE-tubing. The JV catheter flushing procedure was as follows. First, the pin from the catheter was removed and put in 70 % ethanol. The syringe-tubing assembly was then connected to the access port of the catheter via the connector piece and the lock solution (PVP) and blood (~50 µl) were gently withdrawn and

discarded. If the first aspiration attempt failed, we tried to inject saline through the catheter. If this was successful, a second aspiration attempt was made with a clean syringe-tubing assembly. The catheter was then flushed with saline by short pull-push movements. Finally, the catheter was filled with 100 µl sterile heparinized PVP and the pin was replaced.
The IG catheter was rinsed with 1-2 ml sterile saline using a 10 ml filled syringe-tubing construction. No fluids were withdrawn and no heparinized PVP was added.

3.4 Blood collection procedures

3.4.1 Blood sampling via JV catheter

3.4.1.1 Preparation of materials

The preparations for blood sampling were similar to the preparations for catheter flushing (see Chapter 3.3.1), but the following additional materials were used: 1 ml syringes (Injekt®, B.Braun, Melsungen, Germany) which were attached to long 20 G blunted needles, 0.6 ml Eppendorf tubes, small glass tubes (Schmidlin Labor & Service AG, Neuheim, Switzerland) and EDTA (Titriplex 3, Merck, Art.1.08418.025) as an anticoagulant (100 mg dissolved in 1.0 ml distilled water). Seven µl EDTA suspension was put into Eppendorf tubes before blood sampling (7 µl/0.45 ml whole blood).

3.4.1.2 Blood sampling procedures

After flushing the catheters as described above (see Chapter 3.3.3), a small air bubble, about 2 mm long, was introduced into the catheter by briefly opening the connection between tubing and needle. This air bubble was then sent down the PE-tubing by gently infusing saline until it remained just inside the adapter part of the catheter. In this way the dead space was minimized because the air bubble separated the circulating blood from the infusion solution (saline). In the next step

100 µl blood was aspirated which was given back later with about 500 µl saline. The used syringe was then exchanged for a clean, dry 1ml syringe with a long 20 G blunted needle on top and 510 µl blood was aspirated of which 350 µl were transferred into an Eppendorf tube (containing 7 µl EDTA solution) for later analysis of plasma parameters. The remaining 160 µl blood was transferred into a small glass tube for later analysis of serum parameters. Finally, 100 µl sterile PVP mixed with 1ml saline (between 2 blood sampling time points) or sterile heparinized PVP (after the last blood sample) was added and the pin was replaced. The Eppendorf tubes were immediately put on wet ice and centrifuged (8 min, 8000 rpm, 4°C) within 20 min. The plasma was transferred into Cobas-Mira analyzer cups (Hoffmann La Roche, Basel) and stored at -20°C until analysis. The blood in the glass tubes was allowed to clot for 4-5 hours at room temperature (RT) and the serum was then transferred into Cobas-Mira analyzer cups. Serum was stored at 4°C until analysis, which took place on the same day.

3.4.2 Blood sampling via Cardiac puncture

This technique was used for collection of a one-time single, large-volume blood sample (10 – 15 ml) to be used as donor blood, i.e., to replace some of the blood volume of experimental rats after repetitive blood sampling. The cardiac puncture was done under terminal inhalation anesthesia with a mixture of isoflurane in oxygen-dinitrogenoxide. Anesthesia was induced as described above and after reaching surgical tolerance a small plastic barrel containing paper towel soaked in isoflurane anesthetic was placed over the rat's nose during the procedure to ensure prolonged anesthesia. The blood sample was taken from the heart, preferably from the right atrium after thoracotomy. The heart was punctured with a 21 G needle and blood was slowly withdrawn with a 10 ml syringe filled with 1.5 ml ACD solution (0.078 g Acidum citricum $1H_2O$, 0.22 g Natriumcitrat $2H_2O$ and 0.245 g glucose $1H_2O$ in 10 ml; Kantonsapotheke Zurich, Switzerland).

3.5 Experimental diets and drugs

3.5.1 Standard chow diet (see Appendix)

After arrival all animals (n=10) were adapted to standard laboratory chow diet (Extrudate 15 mm round; No. 3436, Provimi Kliba Nafag, Kaiseraugst, Switzerland) with a metabolizable energy content of 13.1MJ/kg. The diet contained, by weight, 4.5 % crude fat, 35.0 % starch, 18.5 % crude protein and 4.5 % crude fiber.

3.5.2 High fat diet (see Appendix)

One week after arrival, 5 rats were switched to a high fat diet (HFD: 60 % kcal %fat; Pellets 10 mm round; No. 2127, Provimi Kliba Nafag, Kaiseraugst, Switzerland) with a metabolizable energy content of 22.0 MJ/kg. The diet contained, by weight, 35.0 % crude fat, 1.0 % starch, 23.9 % crude protein and 4.9 % crude fiber. The ingredients were lard, casein, maltodextrin, sucrose, cellulose, refined soybean oil, minerals, vitamins and amino acids.

3.5.3 5 g HFD test meal including 9.1 ($^{w}/_{w}$) % C17:0

In the last experiment (Experiment 3; see Chapter 3.6.3), at dark onset all animals received a single 5 g HFD test meal (10:00) which contained 9.1 ($^{w}/_{w}$) % of the non-naturally-occurring FA C17:0 [454.5 mg C17:0/5 g HFD; Heptadecanoic acid (17:0), Fluka No. 51610, Sigma-Aldrich, Buchs, Switzerland]. This special experimental diet was self-made by mixing 5000 mg ground HFD with 500 mg C17:0 FA (solid) until a homogenous mixture was obtained, which was then pressed to 10-20 mm long round pellets.

3.5.4 Preparation of DGAT1i01 suspension

3.5.4.1 Vehicle preparation

Hydroxypropylmethylcellulose [0.5 g/100 ml] (HPMC $_{powder}$; Methocel E4M, Colorcon Limited, Kent, England) was dispersed under continuous stirring in a 100 ml Erlenmeyerkolben which was filled with ~30 ml hot (>80°C) milipore water. Thereafter, cold milipore water was added to the residual content. The mixture was then cooled down under continuous stirring using a magnetic stirrer. Tween 80 solution [0.1 g/100 ml] (Sigma-Aldrich, Steinheim, Germany) was added and the solution was stirred again until the Tween 80 solution was dissolved.

3.5.4.2 DGAT1-inhibitor (DGAT1i01) solution preparation

0.015 g [3 mg DGAT1i01$_{solid}$/5 ml Vehicle] or 0.045 g [9 mg DGAT1i01$_{solid}$/5 ml Vehicle] DGAT1i01 solid research sample (AstraZeneca, Cheshire, United Kingdom) were accurately weighed in a suitable vial (25 ml Erlenmeyerkolben). HPMC/Tween 80 solution (see above) was then added to 90 % of the required final volume (25 ml) and the suspension was stirred vigorously for some minutes using a magnetic stirrer. Afterwards, the magnetic stirrer was removed and the additional HPMC/Tween 80 solution was added to the final volume. The suspension was continuously stirred (with a magnetic stirrer) until the experiments started.

3.5.4.3 Handling instructions and stability

The suspension of DGAT1i01 was always prepared on the day before the experiments and the suspension was continuously stirred at ambient temperature overnight to ensure adequate particle size reduction. The suspension was physically stable for at least seven days when stored at room temperature, protected from light and stirred continuously. Chemical stability was not assessed, but no problems were expected there based on discussions with Physical

Chemistry Group of AstraZeneca. There were no anticipated stability problems at the pH of the suspension (pH 3.03 to 3.54) over a seven day period.

3.6 Experimental procedures

3.6.1 Experiment 1: Effect of an IG DGAT1i01 infusion on food intake in Chow- and HFD-fed rats (2 trials: 3 mg/kg and 9 mg/kg)

3.6.1.1 Experimental design

The acute eating-inhibitory effect of DGAT1i01 was tested in 9 male SD rats (weight range during tests, 338-441 g and 362-489 g, respectively) which were equipped with a JV and IG catheter (one rat died after surgery). Rats had continuous *ad libitum* access to tap water and were fed standard laboratory chow (n=5; No.3436, Provimi Kliba, Kaiseraugst, Switzerland) or a high fat diet (HFD) (n=5; No.2127, Provimi Kliba, Kaiseraugst, Switzerland) as indicated (see Chapter 3.5). All animals were adapted to an 8h feeding schedule (food access from 10:00 to 18:00) for 2 weeks (wk). During these 2 wk all rats were also adapted to the intragastric (IG) infusion procedure with 5 ml/kg BW saline and to FI measurements during the dark phase (procedure see below). The experiment was divided into two trials (a, b). In Experiment 1a, 3 mg/kg DGAT1i01 were IG administered (5 ml/kg) 1h before dark onset (09:00). This design was chosen based on previous demonstrations of the compound's eating-inhibitory potency by our collaborating group of AstraZeneca. Five days later in Experiment 1b we tested the effect of 9 mg/kg DGAT1i01 (5 ml/kg) under otherwise identical conditions. In both experiments the vehicle (HPMC/Tween 80 solution, 5 ml/kg)) was used as control. After IG DGAT1i01 or vehicle infusion the IG catheters were rinsed with 0.5 ml saline.

3.6.1.2 Food intake measurements

In Experiments 1a and 1b, cumulative food intake [g] was measured at 2, 4, 6, 8 and 9 h after infusion (i.e., at 11:00, 13:00, 15:00, 17:00 and 18:00). Before experiments, all food cups were filled with approximately the same amount of chow (47-55 g) or HFD (28-34 g). At each time point of food intake measurements the food cups were taken out of the cages, weighed (± 0.1 g) on an electronic balance (Mettler PM 3000, Mettler-Toledo AG, Greifensee, Switzerland) and returned to the cages immediately. In both parts of this experiment a within-subjects cross over design (in random order) was used with at least 1 d between cross over trials.

3.6.1.3 Statistical analysis

Food intakes at each time point were analyzed using a paired two-tailed Student t-test (GraphPad Prism version 5.00 for windows, GraphPad Software, Inc., La Jolla, CA, USA). Data are expressed as means ± SEM for n=4 (Standard Chow diet) and n=5 (HFD) animals, respectively. The minimal level of statistical significance was $p < 0.05$ throughout.

3.6.2 Experiment 2: Effect of an IG DGAT1i01 infusion on serum and plasma metabolites after a 5g HFD test meal (TG, Glyc, FFA, BHB)

3.6.2.1 Experimental design

Six weeks later the effect of IG DGAT1i01 infusion on serum and plasma metabolites was tested in the same 8 male SD rats (weight range during test, 462-642 g; one rat died during the flushing procedure) which were equipped with JV and IG catheters. All animals were adapted to HFD for at least 4 wk and furthermore adapted to the IG infusion procedure with 5 ml/kg BW saline for

several times. Four days prior to the experiment we changed the feeding schedule (food access from 10:00 to 18:00) as follows: A 5 g HFD test meal was offered at the beginning of the dark phase (10:00) and access to the HFD was reestablished 4 h later (14:00) until 18:00. DGAT1i01 (9 mg/kg BW) or vehicle (see above) was IG infused (5 ml/kg) 1h before dark onset (09:00) and the catheter was rinsed as described above. Blood samples were taken via the JV catheter (see Chapter 3.4.1.2) at 08:45 (shortly before IG infusion), 11:00 (2 h after IG infusion, 1 h after test meal), 12:00 (3 h after IG infusion, 2 h after test meal) and 14:00 (5 h after IG infusion, 4 h after test meal). Serum and plasma samples were prepared as described above and stored at -20°C until analysis, which was usually done on the same day. All animals received 1.5 ml donor blood (preparation see Chapter 3.4.2) after the last blood sampling at 14:00. The experiment was designed as a within-subjects cross over test with the treatments given in random order and with at least 2 days between trials.

3.6.2.2 Biochemical assays of serum and plasma metabolites

We determined serum triglycerides (TG), plasma glycerol (Glyc), free fatty acids (FFA) and β-Hydroxybutyrat (BHB), concentrations using standard colorimetric and enzymatic methods adapted for the Cobas MIRA® autoanalyzer (Hoffman LaRoche, Basel, Switzerland).

3.6.2.3 Data collection and statistical analysis

Serum and plasma parameters were analyzed with two-way repeated measures ANOVA (SAS 9.1, SAS Institute, Cary NC, USA) with subjects (animals) and drug treatment (DGAT1i01, vehicle) as factors and time points of blood sampling as repeated measures. Significant ANOVA effects were followed up by planned pairwise comparisons with the Bonferroni-Holm test [HOLM, 1978]. To identify outliers, data were converted to standard scores using the medians and median

absolute deviates x 1.48 (which estimates the standard deviation), and values > 2.57 (i.e., $P < 0.01$) were excluded. Differences were considered significant when $P < 0.05$. Graphs were generated using GraphPad Prism (GraphPad Prism version 5.00 for windows, GraphPad Software, Inc., La Jolla, CA, USA). Data are expressed as means ± SEM for n=8 and n=7, respectively.

3.6.3 Experiment 3: Effect of DGAT1i01 on fatty acid oxidation in small intestinal enterocytes after a 5g HFD+C17:0 test meal

3.6.3.1 Experimental design

The effect of IG DGAT1i01 infusion on fatty acid oxidation (FAO) in small intestinal enterocytes was tested in 16 male SD rats (8 rats from the previous experiment, weight range during experiment 467-645 g, and 8 additional rats (weight range during the experiment 548-600 g), which were housed and treated similarly). All animals were equipped with IG catheters and adapted to the IG infusion procedure with 5 ml/kg BW saline. Furthermore, all animals were adapted to the HFD for at least 3 weeks. Four days prior to the experiment we changed the feeding schedule (food access from 10:00 to 18:00) as in Experiment 2, i.e., a 5 g HFD test meal was offered at the beginning of the dark phase (10:00) after 16 h of food deprivation. At 14:00 food access to HFD was reestablished until 18:00. DGAT1i01 (9 mg/kg in 5 ml) or vehicle (5 ml/kg) (n=8, each) was administered IG 1h before dark onset (09:00) and the catheters were flushed as described. On the day of the Experiment a 5 g HFD test meal including 9.1 ($^{w}/_{w}$) % C17:0 (see Chapter 3.5.3) was offered to all animals simultaneously at the time of usual food access (dark onset). Two hours later (12:00), the first rat was sacrificed and tissue samples were taken out of the small intestine as described below. After 20 min the tissue sampling was finished and the next rat was prepared for sacrificing. The

experiment was designed as a random cross over test which was subdivided in 4 days (4 rats per day) within 2 weeks.

3.6.3.2 Tissue sampling and preparation – A scraping technique

(According to [DIETSCHY et al., 1965] modified)
Each animal was anesthetized with isoflurane and the abdominal cavity was opened. The first 30cm of the small intestine were excised and divided into 3 parts of about 10cm length, each. The 3 segments were immediately placed in ice-cold 0.9% saline and labeled (A = 0-10, B = 10-20, C = 20-30 cm; from proximal to distal). The bowel segments were then cut open longitudinally along the antimesenteric border and the intestinal contents were thoroughly removed from each segment by flushing with fresh ice-cold 0.9 % saline. Thereafter the segments were swabbed on a cellulose wadding swab (Cellodent®) to remove most of the saline, and were laid on a plastic Petri dish with the mucosal side up. The Petri dishes were kept on ice during the preparation. The mucosa was scraped off gently with the edge of a glass microscope slide, attention being paid to not taking along fat tissue and to leaving the denuded smooth muscle layer intact. The mucosal scrapings were homogenized with the glass slide on the Petri dish and 200 µl of the homogenate was pipetted into a chilled round bottom Eppendorf tube and subsequently stored at -80°C until fatty acid analysis by gas chromatography.

3.6.3.3 Lipid extraction from small intestine mucosa sample

Fatty acids were extracted from the small intestinal mucosa samples as described elsewhere ([FOLCH et al., 1957] and modified by Mansouri and Koss [MANSOURI et al., 2008b]. Briefly, the 200 µl sample was thawed at room temperature, mixed and homogenized in 1.0 ml methanol (Fluka No.65548, Sigma-Aldrich, Buchs, Switzerland) using the polytron (Kinematica AG, Littau, Switzerland. The mixture

was then transferred into a glass tube, which was degreased with hexan (Sigma-Aldrich, Buchs, Switzerland) and sealed with a Teflon screw cap. Thereafter, 2 ml of chloroform (Fluka No.25697, Sigma-Aldrich, Buchs, Switzerland) were added and the mixture was incubated overnight (>12 h) at 50°C under continuous shaking. Then the solution was washed with 3 ml of 0.9 % saline and centrifuged (1000 x *g*, 5 min) to separate the two phases (chloroform and water). The lipid-containing chloroform phase (lower) was then transferred into a new glass tube; special care was taken not to transfer water or cell debris.

3.6.3.4 Acid-catalyzed transesterification with methanol

(According to [LEWIS et al., 2000] modified)

The chloroform phase was further used and 3 ml of 10% $^{v}/_{v}$ sulfuric acid (Riedel-de-Haenen No.30723, Sigma-Aldrich, Buchs, Switzerland) in methanol (90 ml methanol+10 ml sulfuric acid) were added. The reaction mixture was then incubated at 50°C overnight in a tightly closed tube. On the next day the mixture was cooled down to room temperature and washed with a large volume of 2 M NaCl. After washing, the mixture was centrifuged again (1000 x *g*, 5 min) to recover the chloroform phase. The lipid-containing chloroform phase was then transferred again into a new glass tube and washed a second time with 2 M NaCl. Finally, the upper phase (~2.5 ml) was discarded and the chloroform phase was transferred into an auto sampler vial for gas chromatography.

3.6.3.5 Preparation of a FAME standard and controls

A FAME (fatty acid methyl ester) standard was generated with C17:0, C15:0, C13:0 and C11:0 fatty acids (FAs). Ten mg of each fatty acid was weighed in a glass tube and 160 µl of water was added. This mixture was then treated in the same way as the samples (see above; Chapters 3.6.3.3 and 3.6.3.4). Before the chloroform phase was transferred into an auto sampler vial it was diluted with chloroform 1:1000 (0.01 mg of each FA) and 1:100 (0.1 mg of each FA). For the preparation of the controls, 1000 mg of the normal HFD and 1000 mg of the HFD + 9.1 % C17:0 (Preparation see above; Chap. 3.5.3) were homogenized in 5 ml of methanol using the polytron. 200 µl of this homogenate were used instead of the samples (~36 mg HFD and 32.8 mg HF + 3.2 mg C17:0 respectively) and were treated in the same way. Prior to the final step the chloroform phase was also diluted with chloroform (1:1000 (0.01 mg of each FA) and 1:100 (0.1 mg of each FA).

3.6.3.6 Fatty acids analysis (Gas chromatography)

The FA profile of the liquid containing chloroform phase was analyzed by gas chromatography using a gas chromatograph (HP 6890, Hewlett-Packard, Philadelphia, PA, USA) equipped with a Supelcowax-10 column (30 m x 0.32 mm, 0.25 m; Supelco Inc., Bellefonte, PA, USA).

3.6.3.7 Data collection and statistical analysis

Data were analyzed using a paired two-tailed Student t-test (GraphPad Prism version 5.00 for windows, GraphPad Software, Inc., La Jolla, CA, USA) and values are expressed as means ± SEM for treatment (n=8) and control (n=8). Differences were considered significant when $P < 0.05$.

4 RESULTS

4.1 Experiment 1: Effect of IG DGAT1i01 infusions on food intake

4.1.1 Experiment 1a

IG infusions of DGAT1i01 (3 mg/kg BW) significantly decreased cumulative food intake during the dark phase (10:00 – 18:00) at 6 h (~16 %) and 8 h (~18%) after infusion onset (9:00) in HFD-fed rats (n=5) compared to control. The food intake in chow-fed rats (n=4) was not significantly affected by the IG DGAT1i01 infusion (see Figure 4.1).

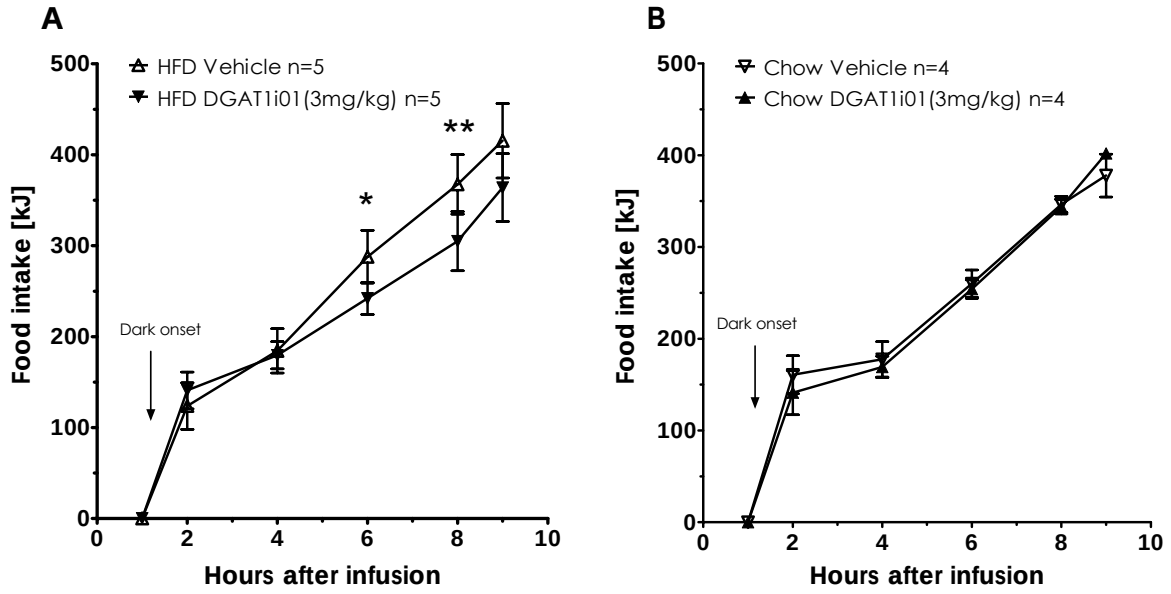

Figure 4.1: Effects of IG DGAT1i01 (3mg/kg BW) or Vehicle (HPMC/Tween 80 solution) infusion on cumulative food intake [kJ] in HFD-fed rats (A) and Chow-fed rats (B).

All animals were food deprived for 16 h and re-fed at dark onset (10:00). The infusions (5ml/kg) were done 1h before dark onset (9:00). Data are means ± SEM. * Significantly lower than corresponding control (paired t-test, *$p < 0.05$; **p < 0.01).

4.1.2 Experiment 1b

IG infusions of DGAT1i01 (9 mg/kg BW) significantly decreased cumulative food intake during the dark phase (10:00 – 18:00) at 4 h (23.7 %), 6 h (17.7 %), 8 h (21.0%) and 9 h (22.5 %) after infusion onset compared to control. The food intake in chow-fed rats (n=4) was not significantly affected by the IG DGAT1i01 infusion (see Figure 4.2).

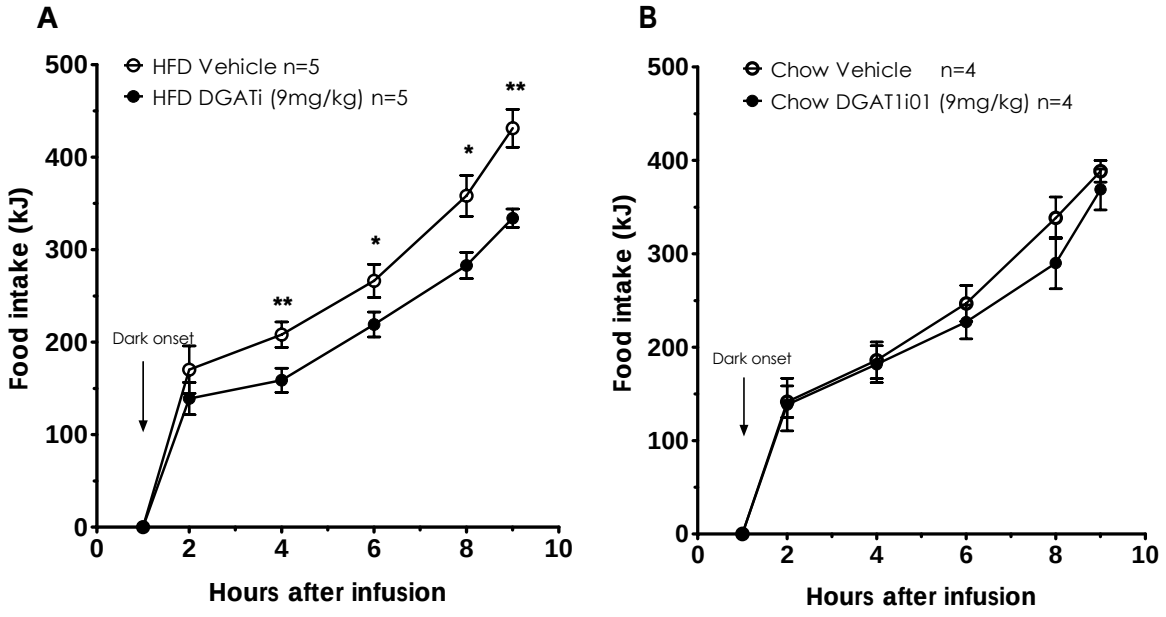

Figure 4.2: Effects of IG DGAT1i01 (9mg/kg BW) or Vehicle (HPMC/Tween 80 solution) IG infusion on cumulative food intake [kJ] in HFD-fed rats (A) and Chow-fed rats (B).

All animals were food deprived for 16h and re-fed at dark onset (10:00). The infusions (5 ml/kg) were done 1h before dark onset (9:00). Data are means ± SEM. * Significantly lower than corresponding control (paired t-test, *$p < 0.05$; **$p < 0.01$).

4.2 Experiment 2: Effect of IG DGAT1i01 infusions on serum and plasma metabolites

The serum triglyceride (TG) (A), plasma free glycerol (Glyc) (B) and free fatty acid (FFA) (C) levels increased (significantly higher than baseline at 3h) and the plasma BHB (D) levels decreased (significantly lower than baseline at 5 h) in the control (vehicle) condition after the 5 g HFD meal at dark on set in 16 h-fasted rats (n=8 and n=7, respectively). IG DGAT1i01 (9 mg/kg BW) infusions (1h before dark onset) blunted these changes (A, B, C, D). Serum TG (see Figure 4.3 (A)) as well as plasma free glycerol and FFA levels (see Figure 4.3 (B and C)) were significantly lower 3 h after DGAT1i01 infusion than after vehicle infusion ($F_{3/36}$ = 8.84, $p < 0.001$) (A), $F_{3/35}$ = 9.25, $p < 0.001$ (B) and $F_{3/34}$ = 4.07, $p < 0.05$ (C), respectively), whereas plasma BHB levels (D) were significantly higher than after vehicle at 5 h after infusion ($F_{3/15}$ = 9.43, $p = 0.001$; see Figure 4.3 (D)). In addition, serum TG levels 2 h after DGAT1i01 infusion were significantly lower than at baseline ($F_{3/36}$ = 8.84, $P < 0.001$ (A)). There was no significant difference in plasma levels of Glyc, FFA, and BHB at 3 h and 5 h after DGAT1i01 infusion compared to baseline (see Figure 4.3 (B, C, D)).

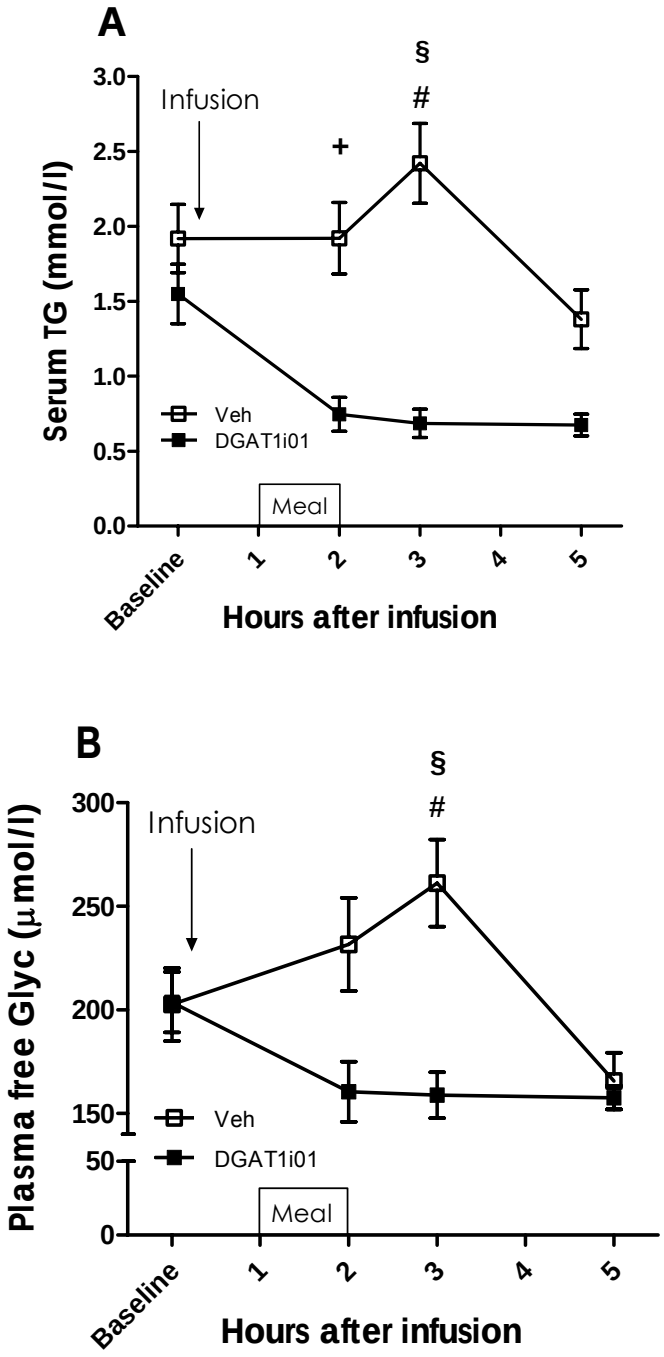
A
§
#
+
Infusion
Serum TG (mmol/l)
3.0
2.5
2.0
1.5
1.0
0.5
0.0
Veh
DGAT1i01
Meal
Baseline
1
2
3
4
5
Hours after infusion
B
§
#
Infusion
Plasma free Glyc (μmol/l)
300
250
200
150
50
0
Veh
DGAT1i01
Meal
Baseline
1
2
3
4
5
Hours after infusion

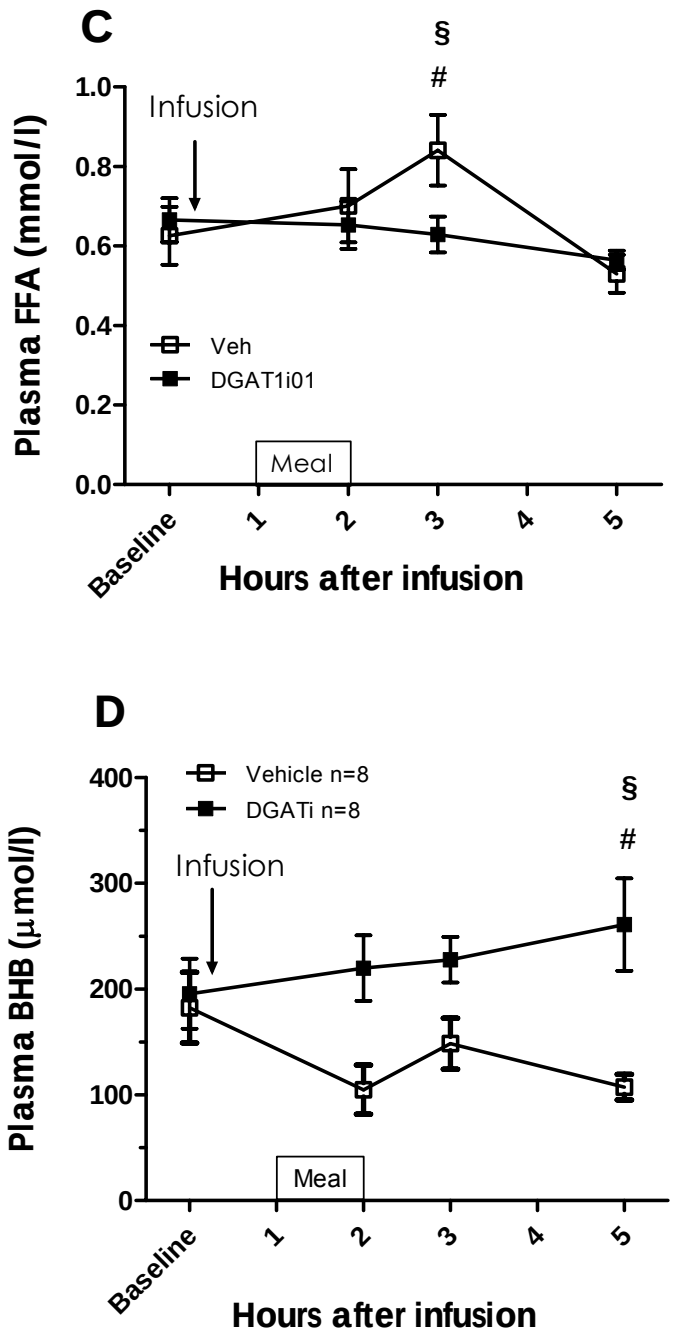

Figure 4.3: Effects of DGAT1i01 (9 mg/kg BW) or Vehicle (Veh; HPMC/Tween 80 solution) IG infusion on serum and plasma metabolites in 16-h food-deprived HFD-fed rats.

The infusions were done 1 h before dark onset (09:00) with a dose volume of 5 ml/kg BW. At dark onset (10:00) rats had access to a meal of 5 g HFD for 1 h. Each time point represents

the mean ± SEM of n=8 (A, B, D) or n=7 (C) animals. # Significantly different from the corresponding vehicle condition; + Significantly lower than baseline levels; § Significantly different from baseline levels (A, B, C, D) (Bonferroni-Holm post-hoc test after significant ANOVA). A: Serum triglyceride (TG); B: Plasma free glycerol (Glyc); C: Plasma free fatty acids (FFA); D: Plasma β-Hydroxybutyrat (BHB)

4.3 Experiment 3: Effect of DGAT1i01 IG infusion on FAO in small intestinal enterocytes after a 5 g HFD test meal including 9.1 ($^{w}/_{w}$) % C17:0 FA

The measured C15:0 FA content in the small intestine mucosa sections (A, B, and C), which was generated by mucosal β-oxidation of C17:0 FA, did not differ significantly from vehicle treatment (see Figure 4.4). IG DGAT1i01 (9 mg/kg BW) infusions (5 ml/kg BW; 1 h prior to dark onset) did not significantly affect FAO in small intestinal enterocytes 3 h after infusions onset in 16-h-fasted and re-feed rats (5 g HFD test meal including 9.1($^{w}/_{w}$) % C17:0).

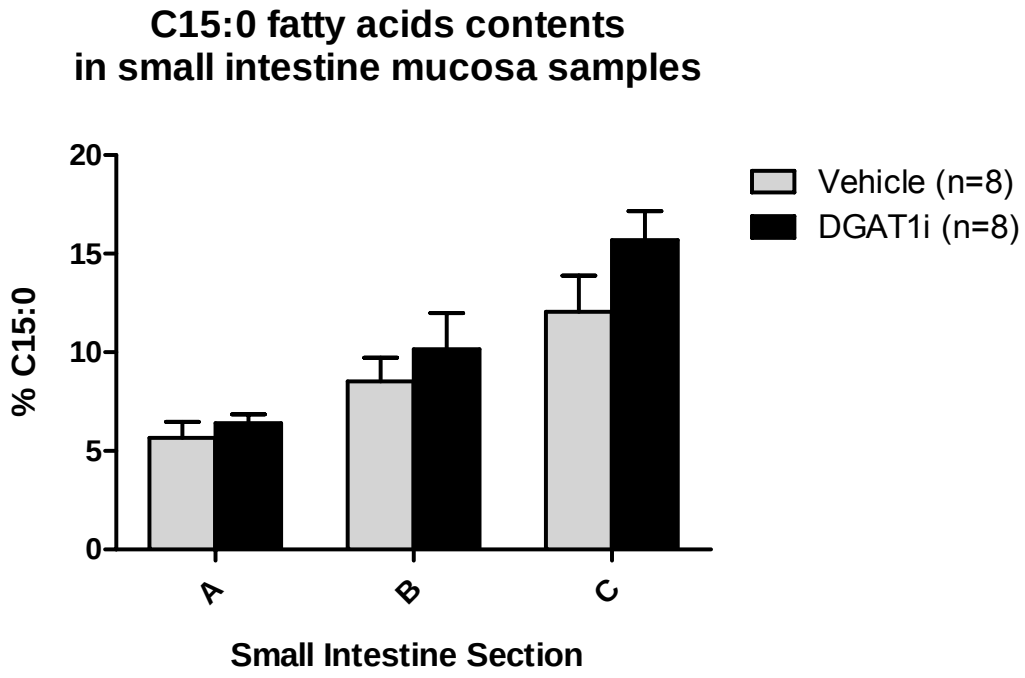

Figure 4.4: C15:0 fatty acids contents of small intestine mucosa after IG DGAT1i01 (9mg/kg BW) or Vehicle infusion.

C15:0 fatty acid contents of small intestine mucosa samples (A, B, C) are expressed as percentage (%) of the total amount of FAs C17:0 + C15:0 (100%). A = section most proximal and C = section most distal to the stomach; each section about 10 cm. Each bar represents the mean ± SEM of eight rats (Student's t-test).

5 DISCUSSION

5.1 Experiment 1: Effect of IG DGAT1i01 infusions (3 and 9 mg/kg BW) on food intake in Chow- and HFD-fed rats

This study was designed to test the hypothesis that an acute IG DGAT1 inhibitor (DGAT1i01) infusion inhibits FI in rats. The results confirmed the hypothesis, demonstrating that IG infused DGAT1i01 (9 mg/kg BW and 3 mg/kg BW, respectively) reduced food intake in HFD-fed rats starting at 4 or 6 hours after administration, but not in chow-fed rats. These results indicate that the fat content of the diet is crucial for this eating-inhibitory effect of DGAT1i01; given the primary localization of DGAT, the results are consistent with the idea that some aspect of intestinal epithelial cell fat handling is involved. Thus, it appears that a shift of intracellular fat metabolism from TG synthesis to fatty acid oxidation could be involved, but no firm conclusion can be drawn based on the present data. Furthermore, the eating-inhibitory effect of DGAT1i01 appears to be dose-dependent, but a direct comparison of the effectiveness of the two doses is not possible because they were administered in two different trials. Interestingly, however, our collaborating group at AstraZeneca (AZ) observed that the oral administration of DGAT1i01 (supramaximal dose of 30 mg/kg BW) led to a rapid onset inhibition of eating at 2 hours after administration in 20 h fasted rats which were also adapted to a HFD. This demonstrates that the eating-inhibitory effect is not limited to our experimental design, but may differ depending on the exact experimental conditions. At present, however, it remains unclear whether DGAT1i01 reduces food intake in both experimental paradigms by exactly the same mechanism.

5.2 Experiment 2: Effect of IG DGAT1i01 infusions on serum and plasma metabolites

The aim of this study was to investigate the effects of an acute IG DGAT1i01 infusion on circulating metabolites in rats. We determined serum TG, plasma glycerol, FFA and BHB in rats which were fasted for 16 h and re-fed with a 5 g HFD test meal 1 h after administration of DGAT1i01 (9 mg/kg BW) or vehicle. As expected, serum TG and plasma glycerol levels increased in control animals after the HFD meal. Further, we could show that DGAT1i01 eliminated this increase and even decreased TG and glycerol levels. This decrease in both metabolites was unexpected and is hard to explain, if the action of DGAT1i01 is limited to enterocytes. We speculated that DGAT1i01 may also have some effect on the liver, inhibiting hepatic TG synthesis and thereby enhancing hepatic FAO. We therefore checked whether plasma β-hydroxybutyrate (BHB) levels were affected. Interestingly, our results showed that DGAT1i01 administration resulted in a significant increase in plasma BHB, which appears to confirm our hypothesis of an additional hepatic action. We could further show that plasma FFA levels after DGAT1i01 infusion did not increase after the test meal, as after vehicle infusion, but rather decreased. This could be due to a decrease in LPL-mediated TG hydrolysis and uptake of FFA and glycerol into tissues that is secondary to the decreased circulating TG levels resulting from decreased intestinal TG synthesis. In general, however, our rat model (chronically eating a 60 % HDF for more than two months) appears to be hypertriglyceridemic (serum TGs ~2 mM).

In summary, these results suggest that inhibition of DGAT1 and, hence, interfering with its role in intestinal fat absorption has metabolic effects that may contribute to the eating-inhibitory effect observed in Experiment 1. Moreover, the results suggest that DGAT1 inhibition may also occur in the liver, where TGs are synthesized. Further investigations are necessary to critically examine the hypothesis of enhanced enterocyte FAO in response to DGAT1i01.

5.3 Experiment 3: Effect of DGAT1i01 IG infusion on FAO in small intestinal enterocytes after a 5g HFD test meal including 9.1 ($^{w}/_{w}$) % C17:0 FA

One possible explanation for the behavioral results in Experiment 1 is that DGAT1i01 administration reduced food intake by indirectly stimulating intestinal epithelial cell fatty acid oxidation. This has recently been hypothesized to be one metabolic mechanism controlling eating [LANGHANS, 2008]. There is also evidence that intestinal FAO is increased when mice are adapted to a diet enriched with PUFAs or TGs when compared to diets without additional fat [MORI et al., 2007]. Also, men showed a lower respiratory quotient (RQ; CO_2 expired/O_2 consumed) after a HF meal compared to an isocaloric low fat meal, indicating that high fat intake increases fat oxidation [SURINA et al., 1993]. Based on prior work by AZ, DGAT1 inhibition also lowers RQ in low-fat and chow-fed C57BL/6 mice when compared to controls, which suggests an enhanced whole body FAO. Therefore, the aim of this experiment was to determine whether FAO in small intestinal mucosa samples from HFD adapted rats was enhanced after an IG DGAT1i01 infusion (9 mg/kg BW) when compared to vehicle infused rats. However, under the conditions tested, we could not find a significant difference in intestinal epithelial cell fatty acid oxidation after DGAT1i01 and vehicle administration. But there seemed to be a tendency for increased FAO, in particular in the most distal intestine mucosa sections. Based on our findings, it could be speculated that DGAT1 inhibition in enterocytes may enhance mucosal FAO and therefore inhibit eating. To revisit this possible effect of DGAT1 inhibition on enterocyte FAO we have to optimize our techniques for mucosa isolation and FAO measurement, and we have to reconsider the time point of small intestine tissue sampling. Furthermore, we should turn our attention more to the mid jejunum

because our data suggest that FAO is highest in the section most distal to the stomach (Section C; last 10 cm of the intestine excision).

6 GENERAL DISCUSSION

DGAT1 is one of two known DGAT enzymes that catalyzes the final and only committed step in TG synthesis (reviewed in [FARESE, JR. et al., 2000]. Many studies used DGAT1-deficient mice to investigate the biological function of DGAT1 [BUHMAN et al., 2002; CHEN et al., 2002b; CHEN et al., 2002c; CHEN, 2006; FARESE, JR. et al., 2000; SMITH et al., 2000], but the effects of DGAT1 deficiency on FI have not been systematically examined yet. Furthermore, currently only little is known about synthetic DGAT1 inhibitors and their effects on behavior. Therefore, this is the first study that begins to thoroughly investigate the effect of a molecular DGAT1 inhibitor (generously provided by AstraZeneca) on food intake and that tries to identify the underlying mechanism of action.

In summary, the results of our three experiments show that an intragastrically administrated DGAT1 inhibitor 1) decreases food intake in rats when the dietary fat content is high and 2) induces metabolic effects that are consistent with the hypothesis that a shift from TG synthesis to fatty acid oxidation is the underlying mechanism of the observed eating-inhibitory effect. As DGAT1 is primarily located in enterocytes, our data are consistent with previous findings (see [LANGHANS, 2008]Langhans, 2008) in suggesting that it is not primarily hepatic fatty acid oxidation that affects food intake. Rather, fatty acid oxidation in enterocytes appears to be affected by DGAT1i01 and may thus contribute to the control of eating.

This working hypothesis is a novel concept for the metabolic control of eating because so far all hypotheses explaining the effects of peripheral metabolism on food intake focused on the liver. Several considerations make the intestine, and in particular the intestinal epithelial cells in fact a similarly – or even more – likely site

where metabolic events might be sensed by the body to affect eating. In general it is known that enterocytes use glutamine, glucose and ketone bodies as energy source, but there is also evidence that enterocytes oxidize fatty acids in addition to the other substrates (reviewed by [LANGHANS, 2008]).
Furthermore, there are vagal afferents present that are close to enterocytes and may therefore be in the position to convey sensory information from these cells to the CNS [BERTHOUD et al., 2004]. Recently, it has been demonstrated that intact vagal afferents are necessary for the stimulation of eating after intraperitoneal injection of the fatty acid oxidation inhibitor mercaptoacetate in rats [BRANDT et al., 2007]. Of course, there are several open questions regarding the idea that vagal afferents can sense metabolic changes in enterocytes and generate signals that affect eating. Foremost, the transduction mechanism of the signal from enterocytes to vagal afferents is unknown. Another remaining question is whether the sensing mechanism is specific for fatty acid oxidation or whether it also senses the utilization of other nutrients, such as glucose or amino acids.

Therefore, further studies are necessary to critically address these open issues before the idea of an eating control mechanism based on changes in enterocyte fatty acid oxidation (or metabolism) can be adopted.

In any case, however, the present findings might provide clues to an understanding of the mechanisms underlying the effects of a DGAT1-inhibitor on lipid metabolism and thus help to elucidate the possible role of intestinal FA catabolism in the control of food intake.

7 SUMMARY

This thesis addresses the effects of a molecular Acyl CoA:diacylglycerol acyltransferase 1 (DGAT 1; a key enzyme in the TG synthesis) inhibitor on food intake and its underlying mechanism of action. The focus was to investigate whether the eating inhibition in response to pharmacological DGAT1 inhibition is due to enhanced fatty acid oxidation in small intestinal enterocytes.

In the first experiment, we investigated the effect of an acute IG DGAT1-inhibitor (DGAT1i01) infusion on FI 16 h-fasted chow-fed or HFD-fed rats (n=9). Doses of 3 and 9 mg/kg DGAT1-inhibitor significantly reduced food intake in HFD-fed rats (18 % and 21 %, respectively, 8 h post infusion), but not in chow-fed rats.

In the second experiment we could show that IG DGAT1i01 infusion (9 mg/kg) had an effect on serum TG, plasma Glyc, FFA and BHB levels after a 5 g HFD test meal in 16 h-fasted rats (n=8). Serum TG, plasma Glyc and FFA levels increased after the HFD meal in response to vehicle infusion, whereas the DGAT1i01 decreased TG, Glyc and FFA levels. Also, DGAT1i01 increased plasma BHB levels compared to vehicle.

In the third experiment the effect of IG DGAT1i01 (9 mg/kg) infusion on mucosal FAO in 16 h-fasted and re-fed rats (n=16) (5 g HFD test meal including 9.1($^{w}/_{w}$) % C17:0) was investigated. However, under the conditions tested, we could not find a significant difference in intestinal epithelial cell FAO after DGAT1i01 and vehicle administration; there seemed to be a tendency for increased FAO, in particular in the most distal intestine mucosa sections.

In conclusion, these results show than an intragastrically administrated DGAT1-inhibitor decreases food intake in rats when the dietary fat content is high. The resulting metabolic effects are consistent with the hypothesis that a shift from TG synthesis to FAO in enterocytes and, perhaps, in liver is the underlying mechanism of the observed eating-inhibitory effect.

8 ZUSAMMENFASSUNG

Die vorliegende Diplomarbeit untersucht den Einfluss eines molekularen Acyl CoA:diacylglycerol acyltransferase 1 (DGAT1; ein Schlüsselenzym in der TG Synthese) Inhibitors auf die Nahrungsaufnahme und die involvierten Mechanismen. Der Schwerpunkt lag dabei auf der Frage, ob die Hemmung der Nahrungsaufnahme durch den Inhibitor auf einer Stimulation der Fettsäurenoxidation in den Darmepithelzellen beruht. In der ersten Studie wurde der Effekt einer akuten intragastralen (IG) Infusion von DGAT1-Inhibitor (DGAT1i01) auf den Verzehr nach 16 h Futterentzug bei Ratten untersucht, die mit einer Standarddiät oder einer Hochfettdiät (HFD) gefüttert wurden (n=9). Dosen von 3 und 9 mg/kg DGAT1i01 reduzierten den Verzehr bei Fütterung mit der HFD nicht jedoch bei Fütterung mit der Standarddiät signifikant (18 bzw. 21 %). Im zweiten Experiment konnten wir zeigen, dass die IG Infusion von DGAT1i01 (9 mg/kg) nach einer 5 g Testmahlzeit und nach 16 h Futterentzug auch die Serumkonzentration von TG sowie die Plasmakonzentrationen von Glyc, FFA und BHB beeinflusste. TG im Serum sowie Glyc und FFA im Plasma stiegen nach Kontrollinfusion an und fielen nach DGAT1i01 Infusion ab. Ferner erhöhte die DGAT i01-Infusion die Plasmakonzentration von BHB. Im dritten Experiment wurde nach 16 Stunden Futterentzug der Einfluss von IG DGAT1i01 (9 mg/kg) auf die Fettäurenoxidation in Darmepithelzellen überprüft. Die HFD-Testmahlzeit enthielt dazu 9.1 (w/w) % C17:0. Unter diesen Bedingungen liess sich kein signifikanter Effekt nachweisen, lediglich in dem am weitesten distal gelegenen Darmabschnitt war die Fettsäurenoxidation tendenziell erhöht. Insgesamt zeigen diese Daten, dass IG DGAT1i01 die Nahrungsaufnahme reduziert, wenn der Fettgehalt der Diät hoch ist. Die beobachteten metabolischen Effekte sind konsistent mit der Hypothese, dass eine Verschiebung von TG-Synthese zu Fettsäurenoxidation in Enterozyten und vielleicht auch in der Leber zu der beobachteten Verzehrsreduktion beiträgt.

9 REFERENCES

ABO-HASHEMA KA, CAKE MH, POWER GW, CLARKE D. Evidence for triacylglycerol synthesis in the lumen of microsomes via a lipolysis-esterification pathway involving carnitine acyltransferases. J Biol Chem 1999; 274: 35577-35582.

BADY I, MARTY N, DALLAPORTA M, EMERY M, GYGER J, TARUSSIO D, FORETZ M, THORENS B. Evidence from glut2-null mice that glucose is a critical physiological regulator of feeding. Diabetes 2006; 55: 988-995.

BAGGIO LL, DRUCKER DJ. Biology of incretins: GLP-1 and GIP. Gastroenterology 2007; 132: 2131-2157.

BASKIN DG, FIGLEWICZ LD, SEELEY RJ, WOODS SC, PORTE D, JR., SCHWARTZ MW. Insulin and leptin: dual adiposity signals to the brain for the regulation of food intake and body weight. Brain Res 1999; 848: 114-123.

BATTERHAM RL, COWLEY MA, SMALL CJ, HERZOG H, COHEN MA, DAKIN CL, WREN AM, BRYNES AE, LOW MJ, GHATEI MA, CONE RD, BLOOM SR. Gut hormone PYY(3-36) physiologically inhibits food intake. Nature 2002; 418: 650-654.

BAUCHE F, SABOURAULT D, GIUDICELLI Y, NORDMANN J, NORDMANN R. 2-Mercaptoacetate administration depresses the beta-oxidation pathway through an inhibition of long-chain acyl-CoA dehydrogenase activity. Biochem J 1981; 196: 803-809.

BAYS HE. Current and investigational antiobesity agents and obesity therapeutic treatment targets. Obes Res 2004; 12: 1197-1211.

BEGLINGER C, DEGEN L. Fat in the intestine as a regulator of appetite--role of CCK. Physiol Behav 2004; 83: 617-621.

BEGLINGER C, DEGEN L. Gastrointestinal satiety signals in humans--physiologic roles for GLP-1 and PYY? Physiol Behav 2006; 89: 460-464.

BENOIT SC, AIR EL, COOLEN LM, STRAUSS R, JACKMAN A, CLEGG DJ, SEELEY RJ, WOODS SC. The catabolic action of insulin in the brain is mediated by melanocortins. J Neurosci 2002; 22: 9048-9052.

BERGE RK, MADSEN L, VAAGENES H, TRONSTAD KJ, GOTTLICHER M, RUSTAN AC. In contrast with docosahexaenoic acid, eicosapentaenoic acid and hypolipidaemic derivatives decrease hepatic synthesis and secretion of triacylglycerol by decreased diacylglycerol acyltransferase activity and stimulation of fatty acid oxidation. Biochem J 1999; 343 Pt 1: 191-197.

BERTHOUD HR, BLACKSHAW LA, BROOKES SJ, GRUNDY D. Neuroanatomy of extrinsic afferents supplying the gastrointestinal tract. Neurogastroenterol Motil 2004; 16 Suppl 1: 28-33.

BRANDT K, ARNOLD M, GEARY N, LANGHANS W, LEONHARDT M. Vagal afferents mediate the feeding response to mercaptoacetate but not to the beta (3) adrenergic receptor agonist CL 316,243. Neurosci Lett 2007; 411: 104-107.

BRUBAKER PL. The glucagon-like peptides: pleiotropic regulators of nutrient homeostasis. Ann N Y Acad Sci 2006; 1070: 10-26.

BUHMAN KK, SMITH SJ, STONE SJ, REPA JJ, WONG JS, KNAPP FF, JR., BURRI BJ, HAMILTON RL, ABUMRAD NA, FARESE RV, JR. DGAT1 is not essential for intestinal triacylglycerol absorption or chylomicron synthesis. J Biol Chem 2002; 277: 25474-25479.

CALLE EE, KAAKS R. Overweight, obesity and cancer: epidemiological evidence and proposed mechanisms. Nat Rev Cancer 2004; 4: 579-591.

CAMPFIELD LA, SMITH FJ. Blood glucose dynamics and control of meal initiation: a pattern detection and recognition theory. Physiol Rev 2003; 83: 25-58.

CAMPFIELD LA, SMITH FJ, BURN P. Strategies and potential molecular targets for obesity treatment. Science 1998; 280: 1383-1387.

CASASCHI A, MAIYOH GK, ADELI K, THERIAULT AG. Increased diacylglycerol acyltransferase activity is associated with triglyceride accumulation in tissues of diet-induced insulin-resistant hyperlipidemic hamsters. Metabolism 2005; 54: 403-409.

CASES S, SMITH SJ, ZHENG YW, MYERS HM, LEAR SR, SANDE E, NOVAK S, COLLINS C, WELCH CB, LUSIS AJ, ERICKSON SK, FARESE RV, JR. Identification of a gene encoding an acyl CoA:diacylglycerol acyltransferase, a key enzyme in triacylglycerol synthesis. Proc Natl Acad Sci U S A 1998; 95: 13018-13023.

CASES S, STONE SJ, ZHOU P, YEN E, TOW B, LARDIZABAL KD, VOELKER T, FARESE RV, JR. Cloning of DGAT2, a second mammalian diacylglycerol acyltransferase, and related family members. J Biol Chem 2001; 276: 38870-38876.

CHEN HC. Enhancing energy and glucose metabolism by disrupting triglyceride synthesis: Lessons from mice lacking DGAT1. Nutr Metab (Lond) 2006; 3: 10-

CHEN HC, FARESE RV, JR. DGAT and triglyceride synthesis: a new target for obesity treatment? Trends Cardiovasc Med 2000; 10: 188-192.

CHEN HC, JENSEN DR, MYERS HM, ECKEL RH, FARESE RV, JR. Obesity resistance and enhanced glucose metabolism in mice transplanted with white adipose tissue lacking acyl CoA:diacylglycerol acyltransferase 1. J Clin Invest 2003; 111: 1715-1722.

CHEN HC, LADHA Z, FARESE RV, JR. Deficiency of acyl coenzyme a:diacylglycerol acyltransferase 1 increases leptin sensitivity in murine obesity models. Endocrinology 2002a; 143: 2893-2898.

CHEN HC, RAO M, SAJAN MP, STANDAERT M, KANOH Y, MIURA A, FARESE RV, JR., FARESE RV. Role of adipocyte-derived factors in enhancing insulin signaling in skeletal muscle and white adipose tissue of mice lacking Acyl CoA:diacylglycerol acyltransferase 1. Diabetes 2004; 53: 1445-1451.

CHEN HC, SMITH SJ, LADHA Z, JENSEN DR, FERREIRA LD, PULAWA LK, MCGUIRE JG, PITAS RE, ECKEL RH, FARESE RV, JR. Increased insulin and leptin sensitivity in mice lacking acyl CoA:diacylglycerol acyltransferase 1. J Clin Invest 2002b; 109: 1049-1055.

CHEN HC, SMITH SJ, TOW B, ELIAS PM, FARESE RV, JR. Leptin modulates the effects of acyl CoA:diacylglycerol acyltransferase deficiency on murine fur and sebaceous glands. J Clin Invest 2002c; 109: 175-181.

CHEN HC, STONE SJ, ZHOU P, BUHMAN KK, FARESE RV, JR. Dissociation of obesity and impaired glucose disposal in mice overexpressing acyl coenzyme a:diacylglycerol acyltransferase 1 in white adipose tissue. Diabetes 2002d; 51: 3189-3195.

CHENG D, MEEGALLA RL, HE B, CROMLEY DA, BILLHEIMER JT, YOUNG PR. Human acyl-CoA:diacylglycerol acyltransferase is a tetrameric protein. Biochem J 2001; 359: 707-714.

CHOI CS, SAVAGE DB, KULKARNI A, YU XX, LIU ZX, MORINO K, KIM S, DISTEFANO A, SAMUEL VT, NESCHEN S, ZHANG D, WANG A, ZHANG XM, KAHN M, CLINE GW, PANDEY SK, GEISLER JG, BHANOT S, MONIA BP, SHULMAN GI. Suppression of diacylglycerol acyltransferase-2 (DGAT2), but not DGAT1, with antisense oligonucleotides reverses diet-induced hepatic steatosis and insulin resistance. J Biol Chem 2007; 282: 22678-22688.

CHUA SC, JR., CHUNG WK, WU-PENG XS, ZHANG Y, LIU SM, TARTAGLIA L, LEIBEL RL. Phenotypes of mouse diabetes and rat fatty due to mutations in the OB (leptin) receptor. Science 1996; 271: 994-996.

CHUNG MY, RHO MC, LEE SW, PARK HR, KIM K, LEE IA, KIM DH, JEUNE KH, LEE HS, KIM YK. Inhibition of diacylglycerol acyltransferase by betulinic acid from Alnus hirsuta. Planta Med 2006; 72: 267-269.

CLARK B, HUBSCHER G. Biosynthesis of glycerides in subcellular fractions of intestinal mucosa. Biochim Biophys Acta 1961; 46: 479-494.

COLEMAN RA, LEE DP. Enzymes of triacylglycerol synthesis and their regulation. Prog Lipid Res 2004; 43: 134-176.

COLEMAN RA, LEWIN TM, MUOIO DM. Physiological and nutritional regulation of enzymes of triacylglycerol synthesis. Annu Rev Nutr 2000; 20: 77-103.

COLL AP, FAROOQI IS, O'RAHILLY S. The hormonal control of food intake. Cell 2007; 129: 251-262.

CROWLEY VE. Overview of human obesity and central mechanisms regulating energy homeostasis. Ann Clin Biochem 2008; 45: 245-255.

CUMMINGS DE. Ghrelin and the short- and long-term regulation of appetite and body weight. Physiol Behav 2006; 89: 71-84.

CUMMINGS DE, OVERDUIN J. Gastrointestinal regulation of food intake. J Clin Invest 2007; 117: 13-23.

DECLERCQ PE, VENINCASA MD, MILLS SE, FOSTER DW, MCGARRY JD. Interaction of malonyl-CoA and 2-tetradecylglycidyl-CoA with mitochondrial carnitine palmitoyltransferase I. J Biol Chem 1985; 260: 12516-12522.

DIETSCHY JM, SIPERSTEIN MD. Cholesterol synthesis by the gastrointestinal tract: localization and mechanisms of control. J Clin Invest 1965; 44: 1311-1327.

DRUCKER DJ. The biology of incretin hormones. Cell Metab 2006; 3: 153-165.

FARESE RV, JR., CASES S, SMITH SJ. Triglyceride synthesis: insights from the cloning of diacylglycerol acyltransferase. Curr Opin Lipidol 2000; 11: 229-234.

FERRARI B, ARNOLD M, CARR RD, LANGHANS W, PACINI G, BODVARSDOTTIR TB, GRAM DX. Subdiaphragmatic vagal deafferentation affects body weight gain and glucose metabolism in obese male Zucker (fa/fa) rats. Am J Physiol Regul Integr Comp Physiol 2005; 289: R1027-R1034.

FLEGAL KM, GRAUBARD BI, WILLIAMSON DF, GAIL MH. Excess deaths associated with underweight, overweight, and obesity. JAMA 2005; 293: 1861-1867.

FOLCH J, LEES M, SLOANE STANLEY GH. A simple method for the isolation and purification of total lipides from animal tissues. J Biol Chem 1957; 226: 497-509.

FRIEDMAN HI, NYLUND B. Intestinal fat digestion, absorption, and transport. A review. Am J Clin Nutr 1980; 33: 1108-1139.

FRIEDMAN MI, HORN CC, JI H. Peripheral signals in the control of feeding behavior. Chem Senses 2005; 30 Suppl 1: i182-i183.

FRIEDMAN MI, TORDOFF MG. Fatty acid oxidation and glucose utilization interact to control food intake in rats. Am J Physiol 1986; 251: R840-R845.

FUJIMOTO K, FUKAGAWA K, SAKATA T, TSO P. Suppression of food intake by apolipoprotein A-IV is mediated through the central nervous system in rats. J Clin Invest 1993; 91: 1830-1833.

GALE SM, CASTRACANE VD, MANTZOROS CS. Energy homeostasis, obesity and eating disorders: recent advances in endocrinology. J Nutr 2004; 134: 295-298.

GEARY N. Endocrine controls of eating: CCK, leptin, and ghrelin. Physiol Behav 2004; 81: 719-733.

GIBBS J, YOUNG RC, SMITH GP. Cholecystokinin decreases food intake in rats. J Comp Physiol Psychol 1973; 84: 488-495.

GOTOH K, LIU M, BENOIT SC, CLEGG DJ, DAVIDSON WS, D'ALESSIO D, SEELEY RJ, TSO P, WOODS SC. Apolipoprotein A-IV interacts synergistically with melanocortins to reduce food intake. Am J Physiol Regul Integr Comp Physiol 2006; 290: R202-R207.

GRIGOR MR, BELL RM. Separate monoacylglycerol and diacylglycerol acyltransferases function in intestinal triacylglycerol synthesis. Biochim Biophys Acta 1982; 712: 464-472.

GUTZWILLER JP, DEGEN L, HEUSS L, BEGLINGER C. Glucagon-like peptide 1 (GLP-1) and eating. Physiol Behav 2004; 82: 17-19.

HAGAN MM. Peptide YY: a key mediator of orexigenic behavior. Peptides 2002; 23: 377-382.

HELLSTROM PM, GELIEBTER A, NASLUND E, SCHMIDT PT, YAHAV EK, HASHIM SA, YEOMANS MR. Peripheral and central signals in the control of eating in normal, obese and binge-eating human subjects. Br J Nutr 2004; 92 Suppl 1: S47-S57.

HEVENER AL, BERGMAN RN, DONOVAN CM. Portal vein afferents are critical for the sympathoadrenal response to hypoglycemia. Diabetes 2000; 49: 8-12.

HILL JO, WYATT HR, REED GW, PETERS JC. Obesity and the environment: where do we go from here? Science 2003; 299: 853-855.

HIRATA T, UNOKI H, BUJO H, UENO K, SAITO Y. Activation of diacylglycerol O-acyltransferase 1 gene results in increased tumor necrosis factor-alpha gene expression in 3T3-L1 adipocytes. FEBS Lett 2006; 580: 5117-5121.

HOLST B, SCHWARTZ TW. Constitutive ghrelin receptor activity as a signaling set-point in appetite regulation. Trends Pharmacol Sci 2004; 25: 113-117.

HORN CC, JI H, FRIEDMAN MI. Etomoxir, a fatty acid oxidation inhibitor, increases food intake and reduces hepatic energy status in rats. Physiol Behav 2004; 81: 157-162.

HUSSAIN MM. A proposed model for the assembly of chylomicrons. Atherosclerosis 2000; 148: 1-15.

KAHLER A, ZIMMERMANN M, LANGHANS W. Suppression of hepatic fatty acid oxidation and food intake in men. Nutrition 1999; 15: 819-828.

KALSCHEUER R, STEINBUCHEL A. A novel bifunctional wax ester synthase/acyl-CoA:diacylglycerol acyltransferase mediates wax ester and triacylglycerol biosynthesis in Acinetobacter calcoaceticus ADP1. J Biol Chem 2003; 278: 8075-8082.

KENNEDY GC. The role of depot fat in the hypothalamic control of food intake in the rat. Proc R Soc Lond B Biol Sci 1953; 140: 578-596.

KUHAJDA FP, PIZER ES, LI JN, MANI NS, FREHYWOT GL, TOWNSEND CA. Synthesis and antitumor activity of an inhibitor of fatty acid synthase. Proc Natl Acad Sci U S A 2000; 97: 3450-3454.

KUMAR V, RANI N, AGGARWAL P, SANNA VK, SINGH AT, JAGGI M, JOSHI N, SHARMA PK, IRCHHAIYA R, BURMAN AC. Synthesis and cytotoxic activity of heterocyclic ring-substituted betulinic acid derivatives. Bioorg Med Chem Lett 2008; 18: 5058-5062.

LAM TK, SCHWARTZ GJ, ROSSETTI L. Hypothalamic sensing of fatty acids. Nat Neurosci 2005; 8: 579-584.

LANDREE LE, HANLON AL, STRONG DW, RUMBAUGH G, MILLER IM, THUPARI JN, CONNOLLY EC, HUGANIR RL, RICHARDSON C, WITTERS LA, KUHAJDA FP, RONNETT GV. C75, a fatty acid synthase inhibitor, modulates AMP-activated protein kinase to alter neuronal energy metabolism. J Biol Chem 2004; 279: 3817-3827.

LANGHANS W. Fatty acid oxidation in the energostatic control of eating-A new idea. Appetite 2008;

LEHNER R, KUKSIS A. Triacylglycerol synthesis by purified triacylglycerol synthetase of rat intestinal mucosa. Role of acyl-CoA acyltransferase. J Biol Chem 1995; 270: 13630-13636.

LEHNER R, KUKSIS A. Biosynthesis of triacylglycerols. Prog Lipid Res 1996; 35: 169-201.

LEONHARDT M, LANGHANS W. Fatty acid oxidation and control of food intake. Physiol Behav 2004; 83: 645-651.

LEVIN BE. Metabolic sensing neurons and the control of energy homeostasis. Physiol Behav 2006; 89: 486-489.

LEWIS T, NICHOLS PD, MCMEEKIN TA. Evaluation of extraction methods for recovery of fatty acids from lipid-producing microheterotrophs. J Microbiol Methods 2000; 43: 107-116.

LIU M, DOI T, SHEN L, WOODS SC, SEELEY RJ, ZHENG S, JACKMAN A, TSO P. Intestinal satiety protein apolipoprotein AIV is synthesized and regulated in rat hypothalamus. Am J Physiol Regul Integr Comp Physiol 2001; 280: R1382-R1387.

LUNG SC, WESELAKE RJ. Diacylglycerol acyltransferase: a key mediator of plant triacylglycerol synthesis. Lipids 2006; 41: 1073-1088.

MANSBACH CM, GORELICK F. Development and physiological regulation of intestinal lipid absorption. II. Dietary lipid absorption, complex lipid synthesis, and the intracellular packaging and secretion of chylomicrons. Am J Physiol Gastrointest Liver Physiol 2007; 293: G645-G650.

MANSOURI A, AJA S, MORAN TH, RONNETT G, KUHAJDA FP, ARNOLD M, GEARY N, LANGHANS W, LEONHARDT M. Intraperitoneal injections of low doses of C75 elicit a behaviorally specific and vagal afferent-independent inhibition of eating in rats. Am J Physiol Regul Integr Comp Physiol 2008a; 295: R799-R805.

MANSOURI A, KOSS MD, BRANDT K, GEARY N, LANGHANS W, LEONHARDT M. Dissociation of mercaptoacetate's effects on feeding and fat metabolism by dietary medium- and long-chain triacylglycerols in rats. Nutrition 2008b; 24: 360-365.

MAYER J. Regulation of energy intake and the body weight: the glucostatic theory and the lipostatic hypothesis. Ann N Y Acad Sci 1955; 63: 15-43.

MAYOREK N, BAR-TANA J. Inhibition of diacylglycerol acyltransferase by 2-bromooctanoate in cultured rat hepatocytes. J Biol Chem 1985; 260: 6528-6532.

MAYOREK N, GRINSTEIN I, BAR-TANA J. Triacylglycerol synthesis in cultured rat hepatocytes. The rate-limiting role of diacylglycerol acyltransferase. Eur J Biochem 1989; 182: 395-400.

MEEGALLA RL, BILLHEIMER JT, CHENG D. Concerted elevation of acyl-coenzyme A:diacylglycerol acyltransferase (DGAT) activity through independent stimulation of mRNA expression of DGAT1 and DGAT2 by carbohydrate and insulin. Biochem Biophys Res Commun 2002; 298: 317-323.

MENDIETA-ZERÓN H, LÓPEZ M, DIÉGUEZ C. Gastrointestinal peptides controlling body weight homeostasis. General and comparative endocrinology 2008; 155: 481-495.

MIGRENNE S, MAGNAN C, CRUCIANI-GUGLIELMACCI C. Fatty acid sensing and nervous control of energy homeostasis. Diabetes Metab 2007; 33: 177-182.

MILLAR JS, STONE SJ, TIETGE UJ, TOW B, BILLHEIMER JT, WONG JS, HAMILTON RL, FARESE RV, JR., RADER DJ. Short-term overexpression of DGAT1 or DGAT2 increases hepatic triglyceride but not VLDL triglyceride or apoB production. J Lipid Res 2006; 47: 2297-2305.

MONDAL MS, DATE Y, YAMAGUCHI H, TOSHINAI K, TSURUTA T, KANGAWA K, NAKAZATO M. Identification of ghrelin and its receptor in neurons of the rat arcuate nucleus. Regul Pept 2005; 126: 55-59.

MORAN TH, SMEDH U, KINZIG KP, SCOTT KA, KNIPP S, LADENHEIM EE. Peptide YY(3-36) inhibits gastric emptying and produces acute reductions in food intake in rhesus monkeys. Am J Physiol Regul Integr Comp Physiol 2005; 288: R384-R388.

MORI T, KONDO H, HASE T, TOKIMITSU I, MURASE T. Dietary fish oil upregulates intestinal lipid metabolism and reduces body weight gain in C57BL/6J mice. J Nutr 2007; 137: 2629-2634.

MORTON GJ, CUMMINGS DE, BASKIN DG, BARSH GS, SCHWARTZ MW. Central nervous system control of food intake and body weight. Nature 2006; 443: 289-295.

NAMMI S, KOKA S, CHINNALA KM, BOINI KM. Obesity: an overview on its current perspectives and treatment options. Nutr J 2004; 3: 3-

NOGUEIRAS R, TSCHOP MH, ZIGMAN JM. Central nervous system regulation of energy metabolism: ghrelin versus leptin. Ann N Y Acad Sci 2008; 1126: 14-19.

OBICI S, FENG Z, KARKANIAS G, BASKIN DG, ROSSETTI L. Decreasing hypothalamic insulin receptors causes hyperphagia and insulin resistance in rats. Nat Neurosci 2002; 5: 566-572.

OGDEN CL, CARROLL MD, CURTIN LR, MCDOWELL MA, TABAK CJ, FLEGAL KM. Prevalence of overweight and obesity in the United States, 1999-2004. JAMA 2006; 295: 1549-1555.

OWEN MR, CORSTORPHINE CC, ZAMMIT VA. Overt and latent activities of diacylglycerol acytransferase in rat liver microsomes: possible roles in very-low-density lipoprotein triacylglycerol secretion. Biochem J 1997; 323 (Pt 1): 17-21.

RAO GA, JOHNSTON JM. Purification and properties of triglyceride synthetase from the intestinal mucosa. Biochim Biophys Acta 1966; 125: 465-473.

REMIE R. Experimental Surgery. 2000; 523-560.

REMIE R, COPPES RP, MEURS H, ROFFEL AF, ZAAGSMA J. Characterization of presynaptic vascular muscarinic receptors inhibiting endogenous noradrenaline overflow in the portal vein of the freely moving rat. Br J Pharmacol 1990; 99: 223-226.

RONNETT GV, KIM EK, LANDREE LE, TU Y. Fatty acid metabolism as a target for obesity treatment. Physiol Behav 2005; 85: 25-35.

ROORDA BD, HESSELINK MK, SCHAART G, MOONEN-KORNIPS E, MARTINEZ-MARTINEZ P, LOSEN M, DE BAETS MH, MENSINK RP, SCHRAUWEN P. DGAT1 overexpression in muscle by in vivo DNA electroporation increases intramyocellular lipid content. J Lipid Res 2005; 46: 230-236.

ROS E. Intestinal absorption of triglyceride and cholesterol. Dietary and pharmacological inhibition to reduce cardiovascular risk. Atherosclerosis 2000; 151: 357-379.

RUSTAN AC, NOSSEN JO, CHRISTIANSEN EN, DREVON CA. Eicosapentaenoic acid reduces hepatic synthesis and secretion of triacylglycerol by decreasing the

activity of acyl-coenzyme A:1,2-diacylglycerol acyltransferase. J Lipid Res 1988; 29: 1417-1426.

SANDOVAL D, COTA D, SEELEY RJ. The integrative role of CNS fuel-sensing mechanisms in energy balance and glucose regulation. Annu Rev Physiol 2008; 70: 513-535.

SCHARRER E, LANGHANS W. Control of food intake by fatty acid oxidation. Am J Physiol 1986; 250: R1003-R1006.

SCHWARTZ MW, MORTON GJ. Obesity: keeping hunger at bay. Nature 2002; 418: 595-597.

SCHWARTZ MW, WOODS SC, PORTE D, JR., SEELEY RJ, BASKIN DG. Central nervous system control of food intake. Nature 2000; 404: 661-671.

SHEN H, HOWLES P, TSO P. From interaction of lipidic vehicles with intestinal epithelial cell membranes to the formation and secretion of chylomicrons. Adv Drug Deliv Rev 2001; 50 Suppl 1: S103-S125.

SHEN L, PEARSON KJ, XIONG Y, LO CM, TSO P, WOODS SC, DAVIDSON WS, LIU M. Characterization of apolipoprotein A-IV in brain areas involved in energy homeostasis. Physiol Behav 2008; 95: 161-167.

SHI Y, BURN P. Lipid metabolic enzymes: emerging drug targets for the treatment of obesity. Nat Rev Drug Discov 2004; 3: 695-710.

SHIAU YF. Mechanisms of intestinal fat absorption. Am J Physiol 1981; 240: G1-G9.

SHIIYA T, NAKAZATO M, MIZUTA M, DATE Y, MONDAL MS, TANAKA M, NOZOE S, HOSODA H, KANGAWA K, MATSUKURA S. Plasma ghrelin levels in lean and obese humans and the effect of glucose on ghrelin secretion. J Clin Endocrinol Metab 2002; 87: 240-244.

SMALL CJ, BLOOM SR. Gut hormones and the control of appetite. Trends Endocrinol Metab 2004; 15: 259-263.

SMITH PM, FERGUSON AV. Neurophysiology of hunger and satiety. Dev Disabil Res Rev 2008; 14: 96-104.

SMITH SJ, CASES S, JENSEN DR, CHEN HC, SANDE E, TOW B, SANAN DA, RABER J, ECKEL RH, FARESE RV, JR. Obesity resistance and multiple mechanisms of triglyceride synthesis in mice lacking Dgat. Nat Genet 2000; 25: 87-90.

STEFFENS AB. A Method for frequent sampling of blood and continuous infusion of fluids in the rat without disturbing the animal. Physiol Behav 1969; 4: 833-836.

STONE SJ, LEVIN MC, FARESE RV, JR. Membrane topology and identification of key functional amino acid residues of murine acyl-CoA:diacylglycerol acyltransferase-2. J Biol Chem 2006; 281: 40273-40282.

STONE SJ, MYERS HM, WATKINS SM, BROWN BE, FEINGOLD KR, ELIAS PM, FARESE RV, JR. Lipopenia and skin barrier abnormalities in DGAT2-deficient mice. J Biol Chem 2004; 279: 11767-11776.

SURINA DM, LANGHANS W, PAULI R, WENK C. Meal composition affects postprandial fatty acid oxidation. Am J Physiol 1993; 264: R1065-R1070.

TABATA N, ITO M, TOMODA H, OMURA S. Xanthohumols, diacylglycerol acyltransferase inhibitors, from Humulus lupulus. Phytochemistry 1997; 46: 683-687.

TARTAGLIA LA, DEMBSKI M, WENG X, DENG N, CULPEPPER J, DEVOS R, RICHARDS GJ, CAMPFIELD LA, CLARK FT, DEEDS J, MUIR C, SANKER S, MORIARTY A, MOORE KJ, SMUTKO JS, MAYS GG, WOOL EA, MONROE CA, TEPPER RI. Identification and expression cloning of a leptin receptor, OB-R. Cell 1995; 83: 1263-1271.

THUPARI JN, LANDREE LE, RONNETT GV, KUHAJDA FP. C75 increases peripheral energy utilization and fatty acid oxidation in diet-induced obesity. Proc Natl Acad Sci U S A 2002; 99: 9498-9502.

TOMODA H, ITO M, TABATA N, MASUMA R, YAMAGUCHI Y, OMURA S. Amidepsines, inhibitors of diacylglycerol acyltransferase produced by Humicola sp. FO-2942. I. Production, isolation and biological properties. J Antibiot (Tokyo) 1995; 48: 937-941.

TOMODA H, OHYAMA Y, ABE T, TABATA N, NAMIKOSHI M, YAMAGUCHI Y, MASUMA R, OMURA S. Roselipins, inhibitors of diacylglycerol acyltransferase, produced by Gliocladium roseum KF-1040. J Antibiot (Tokyo) 1999; 52: 689-694.

TOMODA H, OMURA S. Potential therapeutics for obesity and atherosclerosis: inhibitors of neutral lipid metabolism from microorganisms. Pharmacol Ther 2007; 115: 375-389.

TSCHOP M, SMILEY DL, HEIMAN ML. Ghrelin induces adiposity in rodents. Nature 2000; 407: 908-913.

TSCHOP M, WEYER C, TATARANNI PA, DEVANARAYAN V, RAVUSSIN E, HEIMAN ML. Circulating ghrelin levels are decreased in human obesity. Diabetes 2001; 50: 707-709.

TSO P, LIU M. Apolipoprotein A-IV, food intake, and obesity. Physiol Behav 2004; 83: 631-643.

TSO P, LIU M, KALOGERIS TJ, THOMSON AB. The role of apolipoprotein A-IV in the regulation of food intake. Annu Rev Nutr 2001; 21: 231-254.

UNGER RH. Lipotoxic diseases. Annu Rev Med 2002; 53: 319-336.

VAN DEN TOP M, SPANSWICK D. Integration of metabolic stimuli in the hypothalamic arcuate nucleus. Prog Brain Res 2006; 153: 141-154.

WANG YC, GORTMAKER SL, SOBOL AM, KUNTZ KM. Estimating the energy gap among US children: a counterfactual approach. Pediatrics 2006; 118: e1721-e1733.

WATERMAN IJ, PRICE NT, ZAMMIT VA. Distinct ontogenic patterns of overt and latent DGAT activities of rat liver microsomes. J Lipid Res 2002; 43: 1555-1562.

WEISS SB, KENNEDY EP, KIYASU JY. The enzymatic synthesis of triglycerides. J Biol Chem 1960; 235: 40-44.

WILBORN C, BECKHAM J, CAMPBELL B, HARVEY T, GALBREATH M, LA BOUNTY P, NASSAR E, WISMANN J, KREIDER R. Obesity: prevalence, theories, medical consequences, management, and research directions. J Int Soc Sports Nutr 2005; 2: 4-31.

WILLIAMS G, BING C, CAI XJ, HARROLD JA, KING PJ, LIU XH. The hypothalamus and the control of energy homeostasis: different circuits, different purposes. Physiol Behav 2001; 74: 683-701.

WOODS SC. Gastrointestinal satiety signals I. An overview of gastrointestinal signals that influence food intake. Am J Physiol Gastrointest Liver Physiol 2004a; 286: G7-13.

WOODS SC. Neurobiology of Food and Fluid Intake. 2004b; 2nd: 243-264.

WOODS SC, SCHWARTZ MW, BASKIN DG, SEELEY RJ. Food intake and the regulation of body weight. Annu Rev Psychol 2000; 51: 255-277.

WOODS SC, SEELEY RJ. Insulin as an adiposity signal. Int J Obes Relat Metab Disord 2001; 25 Suppl 5: S35-S38.

WOODS SC, SEELEY RJ, PORTE D, JR., SCHWARTZ MW. Signals that regulate food intake and energy homeostasis. Science 1998; 280: 1378-1383.

WREN AM, SEAL LJ, COHEN MA, BRYNES AE, FROST GS, MURPHY KG, DHILLO WS, GHATEI MA, BLOOM SR. Ghrelin enhances appetite and increases food intake in humans. J Clin Endocrinol Metab 2001; 86: 5992-

YEN CL, MONETTI M, BURRI BJ, FARESE RV, JR. The triacylglycerol synthesis enzyme DGAT1 also catalyzes the synthesis of diacylglycerols, waxes, and retinyl esters. J Lipid Res 2005; 46: 1502-1511.

YEN CL, STONE SJ, KOLIWAD S, HARRIS C, FARESE RV, JR. Thematic Review Series: Glycerolipids. DGAT enzymes and triacylglycerol biosynthesis. J Lipid Res 2008; 49: 2283-2301.

YU XX, MURRAY SF, PANDEY SK, BOOTEN SL, BAO D, SONG XZ, KELLY S, CHEN S, MCKAY R, MONIA BP, BHANOT S. Antisense oligonucleotide reduction of DGAT2 expression improves hepatic steatosis and hyperlipidemia in obese mice. Hepatology 2005; 42: 362-371.

YU YH, ZHANG Y, OELKERS P, STURLEY SL, RADER DJ, GINSBERG HN. Posttranscriptional control of the expression and function of diacylglycerol acyltransferase-1 in mouse adipocytes. J Biol Chem 2002; 277: 50876-50884.

ZAMMIT VA. Role of insulin in hepatic fatty acid partitioning: emerging concepts. Biochem J 1996; 314 (Pt 1): 1-14.

ZHANG Y, PROENCA R, MAFFEI M, BARONE M, LEOPOLD L, FRIEDMAN JM. Positional cloning of the mouse obese gene and its human homologue. Nature 1994; 372: 425-432.

ZHAO G, SOUERS AJ, VOORBACH M, FALLS HD, DROZ B, BRODJIAN S, LAU YY, IYENGAR RR, GAO J, JUDD AS, WAGAW SH, RAVN MM, ENGSTROM KM, LYNCH JK, MULHERN MM, FREEMAN J, DAYTON BD, WANG X, GRIHALDE N, FRY D, BENO DW, MARSH KC, SU Z, DIAZ GJ, COLLINS CA, SHAM H, REILLY RM, BRUNE ME, KYM PR. Validation of diacyl glycerolacyltransferase I as a novel target for the treatment of obesity and dyslipidemia using a potent and selective small molecule inhibitor. J Med Chem 2008; 51: 380-383.

10 APPENDIX

KLIBA NAFAG

2127

Maus und Ratte
Souris et rat
Mouse and rat

Experimentalfutter, purified diet
Diète expérimentale, purified diet
Experimental diet, purified diet

High Fat Diet: 60 % kcal % fat

Inhaltsstoffe | Substances | Major Nutrients

Trockensubstanz | Matière sèche | Dry matter	92.0 %
Rohprotein | Protéines brutes | Crude protein	23.9 %
Rohfett | Graisses brutes | Crude fat	35.0 %
Rohfaser | Fibres brutes | Crude fiber	4.9 %
Rohasche | Cendres brutes | Crude ash	5.0 %
NfE | ENA | NFE	23.2 %
Bruttoenergie | Energie brute | Gross energy	23.8 MJ/kg
Umsetzbare Energie | Energie métabolisable | Metabol. energy	22.0 MJ/kg
Stärke | Amidon | Starch	1.0 %

Aminosäuren | Acides aminés | Amino acids

Arginin | Arginine | Arginine	0.93 %
Lysin | Lysine | Lysine	1.62 %
Methionin | Méthionine | Methionine	0.54 %
Methionin + Cystin | Méthionine + cystine | Methionine + cystine	0.98 %
Tryptophan | Tryptophane | Tryptophan	0.39 %
Threonin | Thréonine | Threonine	0.93 %

Mengenelemente | Macro-éléments | Major mineral elements

Calcium | Calcium | Calcium	0.83 %
Phosphor | Phosphore | Phosphorus	0.50 %
Magnesium | Magnésium | Magnesium	0.08 %
Natrium | Sodium | Sodium	0.27 %
Kalium | Potassium | Potassium	0.57 %
Chlor | Chlore | Chlorine	0.21 %

Spurenelemente | Oligo-éléments | Trace elements

Eisen | Fer | Iron	80 mg/kg
Zink | Zinc | Zinc	48 mg/kg
Kupfer | Cuivre | Copper	8 mg/kg
Jod | Iode | Iodine	0.6 mg/kg
Mangan | Manganèse | Manganese	14 mg/kg
Selen | Sélénium | Selenium	0.2 mg/kg

Vitamine | Vitamines | Vitamins

Vitamin A | Vitamine A | Vitamin A	10'400 IE|UI|IU/kg
Vitamin D_3 | Vitamine D_3 | Vitamin D_3	1'040 IE|UI|IU/kg
Vitamin E | Vitamine E | Vitamin E	357 mg/kg
Vitamin K_3 | Vitamine K_3 | Vitamin K_3	6 mg/kg
Vitamin B_1 | Vitamine B_1 | Vitamin B_1	23 mg/kg
Vitamin B_2 | Vitamine B_2 | Vitamin B_2	15 mg/kg
Vitamin B_6 | Vitamine B_6 | Vitamin B_6	11 mg/kg
Vitamin B_{12} | Vitamine B_{12} | Vitamin B_{12}	0.05 mg/kg
Nicotinsäure | Acide nicotinique | Nicotinic acid	47 mg/kg
Pantothensäure | Acide pantothénique | Pantothenic acid	39 mg/kg
Folsäure | Acide folique | Folic acid	2 mg/kg
Biotin | Biotine | Biotin	0.2 mg/kg
Cholin | Choline | Choline	1'350 mg/kg

Rohstoffe | Ingrédients | Ingredients

Schweinefett, Casein, Maltodextrin, Zucker, Zellulose, Sojaöl raffiniert, Mineralstoffe, Vitamine, Aminosäuren

Graisse de porc, caséine, maltodextrine, sucre, cellulose, huile de soja raffinée, substances minérales, vitamines, acides aminés

Lard, casein, maltodextrin, sucrose, cellulose, refined soybean oil, minerals, vitamins, amino acids

Bemerkungen | Remarques | Remarks

- Experimentalfutter für Mäuse und Ratten
- Angegebene Gehalte sind berechnete Mittelwerte bezogen auf lufttrockene Substanz
- Herstellung auf Anfrage

- Diète expérimentale pour souris et rats
- Les teneurs indiquées sont des valeurs moyennes se rapportant à la matière séchée à l'air
- Fabrication sur demande

- Experimental diet for mice and rats
- Given values are calculated averages in air-dry feed
- Production on demand

Bestellform | Conditionnements | Delivery form

Pellets 10 mm rund | Pellets ronds 10 mm | Pellets 10 mm round

2127.0.99:
Variable Verpackung nach Bedarf
Conditionnement variable, selon besoin
Packaging according to order

KLIBA NAFAG | PROVIMI KLIBA AG | CH-4303 Kaiseraugst | Tel. +41 61 816 16 16 | Fax +41 61 816 18 00 | kliba-nafag@provimi-kliba.ch | www.kliba-nafag.ch

KLIBA NAFAG

3436

Maus und Ratte
Souris et rat
Mouse and rat

Haltung
Entretien
Maintenance

Extrudat | Extrudat | Extrudate

Inhaltsstoffe | Substances | Major Nutrients

Trockensubstanz | Matière sèche | Dry matter	88.0 %
Rohprotein | Protéines brutes | Crude protein	18.5 %
Rohfett | Graisses brutes | Crude fat	4.5 %
Rohfaser | Fibres brutes | Crude fiber	4.5 %
Rohasche | Cendres brutes | Crude ash	6.5 %
NfE | ENA | NFE	54.0 %
Bruttoenergie | Energie brute | Gross energy	16.1 MJ/kg
Umsetzbare Energie | Energie métabolisable | Metabol. energy	13.1 MJ/kg
Stärke | Amidon | Starch	35.0 %

Aminosäuren | Acides aminés | Amino acids

Arginin | Arginine | Arginine	1.10 %
Lysin | Lysine | Lysine	1.00 %
Methionin | Méthionine | Methionine	0.39 %
Methionin + Cystin | Méthionine + cystine | Methionine + cystine	0.76 %
Tryptophan | Tryptophane | Tryptophan	0.20 %
Threonin | Thréonine | Threonine	0.65 %

Mengenelemente | Macro-éléments | Major mineral elements

Calcium | Calcium | Calcium	1.05 %
Phosphor | Phosphore | Phosphorus	0.80 %
Magnesium | Magnésium | Magnesium	0.20 %
Natrium | Sodium | Sodium	0.20 %
Kalium | Potassium | Potassium	0.78 %
Chlor | Chlore | Chlorine	0.36 %

Spurenelemente | Oligo-éléments | Trace elements

Eisen | Fer | Iron	250 mg/kg
Zink | Zinc | Zinc	60 mg/kg
Kupfer | Cuivre | Copper	14 mg/kg
Jod | Iode | Iodine	1 mg/kg
Mangan | Manganèse | Manganese	60 mg/kg
Selen | Sélénium | Selenium	0.3 mg/kg

Vitamine | Vitamines | Vitamins

Vitamin A | Vitamine A | Vitamin A	14'000 IE | UI | IU/kg
Vitamin D_3 | Vitamine D_3 | Vitamin D_3	1'000 IE | UI | IU/kg
Vitamin E | Vitamine E | Vitamin E	110 mg/kg
Vitamin K_3 | Vitamine K_3 | Vitamin K_3	2 mg/kg
Vitamin B_1 | Vitamine B_1 | Vitamin B_1	30 mg/kg
Vitamin B_2 | Vitamine B_2 | Vitamin B_2	20 mg/kg
Vitamin B_6 | Vitamine B_6 | Vitamin B_6	14 mg/kg
Vitamin B_{12} | Vitamine B_{12} | Vitamin B_{12}	0.05 mg/kg
Nicotinsäure | Acide nicotinique | Nicotinic acid	70 mg/kg
Pantothensäure | Acide pantothénique | Pantothenic acid	33 mg/kg
Folsäure | Acide folique | Folic acid	2 mg/kg
Biotin | Biotine | Biotin	0.22 mg/kg
Cholin | Choline | Choline	2'000 mg/kg
Vitamin C | Vitamine C | Vitamin C	40 mg/kg

Rohstoffe | Ingrédients | Ingredients

Weizenkleie, Weizen, Gerste, Sojaextraktionsschrot (NGVO), Mais (NGVO), Geflügelfleischmehl, Weizenstärke, Molkenpulver, Sojaöl, Sonnenblumenkuchen, Bierhefe, Mineralstoffe, Vitamine, Aminosäuren

Son de blé, blé, orge, tourteau d'extraction de soja (sans OGM), maïs (sans OGM), farine de viande de volaille, amidon de blé, petit lait en poudre, huile de soja, tourteau de pression de tournesol, levure de bière, substances minérales, vitamines, acides aminés

Wheat middlings, wheat, barley, soybean meal (NGMO), corn (NGMO), poultry meal, wheat starch, whey powder, soybean oil, sunflower cake, brewer's dried yeast, minerals, vitamins, amino acids

Bemerkungen | Remarques | Remarks

- Alleinfuttermittel für Mäuse und Ratten
- Angegebene Gehalte sind berechnete Mittelwerte bezogen auf lufttrockene Substanz

- Aliment complet pour souris et rats
- Les teneurs indiquées sont des valeurs moyennes se rapportant à la matière séchée à l'air

- Complete food for mice and rats
- Given values are calculated averages in air-dry feed

Bestellform | Conditionnements | Delivery form

Extrudat 15 mm rund | Extrudat rond 15 mm | Extrudate 15 mm round

3436.EX.E05:
5 kg in Eimern mit Sicherheitsverschluss
5 kg en seaux avec couverde de sécurité
5 kg in pails with safety cap

3436.EX.F12:
12.5 kg in Papiersäcken mit verschweisster Plastiksackeinlage
12.5 kg en sacs en papier avec sache en plastique thermo-soudable
12.5 kg in paper bags with welded plastic lining

3436.EX.S12:
12.5 kg in Papiersäcken
12.5 kg en sacs en papier
12.5 kg in paper bags

06/2007

KLIBA NAFAG | PROVIMI KLIBA AG | CH-4303 Kaiseraugst | Tel. +41 61 816 16 16 | Fax +41 61 816 18 00 | kliba-nafag@provimi-kliba.ch | www.kliba-nafag.ch

CURRICULUM VITAE

Gudrun Schober

Personal Data	Date of birth:	March 9th ,1982
	Place of birth:	Linz, Austria
	Present address:	Vordergasse 15, 8200 Schaffhausen, Switzerland
	E-mail:	gudrun-schober@ethz.ch gudrun.schober@gmx.at
Studies	2001 – 2002	Johannes Kepler University, Linz, Austria Field of study: Technical Chemistry
	2002 – present	University of Vienna, Austria Field of study: Nutritional Sciences
	2005 – 2006	Guest student at Swiss Federal Institute of Technology Zurich, Switzerland Field of study: Food Science (Winter semester 05/06)
	2008 – 2008	Guest student at Swiss Federal Institute of Technology Zurich, Switzerland Field of study: Food Science (Spring semester 08)
	since April 08	Diploma student at Swiss Federal Institute of Technology Zurich, Institute of Animal Sciences, Switzerland Thesis: Possible mechanism of the eating-inhibitory effect of DGAT-1-inhibition under the guidance of Prof. Dr. Wolfgang Langhans
Education	1988 – 1992	Music Primary School (Violin), Linz, Austria
	1992 – 1996	Bundesrealgymnasium Ramsauerstrasse, Linz, Austria
	1996 – 2001	Bundesoberstufenrealgymnasium for competitive sport (Judo), Honauerstrasse, Linz, Austria
	June 2001	Matura (A-level) at Bundesoberstufenrealgymnasium for competitive sport, Honauerstrasse, Linz, Austria

 Schwerzenbach, am 16. Dezember 2008